

**Characterization and functional analysis of two redundant
MAPKKs in plant immunity**

by

Qian Zhang

B.Sc., Wuhan University, 2012

M.Sc., The University of British Columbia, 2015

A THESIS SUBMITTED IN PARTIAL FULFILLMENT OF
THE REQUIREMENTS FOR THE DEGREE OF

DOCTOR OF PHILOSOPHY

in

THE FACULTY OF GRADUATE AND POSTDOCTORAL STUDIES

(Botany)

THE UNIVERSITY OF BRITISH COLUMBIA

(Vancouver)

September 2020

© Qian Zhang, 2020

The following individuals certify that they have read, and recommend to the Faculty of Graduate and Postdoctoral Studies for acceptance, the dissertation entitled:

Characterization and functional analysis of two redundant MAPKKs in plant immunity

submitted by Qian Zhang in partial fulfillment of the requirements for

the degree of Doctor of Philosophy

in Botany

Examining Committee:

Yuelin Zhang, Associate Professor, Botany, UBC

Supervisor

Liang Song, Assistant Professor, Botany, UBC

Supervisory Committee Member

Richard Hamelin, Professor, Forest and Conservation Science, UBC

University Examiner

George Haughn, Professor, Botany, UBC

University Examiner

Additional Supervisory Committee Members:

Jae-Hyeok Lee, Assistant Professor, Botany, UBC

Supervisory Committee Member

Xin Li, Professor, Botany, UBC

Supervisory Committee Member

Abstract

Mitogen-activated protein kinase (MAPK) cascades are conserved signaling modules that transduce and amplify signals from upstream receptors in eukaryotes. In *Arabidopsis*, two MAP kinase cascades are activated upon treatment of flg22, a conserved peptide of 22 amino acids within the N terminus of bacteria flagellin. One cascade is composed of MEKK1-MKK1/2-MPK4. The other one is composed of MKK4/5-MPK3/6 and previously unknown MAPKKK(s). How signals are transduced to MAP kinase cascades was also not very clear. My Ph.D. research focuses on identification of the previously unknown MAPKKK(s) upstream of MKK4/MKK5-MPK3/MPK6 module and characterization of this MAP kinase cascade in plant immunity.

It is known that YDA-MKK4/5-MPK3/6 cascade regulates stomatal development. I hypothesized that the close homologues of YDA, MAPKKK3 and MAPKKK5, function upstream of MKK4/MKK5-MPK3/MPK6 to regulate plant immunity. The *mapkkk3 mapkkk5* double mutant was found to have significantly reduced MPK3 and MPK6 activation upon multiple elicitor treatment including flg22, suggesting that MAPKKK3 and MAPKKK5 are required for multiple elicitor-induced MPK3/MPK6 activation. The double mutant also shows enhanced susceptibility towards virulent pathogens, reduced cell death and enhanced susceptibility towards avirulent pathogens, suggesting that these two MAPKKKs are required for pathogen resistance. Using *E.coli* expressed proteins, MAPKKK3-MKK5-MPK6 cascade was reconstituted *in vitro*, biochemically confirming that MAPKKK3 is upstream of MKK5 and MPK6. Kinase assays using different mutant versions of MAPKKK3 protein show that the kinase domain and C terminal domain but not the N terminal regulatory domain of MAPKKK3 is required for signaling. Previously, PCRK1 (Pattern-triggered immunity Compromised Receptor-like cytoplasmic Kinase 1) and PCRK2 were shown to interact with flg22 receptor and the *pcrk1 pcrk2* double mutant shows modestly reduced flg22-induced MPK3/MPK6 activation. Co-Immunoprecipitation and biotinylation assays using transient expressed proteins in *Nicotiana benthamiana* showed that MAPKKK3 and MAPKKK5 interact with PCRK2, suggesting PCRK2 may transduce signal from flg22 receptor to MAPKKK3/MPK6.

Altogether, studies in this dissertation identified two MAPKKKs functioning upstream of MKK4/5-MPK3/6, characterized the roles of this MAP kinase cascade in immunity and provided insight on signal transduction from the flg22 receptor to this MAP kinase cascade.

Lay Summary

Like humans, plants also have an immune system that protects them from foreign invaders. In plant immunity, MAPK cascades are important signaling modules that transduce and amplify signals perceived upon pathogen infection. Each MAPK cascade is composed of three kinases that can be sequentially phosphorylated and activated. One of the MAPK cascades activated by pathogen infection has a previously unknown component. The study in this dissertation identified two such redundant kinases in the MAPK cascade and characterized the roles of this MAPK cascade in plant immunity. In addition, a protein that transduces signal from the upstream receptor to this MAPK cascade was identified. Altogether, these discoveries expanded our knowledge on MAPK cascades in plant immunity. Such molecular understanding will be critical for scientists to build more thorough knowledge of plant immunity, which will be essential to improve disease control strategies for crop plants.

Preface

The work presented in this thesis is the result of research performed between January 2015 and March 2020. The candidate and the supervisor Y. Zhang designed the experiments. Part of chapter 3 is modified from an article published as Sun, T. *, Nitta, Y. *, Zhang, Q. *, Wu, D., Tian, H., Lee, JS. and Zhang, Y. 2018. “Antagonistic interactions between two MAP kinase cascades in plant development and immune signaling” (*Co-first authorship). Figure 3.1-Figure 3.7 are modified from the published article mentioned above. The remaining experiments presented in this thesis are original and unpublished.

The candidate primarily conducted the experiments and analyzed the data presented in this thesis except that Dr. Tongjun Sun carried out the following.

1. Generated the *mapkkk3 mapkkk5 mekk1 mekk2 mekk3* mutant and assayed for flg22-induced MPK3/MPK6 phosphorylation in the mutant in figure 3.5.
2. Generated the constructs used in the Co-IP and BiFC experiment and carried out the experiment in figure 3.6.
3. Generated constructs for expressing recombinant MAPKKK3, MKK5, MKK5EE and MPK6 proteins in *E. coli*.

Table of Contents

Abstract.....	iii
Lay Summary	v
Preface.....	vi
Table of Contents	vii
List of Tables	xi
List of Figures.....	xii
List of Abbreviations	xiv
Acknowledgements	xviii
Chapter 1: Introduction	1
1.1 The plant immune system	1
1.2 Pattern-triggered immunity (PTI)	2
1.2.1 Perception of PAMPs by PRR complexes	3
1.2.2 Signalling downstream of PRR complexes.....	4
1.2.3 Receptor-like cytoplasmic kinases (RLCKs) in PTI.....	6
1.3 Effector-triggered susceptibility (ETS).....	8
1.4 Effector-triggered immunity (ETI)	9
1.4.1 Recognition of pathogen effectors by R proteins	10
1.4.2 Autoimmune mutants with constitutive ETI responses	11
1.5 Interplay between PTI and ETI.....	12
1.6 Systemic acquired resistance (SAR).....	15
1.6.1 SA in SAR.....	15

1.6.2	Pipecolic acid (Pip) and N-hydroxypipecolic acid (NHP) in SAR.....	16
1.7	MAPK cascades and plant immunity.....	17
1.7.1	MAPK cascades in plant immunity	19
1.7.2	MAPKKKs in plant immunity	20
1.8	Thesis objective	23
Chapter 2: Method and Materials.....		25
2.1	Plant materials and mutant characterization	25
2.2	Construction of plasmids	26
2.3	Analysis of MAPK activation.....	28
2.4	Gene expression analysis	28
2.5	Pathogen infection assay.....	30
2.6	Measurement of Oxidative Burst	31
2.7	Ion leakage measurement.....	32
2.8	Recombinant protein expression and purification	32
2.9	In vitro kinase assay.....	33
2.10	Bimolecular fluorescence complementation assay	34
2.11	Co-immunoprecipitation and biotinylation assay	34
2.12	Statistical analysis.....	35
Chapter 3: Results.....		36
3.1	flg22-induced activation of MPK3 and MPK6 is comprised in the <i>mapkkk3 mapkk5</i> double mutant.....	36
3.2	MAPKKK3 and MAPKKK5 are required for MPK3/MPK6 phosphorylation induced by multiple elicitors.	40

3.3	Loss of <i>MEKK1</i> , <i>MEKK2</i> , and <i>MEKK3</i> does not enhance the compromised activation of MPK3/MPK6 by <i>flg22</i>	42
3.4	MAPKKK3/MAPKKK5 interact with MKK4/MKK5.	43
3.5	MAPKKK3 and MAPKKK5 are required for PTI and basal resistance.	45
3.6	MAPKKK3 and MAPKKK5 are required for Effector-Triggered Immunity.	47
3.7	The <i>mapkkk3 mapkkk5</i> double mutant can't suppress the autoimmune phenotypes in <i>chs3-2D</i> and <i>mekk1-1</i>	48
3.8	MAPKKK3 and MAPKKK5 are required for ETI-induced cell death.	50
3.9	SAR induced by <i>Pto</i> DC3000 <i>AvrRpt2</i> is compromised in the <i>mapkkk3 mapkkk5</i> double mutant.	54
3.10	The MAPKKK3-MKK5-MPK6 MAPK cascade can be reconstituted <i>in vitro</i>	56
3.11	The kinase domain and C terminal domain, but not the N terminal domain of MAPKKK3 are required for its function <i>in vitro</i>	58
3.12	PCRK2 interacts with MAPKKK3 and MAPKKK5.	60
Chapter 4: Discussion		64
4.1	MAPKKK3 and MAPKKK5 function upstream of MKK4/MKK5-MPK3/MPK6.	64
4.2	MAPKKK3/MAPKKK5-MKK4/MKK5-MPK3/MPK6 cascade play critical roles in PTI and basal resistance.	65
4.3	MAPKKK3 and MAPKKK5 contribute to ETI and are required for <i>AvrRpt2</i> -induced cell death and SAR.	67
4.4	MAPKKK3 kinase activity and C terminal domain but not its N terminal regulatory domain is required for its function in signal transduction.	68

4.5	PCRK2 interacts with MAPKKK3/MAPKKK5 and connects upstream PRRs to the MAPKKK3/MAPKKK5-MKK4/MKK5-MPK3/MPK6 cascade.	70
Bibliography	73

List of Tables

Table 2.1 Primers used in this study.	29
--	----

List of Figures

Figure 1.1 Overview of plant immune responses downstream of immune receptors.....	14
Figure 1.2 Phylogenetic tree of MEKK-type mitogen-activated protein kinase kinase kinases (MAPKKKs) in <i>Arabidopsis</i>	21
Figure 3.1 flg22-induced activation of MPK3 and MPK6 are compromised in the <i>mapkkk3 mapkkk5</i> double mutant.	38
Figure 3.2 ROS burst triggered by flg22 is not affected in <i>mapkkk3 mapkkk5</i>	39
Figure 3.3 The reduced flg22-induced MAPK activation in <i>mapkkk3 mapkkk5</i> can be complemented by MAPKKK3 or MAPKKK5.	40
Figure 3.4 MAPKKK3 and MAPKKK5 are required for elf18, nlp20 and pep23-induced activation of MPK3 and MPK6.	41
Figure 3.5 flg22-induced MAPK activation in <i>mapkkk3 mapkkk5</i> is not further reduced by <i>mekk1 mekk2 mekk3</i>	42
Figure 3.6 MAPKKK3/MAPKKK5 interact with MKK4/MKK5.	44
Figure 3.7 <i>mapkkk3 mapkkk5</i> plants are more susceptible to <i>Pto</i> DC3000 <i>hrcC</i> ⁻ and <i>Pto</i> DC3000.	46
Figure 3.8 Growth of <i>Pto</i> DC3000 <i>AvrRpt2</i> and <i>Pto</i> DC3000 <i>AvrRps4</i> on wild type (WT), <i>mapkkk3</i> , <i>mapkkk5</i> , and <i>mapkkk3 mapkkk5</i> plants.	47
Figure 3.9 <i>mapkkk3 mapkkk5</i> double mutant can't suppress the autoimmune phenotype in <i>mekk1-1</i> and <i>chs3-2D</i>	49
Figure 3.10 <i>mapkkk3 mapkkk5</i> double mutant plants show delayed cell death after infection by <i>Pto</i> DC3000 <i>AvrRpt2</i>	51

Figure 3.11 Mutations in <i>MKK4/MKK5</i> and <i>MPK3/MPK6</i> further reduce ETI-induced cell death and enhance susceptibility to avirulent pathogens in <i>mapkkk3 mapkkk5</i>	54
Figure 3.12 <i>mapkkk3 mapkkk5</i> double mutant shows a defect in <i>Pto</i> DC3000 <i>AvrRpt2</i> induced SAR.....	55
Figure 3.13 MAPKKK3-MKK5-MPK6 cascade can be reconstituted <i>in vitro</i>	57
Figure 3.14 Analysis of the N-terminal domain, the C-terminal domain, and the kinase activity of MAPKKK3 in its function.	60
Figure 3.15 Chitin-induced MAPK activation and <i>FRK1</i> expression are not significantly altered in the <i>pbl27</i> mutant.	61
Figure 3.16 PCRK2 interacts with MAPKKK3 and MAPKKK5 <i>in planta</i>	63
Figure 4.1 MAPKKK3/MAPKKK5-MKK4/MKK5-MPK3/MPK6 cascade plays broad roles in plant immunity.	72

List of Abbreviations

ACC	aminocyclopropane-1-carboxylic acid
ACS2	ACC synthase 2
ACS6	ACC synthase 6
AGD2	aberrant growth and death 2
ALD1	AGD2-like defense response protein 1
ANP1	<i>Arabidopsis</i> NPK-related protein kinase 1
<i>AvrB</i>	an avirulence gene from <i>Pst</i> DC3000
<i>AvrE1</i>	an avirulence gene from <i>Pst</i> DC3000
<i>AvrPphB</i>	an avirulence gene from <i>Pst</i> DC3000
<i>AvrPto</i>	an avirulence gene from <i>Pst</i> DC3000
<i>AvrRpm1</i>	an avirulence gene from <i>Pst</i> DC3000
<i>AvrRps4</i>	an avirulence gene from <i>Pst</i> DC3000
<i>AvrRpt2</i>	an avirulence gene from <i>Pst</i> DC3000
BAK1	BRI1-associated receptor kinase 1
BIK1	<i>Botrytis</i> -induced kinase 1
BIR1	BAK1-interacting receptor-like kinase 1
BIR2	BAK1-interacting receptor-like kinase 2
BIR3	BAK1-interacting receptor-like kinase 3
BR	brassinosteroid
BR11	BR-insensitive 1
BSK1	BR-signaling kinase 1
CAMTA3	calmodulin-binding transcription activator 3
Cas9	CRISPR-associated 9
CBP60g	calmodulin binding protein 60 g
CC	coiled-coil
CERK1	chitin elicitor receptor kinase 1
CHS3	chilling sensitive 3
ChIP	chromatin immunoprecipitation
ChIP-seq	ChIP-sequencing

CNGC2	cyclic nucleotide gated channel 2
CNGC4	cyclic nucleotide gated channel 4
CNL	coiled-coil type NLR
COR	coronatine
CPK	calmodulin-domain protein kinase
CRCK3	calmodulin-binding receptor-like cytoplasmic kinase 3
CRISPR	Clustered Regularly Interspaced Short Palindromic Repeats
CTR1	constitutive triple response 1
DAMP	damage associated molecular pattern
Ecp6	an effector from the biotrophic fungus <i>Cladosporium fulvum</i>
EDR1	enhanced disease resistance 1
EFR	elongation factor (EF)-Tu receptor
EIX	ethylene-inducing xylanase
Eix2	ethylene-inducing xylanase receptor 2
EPF1	epidermal patterning factor 1
EPF2	epidermal patterning factor 2
EPFL4	epidermal patterning factor like 4
EPFL6	epidermal patterning factor like 6
ETI	effector-triggered immunity
ETS	effector-triggered susceptibility
FIR	FLS2-interacting receptor
FLS2	flagellin sensing 2
FMO1	flavin-dependent monooxygenase 1
FRK1	flg22-induced receptor-like kinase 1
HopM1	an avirulence gene from <i>Pst</i> DC3000
HPCA1	hydrogen peroxide-induced Ca ²⁺ increases 1
HR	hypersensitive response
ICS1	isochorismate synthase 1
JA	jasmonic acid
JAZ	jasmonate-ZIM domain

LRR	leucine-rich repeat
LysM	Lysin motif
MAMP	micobe-associated molecular pattern
MAPK	mitogen-activated protein kinase
MAPKKK/MEKK	mitogen-activated protein kinase kinase kinase
Mg3LysM	the homologue of effector Ecp6 from <i>Mycosphaerella graminicola</i>
MKD1	MAPKKK delta 1
MKK/MEK	mitogen-activated protein kinase kinase
<i>N. b.</i>	<i>Nicotiana benthamiana</i>
NB	nucleotide binding
NHP	N-hydroxy-pipecolic acid
NIK1	nuclear shuttle protein-interacting kinase 1
NLP	necrosis and ethylene-inducing peptide 1-like proteins
NLR	NOD-like receptors
NOD	nucleotide-binding oligomerization domain
NPR1	nonexpressor of <i>PR</i> genes 1
P2C	Δ 1-piperidine-2-carboxylic acid
PAD4	phytoalexin deficient 4
PAMP	pathogen-associated molecular pattern
PBL1	PBS like 1
PBS1	AvrPphB susceptible 1
PCR	polymerase chain reaction
PCRK1	PTI compromised receptor-like cytoplasmic kinase 1
PCRK2	PTI compromised receptor-like cytoplasmic kinase 2
PEPR1	pep1 receptor 1
PEPR2	pep1 receptor 2
Pip	pipecolic acid
<i>PR</i> gene	<i>pathogenesis-related</i> gene
PRR	pattern recognition receptor
<i>Pto</i>	<i>Pseudomonas syringae</i> pv. <i>tomato</i>

PTI	PAMP-triggered immunity
R protein	resistance protein
RbohD	respiratory burst oxidase homologue D
RIN4	RPM1 interacting protein 4
RLCK	receptor-like cytoplasmic kinase
RLK	receptor-like kinase
RLP	receptor-like protein
ROS	reactive oxygen species
RPM1	resistance to <i>P. syringae pv maculicola</i> 1
RPP1	recognition of <i>Peronospora parasitica</i> 1
RPS2	resistant to <i>P. syringae</i> 2
RPS4	resistant to <i>P. syringae</i> 4
RPS5	resistant to <i>P. syringae</i> 5
RRS1	resistant to <i>Ralstonia solanacearum</i> 1
SA	salicylic acid
SAR	systemic acquired resistance
SARD1	SAR deficient 1
SARD4	SAR deficient 4
SOBIR1	suppressor of <i>bir1</i> 1
T3SS	type III secretion system
TGA	TGACG sequence-specific binding protein
TIR	Toll interleukin receptor
TNL	TIR type NLR
SUMM2	suppressor of <i>mkk1 mkk2</i> 2
WRKY29	WRKY DNA-binding protein 29
WRKY33	WRKY DNA-binding protein 33

Acknowledgements

I would not have reached this point in my career without the assistance of many people.

First of all, I would like to express my huge appreciation to my supervisor Dr. Yuelin Zhang for his expertise, patience and continuous support. He is an intelligent and diligent scientist with a strong sense of responsibility. He also tried his best to encourage and support me when I had problems in my life. He is an excellent mentor. I am very grateful to have worked with him during my PhD study.

I would also like to thank my committee members Dr. Xin Li and Dr. Jae-Hyeok Lee for their advice and suggestions throughout the course of my Ph.D. career, as well as their contributions to the development of the project in this thesis.

I am grateful to all former and current lab members. Thanks to former lab members Xingchuan Huang for his training and help, Dr. Yaxi Zhang, Dr. Qing Kong and Dr. Zhibin Zhang for their help and advice during my early times in the Zhang lab at National Institute of Biological Sciences, Beijing. I would like to thank former lab member Dr. Yanan Liu for collaboration on an E3 screen that is not mentioned in this dissertation. I would like to thank Dr. Tongjun Sun, Dr. Yukino Nitta, Dr. Di Wu and Dr. Hainan Tian for their contributions and collaboration on the published article, part of which is included in this dissertation. Thanks also go to all the former and current Li lab members for sharing all kinds of resources.

This research is funded by the Natural Sciences and Engineering Research Council (NSERC) of Canada, UBC Four-Year Fellowship and UBC Teaching Assistantship. I appreciate the support from all of these funding sources.

Finally, I would like to thank my lovely family, my children, my partner Tongjun Sun and my mother Huizhen Zhang for their love and support.

Chapter 1: Introduction

1.1 The plant immune system

Plants are sessile and they are constantly exposed to various environmental stresses. Plants not only need to deal with abiotic stress, but also have to face the challenges from different pathogens including bacteria, fungi, oomycetes and viruses. During the process of plant-pathogen interaction, both plants and pathogens have developed strategies to gain advantages in the battle. Plants deploy a sophisticated immune system to protect themselves against pathogens. At the very front line, plants use waxy cuticles and cell walls as physical barriers to limit pathogen invasion (Hückelhoven, 2007; Reina-Pinto & Yephremov, 2009). Some pathogens made their way into plant tissue through wound sites or natural openings such as stomata, antimicrobial enzymes and chemicals are used to inhibit pathogen proliferation (Bednarek & Osbourn, 2009; Maeli Melotto et al., 2017). More importantly, plants have evolved a large number of immune receptors to recognize pathogens and trigger immune responses (Li et al., 2015; Zipfel, 2014). Pathogens secrete phytotoxins and effectors to dampen plant immunity (Möbius & Hertweck, 2009; Toruño et al., 2016). For example, the plant immune system can sense the presence of bacterial pathogens to trigger stomata closure, which limits entry of the bacteria. However, the bacterial pathogen *Pseudomonas syringae pv. tomato (Pto)* DC3000 secretes the phytotoxin coronatine (COR) to induce stomata reopening, which helps pathogen invasion (Melotto et al., 2006; Zeng & He, 2010). In response, plants have evolved additional immune receptors to detect various pathogen effectors and trigger defence responses (Li et al., 2015). Thus plants and pathogens are in a continuous co-evolutionary struggle for dominance.

1.2 Pattern-triggered immunity (PTI)

One class of plant immune receptor localized on the plasma membrane is named pattern recognition receptor (PRR). Receptor proteins in this class are responsible for recognition of conserved molecular features from pathogens/microbes collectively named as pathogen-associated molecular patterns (PAMPs) or microbe-associated molecular patterns (MAMPs) (Jones & Dangl, 2006). MAMPs are evolutionarily conserved and are usually important for microbial fitness. Plant PRRs fall into two large proteins families: the receptor-like kinase (RLK) and receptor-like protein (RLP) families (Liebrand et al., 2014; Monaghan & Zipfel, 2012). Both RLKs and RLPs bear an extracellular ligand-binding domain and a transmembrane motif. However, RLKs but not RLPs have a cytoplasmic kinase domain.

The well-studied PAMPs include flg22 (a 22-amino acid peptide derived from bacterial flagellin) (Felix et al., 1999), elf18 (a 18-amino acid peptide derived from elongation factor Tu) (Kunze et al., 2004), nlp20 (a 20-amino acid peptide derived from necrosis and ethylene-inducing peptide 1-like proteins) (Böhm et al., 2014; Oome et al., 2014), and chitin, an polysaccharide component from the fungal cell wall (Kumar & Klessig, 2003; Shibuya & Minami, 2001). They are recognized by the immune receptors FLAGELLIN SENSING 2 (FLS2) (Gomez-Gomez & Boller, 2000), EF-Tu RECEPTOR (EFR) (Zipfel et al., 2006), RECEPTOR LIKE PROTEIN 23 (RLP23) (Albert et al., 2015) and CHITIN ELICITOR RECEPTOR KINASE 1 (CERK1) (Miya et al., 2007), respectively. Recognition of MAMPs by their cognate PRRs initiates signal transduction from the apoplast into the cytosol and activates pattern-triggered immunity (PTI), which is critical to restrict pathogen colonization.

1.2.1 Perception of PAMPs by PRR complexes

Increasing evidence shows that PRRs recruit various interacting proteins and form complexes upon activation to transduce signals across the plasma membrane. One well-studied example is the recognition of flg22 by FLS2 (Gomez-Gomez & Boller, 2000) (Figure 1.1). The receptor FLS2 contains 28 LRRs in its N terminal extracellular domain, which directly bind flg22. Upon flg22 treatment, another RLK BRASSINOSTEROID-INSENSITIVE 1 (BRI1)- ASSOCIATED RECEPTOR KINASE 1 (BAK1) is rapidly recruited by FLS2 and is required for flg22-triggered signaling (Chinchilla et al., 2007; Schulze et al., 2010). Structural analysis further confirmed that BAK1 functions as a co-receptor of flg22. Heterodimerization of FLS2 and BAK1 leads to trans-phosphorylation of their kinase domains and activation of the PRR complex (Sun et al., 2013). A receptor-like cytoplasmic kinase (RLCK), BOTRYTIS-INDUCED KINASE 1 (BIK1), which associates with both FLS2 and BAK1 in the absence of flg22, was shown to be phosphorylated and released from the activated FLS2 complex upon flg22 perception (Lu et al., 2010). A homologue of BIK1, PBS like 1 (PBL1), was also shown to interact with FLS2 and required for FLS2-mediated immunity (Zhang et al., 2010).

The interaction of FLS2 and BAK1 induced by flg22 is subjected to extensive regulation by several accessory RLKs. BAK1-INTERACTING RLK2 (BIR2) and BIR3 were shown to bind BAK1 in the resting state to negatively regulate the FLS2-BAK1 complex formation (Halter et al., 2014; Imkampe et al., 2017). A study of 200 *Arabidopsis* LRR-RKs showed that BAK1 and APEX are two critical nodes in the LRR-RK interaction network (Smakowska-Luzan et al., 2018). APEX negatively regulates FLS2-BAK1 complex formation while another short LRR-RK identified in the study, FLS2-INTERACTING RECEPTOR (FIR), promotes the FLS2-BAK1 complex

formation (Smakowska-Luzan et al., 2018). Another LRR-RK NUCLEAR SHUTTLE PROTEIN-INTERACTING KINASE1 (NIK1), belonging to the LRR-II-RLK subfamily, as does BAK1, interacts with both BAK1 and FLS2 and negatively regulates the FL2-BAK1 complex formation (Li et al., 2019). It remains unclear how different accessory LRR-RKs are coordinated during elicitor perception and PTI activation.

A number of RLPs have also been shown to function as PRRs. Because RLPs lack a cytoplasmic kinase domain, they rely on associated RLKs to transduce signals. *Arabidopsis* SUPPRESSOR OF BIR1 1 (SOBIR1) was shown to function as an adaptor kinase in multiple LRR-RLP type PRRs complexes (Liebrand et al., 2014). For example, SOBIR1 is required for RLP23-mediated perception of nlp20 (Albert et al., 2015). RLP23 constitutively interacts with SOBIR1 and recruits BAK1 to form a tripartite receptor complex upon binding of nlp20 (Albert et al., 2015). In addition, SOBIR1 is found to be required for RLP1 (Jehle et al., 2013), RLP30 (Wang et al., 2008; Zhang et al., 2013) and RLP42-mediated immune signaling (Zhang et al., 2014).

1.2.2 Signalling downstream of PRR complexes

A number of cellular responses are activated upon perception of PAMPs, which includes calcium influx, reactive oxygen species (ROS) production, mitogen-activated protein kinase (MAPK) cascade activation, transcriptional reprogramming and physiological changes such as increased defence hormone ethylene and salicylic acid (SA) levels (Couto & Zipfel, 2016) (Figure 1.1). Some of these responses such as calcium influx, ROS production and MAPK activation can be detected within a few minutes, while others happen later (Couto & Zipfel, 2016). Together, these responses render enhanced resistance to pathogen infection.

The early responses after activation of PRR complexes contribute to transducing signals further

downstream. For example, Ca^{2+} serves as a secondary messenger in defence signalling. A recent study revealed that CYCLIC NUCLEOTIDE-GATED CHANNEL 2 (CNGC2) and CNGC4 form a Ca^{2+} channel required for calcium influx during PTI (Tian et al., 2019). The channel is phosphorylated and activated by BIK1 upon perception of flg22 (Tian et al., 2019). Ca^{2+} signalling has been shown to play an important role in promoting ROS production in PTI. It is also involved in regulating the biosynthesis of SA. The transcription factor CALMODULIN-BINDING PROTEIN 60-LIKE G (CBP60g) is a positive regulator of SA biosynthesis and CALMODULIN-BINDING TRANSCRIPTION ACTIVATOR 3 (CAMTA3) serves as a negative regulator of SA biosynthesis (Kim et al., 2019; Sun et al., 2019). The activities of both CBP60g and CAMTA3 are modulated by Ca^{2+} .

In *Arabidopsis*, apoplastic ROS production during PTI is mainly catalysed by the NADPH oxidase RESPIRATORY BURST OXIDASE HOMOLOG D (RBOHD) (Torres et al., 2002). RBOHD is a direct substrate of BIK1. Upon perception of PAMPs, RBOHD is rapidly phosphorylated by BIK1 and phosphorylation of RBOHD is essential for PAMP-induced ROS production and stomatal immunity (Kadota et al., 2014; Li et al., 2014). Phosphorylation of RBOHD by CALMODULIN-DOMAIN PROTEIN KINASES (CPKs) also stimulates its activity and promotes production of ROS during PTI (Boudsocq et al., 2010; Dubiella et al., 2013).

MAPK cascades are conserved signalling modules that transduce signals from upstream stimuli and amplify signals in various biological processes. More details about MAPK cascades will be introduced in section 1.7.

Activation of MAPKs during PTI stimulates production of ethylene, a key phytohormone that contributes to positive regulation of plant resistance to both bacterial and fungal pathogens. It was

shown that the ethylene biosynthesis rate limiting enzymes ACC SYNTHASE 2 (ACS2) and ACS6 are the substrates of MPK3 and MPK6, suggesting that ethylene biosynthesis is downstream of MAP kinases (Liu & Zhang, 2004).

Induction of a large number of defense-related genes can be detected a few hours after PAMP treatment. Examples of PAMP-induced genes include commonly used PTI marker genes such as *FLG22-INDUCED RECEPTOR-LIKE KINASE 1 (FRK1)* and *WRKY DNA-BINDING PROTEIN 29 (WRKY29)* (Asai et al., 2002).

Callose deposition and accumulation of SA are observed at a late stage of PTI (Boller & Felix, 2009). Callose deposition may help to strengthen plant cell wall and limit the invasion of pathogen (Piršelová & Matušíková, 2013). SA contributes to immunity by promoting the expression of a large number of defence-related genes (Zhang et al., 2010), many of which are used as defence marker genes, such as *Pathogenesis-Related (PR)* genes

1.2.3 Receptor-like cytoplasmic kinases (RLCKs) in PTI

Arabidopsis genome encodes 147 RLCKs that are divided into 17 subfamily based on the sequence homology (Shiu et al., 2004). Most RLCKs only have a Ser/Thr-specific cytoplasmic kinase domain. A number of RLCKs have been shown to physically associate with RLKs to transduce defence signals. They are activated by the PRR complexes during PTI. For example, BIK1 is phosphorylated by FLS2/BAK1 upon flg22 perception and then released from the complex to activate downstream signalling (Lu et al., 2010). As mentioned previously, BIK1 was shown to regulate calcium influx and ROS burst by directly phosphorylating the Ca²⁺ channels

CNGC2/CNGC4 and NADPH oxidase RBOHD, respectively. Interestingly, BIK1 was also observed in the nucleus and it directly interacts with multiple WRKY transcription factors to promote defence gene expression (Lal et al., 2018).

BIK1 belongs to the RLCK subfamily VII. Several members of the RLCK subfamily VII have been shown to play critical roles in PTI. Expression of the *P. syringae* effector AvrPphB, which cleaves BIK1, its close homologue PBL1 and other PBL proteins, greatly inhibits flg22-induced immune responses (Zhang et al., 2010). Both *bik1* and *pbl1* mutants are diminished in multiple PAMP-induced responses and show enhanced susceptibility towards *Pto* DC3000 *hrcC*, a bacterial strain that is deficient in Type-III secretion system and can only trigger PTI, suggesting that BIK1 and its homologues play indispensable roles in PTI (Zhang et al., 2010).

PATTERN-TRIGGERED IMMUNITY (PTI) COMPROMISED RECEPTOR-LIKE CYTOPLASMIC KINASE 1 (PCRK1) and PCRK2 are two redundant RLCKs that also function in PTI. The *pcrk1 pcrk2* double mutant was found to be more susceptible to virulent pathogens in a reverse genetic screen (Kong et al., 2016). It displays unaltered flg22-induced ROS production but reduced flg22-induced MAPK activation and defence gene expression (Kong et al., 2016). Co-immunoprecipitation experiments showed that both PCRK1 and PCRK2 interact with FLS2 and phosphorylation of both proteins can be observed after flg22 treatment (Kong et al., 2016). Plants lacking both PCRK1 and PCRK2 have reduced pathogen-induced SA accumulation and allow significantly more *Pto* DC3000 *hrcC* growth, suggesting that these two proteins play important roles in PTI (Kong et al., 2016). It was proposed that PCRK1 and PCRK2 are involved in transducing defence signal from FLS2 to activate downstream MAPKs.

Another RLCK, BR-SIGNALING KINASE1 (BSK1), was reported to interact with and

phosphorylate the N terminus of MITOGEN-ACTIVATED PROTEIN KINASE KINASE KINASE 5 (MAPKKK5) *in vitro* (Yan et al., 2018). BSK1 is the substrate of BR receptor BRASSINOSTEROID INSENSITIVE 1(BRI1) (Tang et al., 2008). The *bsk1* mutant shows enhanced susceptibility to virulent and avirulent pathogens (Shi et al., 2013). Interestingly, BSK1 can physically interact with FLS2 and is required for flg22-induced ROS production and *PR* gene expression (Shi et al., 2013). However, flg22-induced MAP kinase activation is not affected in the *bsk1* mutant (Shi et al., 2013). It remains unclear whether flg22-induced MAPK activation will be reduced when BSK1 and its homologues are mutated.

1.3 Effector-triggered susceptibility (ETS)

To overcome PTI responses, pathogens evolved effectors to interfere with different steps of PTI, causing effector-triggered susceptibility (ETS) (Jones & Dangl, 2006). Many bacterial pathogens use a needle-like structure called type III secretion system (T3SS) to inject effector proteins into plant cells (Galan & Collmer, 1999) (Figure 1.1). Most of the pathogen effectors target important components of PTI signalling to attenuate PTI responses. For example, the *Pseudomonas* effector AvrPto can directly bind FLS2 and possibly other PRRs to inhibit their kinase activity and suppress PTI (Xiang et al., 2008). The previously mentioned effector AvrPphB interacts with and triggers cleavage of BIK1 and its homologues (Zhang et al., 2010). Alternatively, some pathogen effectors prevent recognition by host plants to evade immune responses. The effector Ecp6 from the biotrophic fungus *Cladosporium fulvum* sequesters chitin oligosaccharides that are released from the cell walls of invading hyphae to prevent elicitation of host immunity in tomato (de Jonge et al., 2010). The homologue of Ecp6, Mg3LysM from *Mycosphaerella graminicola*, similarly helps

pathogens to evade chitin recognition in wheat (Lee et al., 2014).

Recently it was shown that effectors such as AvrE1 and HopM1 are critical for the formation of the aqueous environment in the apoplast, which is crucial for the growth of the bacteria (Xin et al., 2016). High humidity allows greater amount of *Pto* DC3000 growth and is associated with the common water soaking disease symptom. Expressing AvrE1 or HopM1 in wild type plants was able to trigger the water soaking phenotype (Xin et al., 2016). Deleting both AvrE1 and HopM1 from *Pto* DC3000 leads to reduced bacterial growth even with high levels of humidity, suggesting that AvrE1 and HopM1 contribute to pathogen virulence by triggering water soaking in the apoplast (Xin et al., 2016).

1.4 Effector-triggered immunity (ETI)

During the arms race between plants and pathogens, plants evolved resistance (R) proteins that can directly or indirectly recognize pathogen effectors and trigger a robust immune response called effector-triggered immunity (ETI) (Jones & Dangl, 2006). ETI is usually coupled with localized cell death known as hypersensitive response (HR), which is likely responsible for limiting the spread of biotrophic pathogens (Jones & Dangl, 2006).

Most plant R proteins are structurally similar to mammalian Nucleotide-Binding oligomerization Domain (NOD)-like receptors. They possess a variable N-terminal domain, a middle nucleotide binding (NB) domain and a C-terminal LRR domain, and are called nucleotide binding leucine-rich repeat receptors (NLRs) (Jacob et al., 2013; Li et al., 2015). There are two main types of typical plant NLR proteins based on the difference in their N-terminus. One group with a Toll-

interleukin receptor (TIR) domain is named TIR-NB-LRR protein or TNL. The other group has a coiled-coil (CC) domain and is named CC-NB-LRR protein or CNL (Jacob et al., 2013; Li et al., 2015).

1.4.1 Recognition of pathogen effectors by R proteins

Three models, namely the direct interaction model, the guard model and the decoy model, have been proposed for recognition of pathogen effectors by plant R proteins (van der Hoorn & Kamoun, 2008). In the direct interaction model, recognition of effectors is achieved by direct binding of R proteins to effectors (van der Hoorn & Kamoun, 2008). For example, *Arabidopsis* RECOGNITION OF PERONOSPORA PARASITICA 1 (RPP1), a TNL, directly interacts with *Hyaloperonospora arabidopsidis* effector ATR1 via its LRR domain and causes HR (Krasileva et al., 2010). Effector AvrRps4 directly interacts with *Arabidopsis* TNLs RESISTANT TO RALSTONIA SOLANACEARUM 1 (RRS1) and RRS1B separately (Saucet et al., 2015). Two pairs of linked TNLs RESISTANT TO P. SYRINGAE 4 (RPS4)-RRS1 and RPS4B-RRS1B independently confer recognition of AvrRps4 (Saucet et al., 2015). A recent study showed that AvrRps4 triggered RRS1 conformation change, releasing the inhibition of RPS4 by RRS1, which leads to activation of ETI (Guo et al., 2020) (Figure 1.1).

Most studied R proteins do not directly interact with pathogen effectors, but they can sense the modification of host targets caused by effectors and trigger ETI. When the effector targets a host protein with a function in immunity, the host protein is designated as a “guardee” in the guard model (van der Hoorn & Kamoun, 2008). For example, RESISTANCE TO P. SYRINGAE PV MACULICOLA 1 (RPM1) INTERACTING PROTEIN 4 (RIN4) is a negative regulator of PTI

and is guarded by two CNLs RPS2 and RPM1. *Pto* DC3000 effector AvrRpt2 cleaves RIN4 for degradation and AvrRpm1/AvrB targets RIN4 for phosphorylation, which are monitored by RPS2 and RPM1 respectively (Chung et al., 2011; Day et al., 2005; M. G. Kim et al., 2005). Modification of RIN4 by AvrRpt2 or AvrRpm1/AvrB leads to activation of ETI (Chung et al., 2011; Day et al., 2005) (Figure 1.1).

In the decoy model, the host proteins targeted by the pathogen effectors have no function in immunity in the absence of its cognate R proteins (Hoorn & Kamoun, 2008). As mentioned above, BIK1 and PBLs are targets of the effector protein AvrPphB, which functions as a cysteine protease to cleave these kinases (Zhang et al., 2010). The cleavage of another target of AvrPphB, PBS1, is monitored by the CNL RPS5 and triggers activation of ETI (Figure 1.1). While PBLs are positive regulators of PTI and cleavage of PBLs by AvrPphB inhibits PTI and benefits bacterial colonization in plants that lack RPS5, PBS1 does not play a role in PTI itself and functions as a “decoy” for these PBLs (Ade et al., 2007; Zhang et al., 2010). The use of guardee and decoys expands the recognition capacity of NLRs, allowing limited number of plant NLRs to recognize large number of effectors from different pathogens.

1.4.2 Autoimmune mutants with constitutive ETI responses

As mentioned earlier, ETI is normally initiated by recognition of pathogen effectors by corresponding R proteins and is usually coupled with HR. ETI is a robust defence response and often causes damage to host plants as well. In nature, ETI occurs only when both effectors from pathogen and the corresponding R proteins are present (Gassmann & Bhattacharjee, 2012). The cell death is limited to the infection sites to reduce the damage to the host plants.

However, when the guardee or some regulatory components of ETI is disrupted in mutant plants, ETI response becomes constitutively activated without the presence of pathogen effectors. In association with constitutive ETI response, autoimmune mutants usually have curly leaves and dwarf morphology, indicating a shift of resource from development to immunity. For example, *mekk1* is a seedling lethal mutant with highly elevated *PR* gene expression (Zhang et al., 2012). Mutations in the CNL protein SUMM2 revert the *mekk1* mutant back to wild type-like, indicating that dwarfism is caused by constitutive ETI response mediated by SUMM2 (Zhang et al., 2012). Another mutant *chs3-2D*, which carries a gain-of-function mutation within the TNL CHILLING SENSITIVE 3 (CHS3), also shows severe dwarfism and enhanced resistance to virulent pathogens (Bi et al., 2011). Blocking defence signalling downstream of CHS3 similarly block the dwarfism (Bi et al., 2011).

Since there is a clear correlation between the dwarfism and the level of constitutive defence responses in autoimmune mutants, plant size is often used as an initial indicator of defence responses in these mutants. A number of forward genetic screens have been successfully carried out using increased plant size as the primary phenotype to look for suppressors of autoimmune mutants, which were used to dissect the related immune signalling pathways (Gao et al., 2009; Li et al., 2011; Sun et al., 2019; Wersch et al., 2016).

1.5 Interplay between PTI and ETI

Figure 1.1 summarizes plant immune responses including PTI and ETI mentioned in previous paragraphs. PTI and ETI are two evolutionary intertwined immune responses with distinct

molecular requirement (Jones & Dangl, 2006). PTI occurs when conserved molecular patterns from pathogens meet with plasma membrane-localized PRRs, whereas ETI deploys R proteins to detect the presence of quickly evolving pathogen effectors that are used to subvert PTI and promote virulence. Although PRRs and R proteins serve to detect distinct components of pathogens and there are clear differences in timing and magnitude of defence between PTI and ETI, they share greatly overlapped immune output, including MAP kinase activation, production of ROS, increased accumulation of SA and induction of similar defence-related genes (Boller & Felix, 2009; Kanneganti et al., 2007). Recent studies revealed that PTI and ETI are not two completely separate immune responses and have interesting interactions. ETI primes the upregulation of *BAK1*, *BIK1*, *RBOHD*, *MPK3* and other PTI components (Ngou et al., 2020; Yuan et al., 2020). On the other hand, PTI activation of RBOHD is required for ROS production in ETI and ETI is compromised in *rboh* mutant plants (Ngou et al., 2020; Yuan et al., 2020).

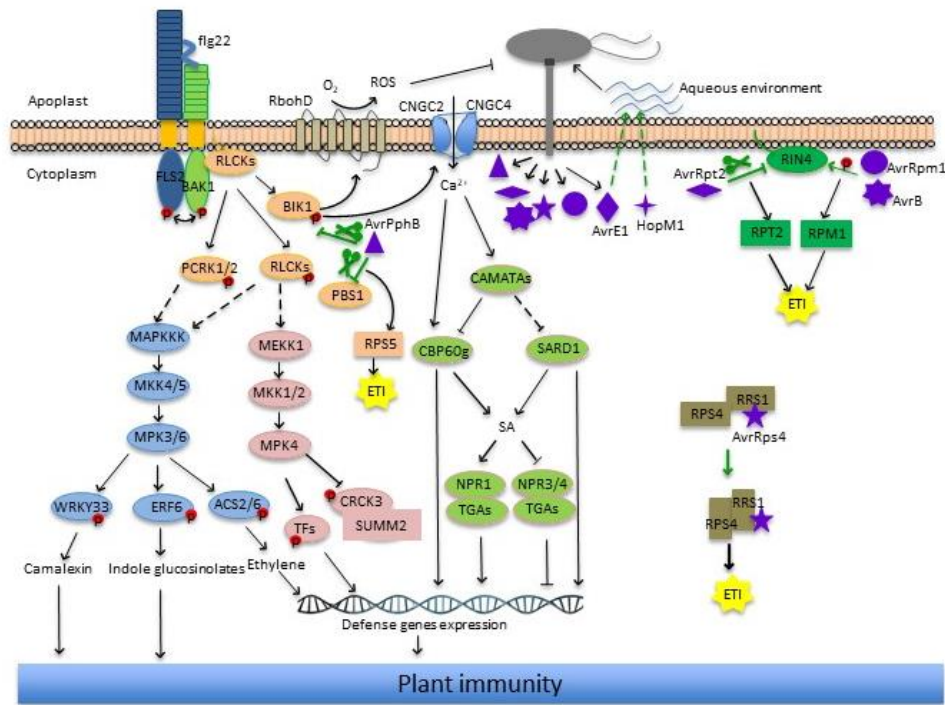


Figure 1.1 Overview of plant immune responses downstream of immune receptors.

Effectors are coloured in purple and effector-triggered modification or changes are shown in green lines. R proteins are represented by rectangle-shaped labels. ETI responses are represented by bright yellow stars. Dashed lines represent indirect actions or direct actions lacking evidence.

The main immune responses mentioned in the introduction part are listed as followed: 1) Perception of flg22 by FLS2 complex activates RLCKs. Activated BIK1 phosphorylates RbohD and CNGC2/CNGC4 to induced ROS production and Ca^{2+} influx separately. Activated PCRK1/PCRK2 and other RLCKs may contribute to MAPK activation. 2) Two MAPK cascades are activated. The MEKK1-MKK1/MKK2-MPK4 cascade negatively regulates SUMM2 mediated ETI and positively contributes to basal immunity. The MKK4/MKK5-MPK3/MPK6 module plays positive roles in immunity. MPK3/MPK6 substrates ACS2/ACS6, WRKY33 and ERF6 promote the biosynthesis of ethylene, camalexin and Indole glucosinolates separately. Ethylene induces defense gene expression and the other two chemicals contribute to immune responses. 3) Ca^{2+} is required for the function of CAMTA transcription factors and CBP60g. CAMTAs negatively regulate two redundant transcription factors SARD1 and CBP60g, which regulate defence gene expression in both SA-dependent and SA-independently manner. 4) *Pto* DC3000 uses a needle-

like type III secretion system to deliver effectors into host plant cell. AvrE1 and HopM1 trigger aqueous environment in the apoplast to promote pathogen growth. AvrPphB triggers cleavage of BIK1, paralogs of BIK, and PBS1. The cleavage of PBS1 leads to RPS5-activated ETI. Cleavage of RIN4 by AvrRpt2 and phosphorylation of RIN4 by AvrRpm1 and AvrB activate RPS2 and RPM1-dependent ETI separately. Effector AvrRps4 directly binds RRS1, changes its conformation and releases the inhibition of RPS4, leading to ETI responses.

1.6 Systemic acquired resistance (SAR)

Both PTI and ETI happen at local infection sites. It is long known that distal parts of plant also gain resistance after activation of local defence by the primary infection, which is called systemic acquired resistance (SAR) (Klessig et al., 2018). SAR can be induced by diverse pathogens and the resistance is broad-spectrum and can be long-lasting. Early studies showed that *PR* genes are strongly induced and there is dramatically increased accumulation of SA at local infection site during the induction of SAR (Klessig et al., 2018).

1.6.1 SA in SAR

Elevated SA accumulation is observed in both local and distal tissue after infection. ISOCHORISMATE SYNTHASE 1 (*ICS1*) is a key enzyme required for pathogen-induced SA biosynthesis in *Arabidopsis* (Wildermuth et al., 2001). In *ics1* mutants, pathogen-induced SA accumulation is blocked and both basal defense and SAR are greatly impaired. On the other hand, exogenous application of SA triggers induction of *PR* genes and resistance in plants. SAR DEFICIENT 1 (*SARD1*) and CBP60g are two redundant transcription factors that are responsible for pathogen induced *ICS1* expression (Zhang et al., 2010). Mutants with mutations in

NONEXPRESSOR OF PR GNENS 1 (NPR1) were isolated from forward genetic screens looking for SA-insensitive mutants (Cao et al., 1997; Ryals et al., 1997; Shah et al., 1997). *npr1* mutants are non-responsive to SA and its analogue INA and BTH, and are compromised in basal defense and SAR, suggesting NPR1 functions downstream of SA.

What the receptors of SA are has been a very interesting research question for several decades. In 2012, direct binding of SA to NPR1 was shown to lead to NPR1 conformation change, suggesting that NPR1 is an SA receptor (Wu et al., 2012). In 2018, SA was shown to bind and inhibit the transcriptional repression activities of NPR4 and its close paralog NPR3 to promote the expression of SA-responsive genes (Ding et al., 2018). Both NPR1 and NPR3/NPR4 interact with TGA transcription factors to carry out their function (Ding et al., 2018; Zhang et al., 1999, 2006). The current understanding on SA perception is that NPR1 and NPR3/4 are SA receptors with opposite roles in regulating transcription of defense related genes and they function in parallel in SA signaling (Figure 1.1).

1.6.2 Pipecolic acid (Pip) and N-hydroxypipicolic acid (NHP) in SAR

Besides SA, pipecolic acid (Pip) was also found to accumulate significantly at local infection site and systemic tissue after pathogen infection (Navarova et al., 2012). Exogenous application of Pip can also prime resistance in wild type plant (Navarova et al., 2012). Three enzymes required for proper establishment of SAR, AGD2-LIKE DEFENSE RESPONSE PROTEIN 1 (ALD1), SAR DEFICIENT 4 (SARD4) and FLAVIN-DEPENDENT MONOOXYGENASE 1 (FMO1), have recently been placed in the pipecolic acid (Pip) and N-hydroxypipicolic (NHP) biosynthesis pathway (Ding et al., 2016; Hartmann et al., 2018). ALD1 is an aminotransferase and SARD4

shows similarity to bacterial ornithine cyclodeaminase. The pip biosynthesis pathway was reconstituted with heterologously expressed ALD1 and SARD4 using L-lysine as the substrate (Ding et al., 2016). The biochemical process of pip biosynthesis involves transamination of L-lysine by ALD1 followed by reduction by SARD4 (Ding et al., 2016). FMO1 was shown to function as a pipecolate N-hydroxylase, catalyzing the biochemical conversion of pip to NHP (Hartmann et al., 2018). As *fmo1* mutant plants accumulate high levels of pip and still show a severe SAR deficiency, NHP but not Pip is considered the signal molecule involved in the establishment of SAR (Hartmann et al., 2018).

1.7 MAPK cascades

MAPK cascades are conserved signalling modules in eukaryotes. A MAPK cascade is composed of a MAP kinase kinase kinase (MAPKKK/MEKK), a MAP kinase kinase (MKK/MEK) and a MAPK/MPK (MAPK-Group, 2002). When upstream signal activates a MAPKKK, the MAPKKK gets phosphorylated, leading to sequential phosphorylations of the corresponding MAPKK, MAPK and then the MAPK substrate. The phosphorylated MAPK substrate then initiates the downstream responses.

MAPK cascades are involved in diverse biological processes such as cell division, stomatal development and plant defence against pathogens (Meng & Zhang, 2013). In *Arabidopsis*, there are about 60 predicted MAPKKKs, 10 MKKs and 20 MAPKs. The existence of a large number of MAPKKKs suggests that they might be required for transducing diverse upstream signals (MAPK-Group, 2002). However, for the majority of the predicted MAPKKKs, there is no biochemical evidence showing that they phosphorylate MKKs. Because of the limited numbers of MKKs and

MAPKs, some MKKs and MPKs are shared components in different MAPK cascades. One big question is how the specificity of MAPK cascade is maintained in plants. It has been shown that spatiotemporal availability of the upstream stimuli and MAPK substrates likely contributes to the specificity of MAPK cascades.

An example of how upstream stimuli determines MAPK specificity is the regulation of stomatal development and localized cell proliferation by the MAPK cascade YDA-MKK4/MKK5-MPK3/MPK6. The peptide ligand EPIDERMAL PATTERNING FACTOR 1 (EPF1) and EPF2, whose perception regulates stomatal development, are expressed specifically in a subset of stomatal lineage cells, defining the role of the downstream YDA-MKK4/MKK5-MPK3/MPK6 cascade in stomatal development (Jewaria et al., 2013). In contrast, EPIDERMAL PATTERNING FACTOR LIKE 4 (EPFL4) and EPFL6, which are perceived by receptors regulating cell division, have highest expression level in inflorescence stem, defining the role of the same MAPK cascade in inflorescence stem growth (Uchida & Tasaka, 2013).

Another example on how substrate availability helps to maintain MAPK specificity is that MPK3/MPK6 can regulate both ethylene biosynthesis and camalexin production (Han et al., 2010; Mao et al., 2011). The MPK3/MPK6 substrates ACS2/ACS6 required for ethylene biosynthesis are localized in cytoplasm while the MPK3/MPK6 substrate WRKY DNA-BINDING PROTEIN 33 (WRKY33) required for camalexin biosynthesis is localized in the nucleus (Han et al., 2010; Mao et al., 2011). The availability of these different substrates determines the output of the downstream responses.

1.7.1 MAPK cascades in plant immunity

As mentioned previously, MAPK cascades are activated upon PRR complex activation. In *Arabidopsis*, there are two MAPK cascades activated upon flg22 treatment. One is composed of MEKK1, MKK1/2 and MPK4, which plays a dual role in plant defence (Gao et al., 2008; Zhang et al., 2012) (Figure 1.1). The integrity of this MAPK cascade is monitored through the phosphorylation status of MPK4 substrate CRCK3 by the NLR protein SUMM2. *mekk1*, *mkk1/2*, *mpk4* knockout mutants all show dwarfism and elevated defence responses due to activation of SUMM2-mediated ETI (Zhang et al., 2012). Interestingly, when the knockout mutant *summ2-8* was crossed into *mekk1* and *mpk4* mutants, the double mutants reverted to wild-type size and show enhanced susceptibility towards virulent pathogens, suggesting that this MAPK cascade plays a positive role in basal defence (Zhang et al., 2012).

The other MAPK cascade is composed of (a) previously unknown MAPKKK(s), MKK4/MKK5 and MPK3/MPK6 (Asai et al., 2002) (Figure 1.1). The activated MPK3/MPK6 promote ethylene biosynthesis, camalexin biosynthesis and defence gene activation. MEKK1 was proposed as the MAPKKK upstream of the MKK4/MKK5-MPK3/MPK6 module, because a truncated version of MEKK1 protein can phosphorylate MKK5 *in vitro* (Asai et al., 2002). However, *mekk1* knockout mutant plants do not show any defect in flg22-induced MPK3/MPK6 phosphorylation compared with wild type plants (Ichimura et al., 2006; Suarez-Rodriguez et al., 2007). There are two possible explanations on the discrepancy between the biochemical and genetic data. One possibility is that there are MEKK1 homologues compensating for the loss of MEKK1 so that flg22-induced MPK3/MPK6 phosphorylation is not altered in the *mekk1* knockout mutant. Alternatively, MEKK1 is simply not the MAPKKK upstream of the MKK4/MKK5-MPK3/MPK6 module. The

truncated MEKK1 was able to phosphorylate MKK5 *in vitro* because the truncated protein lost its specificity.

The MKK4/MKK5-MPK3/MPK6 module plays important role in plant immunity. The chemical-genetically rescued *mpk3 mpk6* double mutant shows defective stomata immunity and enhanced susceptibility towards virulent and avirulent pathogens (Su et al., 2017; Su et al., 2018). Previously mentioned MPK3/MPK6 substrates such as ACS2/ACS6 and WRKY33 contribute separately to ethylene and camalexin biosynthesis to promote resistance against pathogens (Han et al., 2010; Liu & Zhang, 2004; Mao et al., 2011). It is reported that pathogen-induced MPK3/MPK6 activation rapidly alters the expression of photosynthesis-related genes to inhibit photosynthesis and ROS accumulation, which is required for proper establishment of ETI (Su et al., 2018).

1.7.2 MAPKKKs in plant immunity

As mentioned previously, plant MAPKKK family has larger number and more variety in protein primary sequence than the MKKs and MAPKs. The 60 *Arabidopsis* MAPKKKs are divided into two large groups based on sequence analysis: the MEKK-type MAPKKKs and Raf-like MAPKKKs (MAPK-Group, 2002). As shown in figure 1.2, there are 12 MEKKs in *Arabidopsis*, which can be further divided into four subgroups.

The first subgroup includes MEKK1 and its three paralogs, MEKK2, MEKK3 and MEKK4. Among them, MEKK1, MEKK2 and MEKK3 are encoded by three tandemly duplicated genes (Su et al., 2013). As previously mentioned, *mekk1* mutants exhibit constitutively activated SUMM2-mediated ETI response, resulting in extreme dwarfism and a seedling lethal phenotype

(Zhang et al., 2012). MEKK2 is the closest paralog of MEKK1. Interestingly, *mekk2* mutations revert the dwarfism of *mekk1* to wild type-like, suggesting that MEKK2 is required for SUMM2-mediated defense response in *mekk1* (Zhang et al., 2017). A recent study showed that MEKK2 inhibits phosphorylation of MPK4 and its homologues MPK11/MPK13 to promote SUMM2-mediated immunity (Nitta et al., 2020). In a separate study, overexpression of CRCK3 was found to cause cell death in a MEKK2 dependent manner and the kinase activity of MEKK2 is not required the cell death phenotype (Yang et al., 2020). It was proposed that MEKK2 functions as a scaffold between SUMM2 and CRCK3. Both the *mekk3* single mutant and *mekk1 mekk2 mekk3* triple mutant exhibit wild type-like morphology (Su et al., 2013). MEKK4 has an extended N terminal region that contains a TIR domain and a WRKY domain, suggesting that MEKK4 may have a role in plant defense (MAPK-Group, 2002).

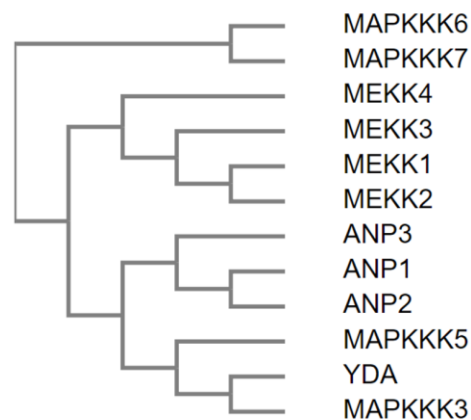


Figure 1.2 Phylogenetic tree of MEKK-type mitogen-activated protein kinase kinase kinases (MAPKKKs) in *Arabidopsis*.

The protein sequences of MEKK-type kinases downloaded from TAIR were used for alignment. Protein sequence alignment was performed at the Clustal Omega website (<https://www.ebi.ac.uk/Tools/msa/clustalo/>).

The second MAPKKK subgroup contains YDA, MAPKKK3 and MAPKKK5. As mentioned earlier, YDA forms a MAPK cascade with MKK4/MKK5 and MPK3/MPK6, regulating stomatal development and cell division (Bergmann et al., 2004). Silencing of a homolog of *MAPKKK3* in *Nicotiana benthamiana* (*N.b.*) was reported to have reduced HR induced by infiltration of *Agrobacteria* carrying AvrPto effector, whereas overexpression of MAPKKK3 homolog causes cell death in *N.b.* leaves, suggesting that MAPKKK3 plays a positive role in plant immunity (del Pozo et al., 2004).

The third subgroup comprises *ARABIDOPSIS* NPK1-RELATED PROTEIN KINASE 1 (ANP1), ANP2 and ANP3. They are homologs of the tobacco NPK1, a MAPKKK involved in cytokinesis (Nishihama et al., 1997). The three ANPs are highly expressed in tissue with active cell division and cytokinesis. Triple knockout of the three genes are lethal while *anp2/3* double mutant shows elevated basal *PR* gene expression and dwarfism (Lian et al., 2018). It was reported that ANP2/3 form a MAPK cascade with MKK6 and MPK4 to suppress immune response that is partially dependent on PHYTOALEXIN DEFICIENT 4 (PAD4), which is required for TNL mediated immunity, suggesting that there might be a TNL protein activated in *anp2/3* (Lian et al., 2018).

The last subgroup has two genes, MAPKKK6 and MAPKKK7, which contribute to cell division and pollen development. The double mutant *mapkkk6 mapkkk7* is lethal (Chaiwongsar et al., 2012). The *mapkkk7* single mutant was shown to have enhance basal resistance and enhanced flg22-induced MAPK activation, suggesting that it also functions as a negative regulator of plant immunity (Mithoe et al., 2016).

Gene expression profile analysis of *Arabidopsis* MEKK type MAPKKKs upon flg22, elf18, chitin and pep2 shows that more than one elicitor can highly induce MEKK1, MEKK3 and MAPKKK5

(Bi et al., 2018). Upon *Pto* DC3000 treatment, MEKK1, MAPKKK3 and MAPKKK5 are also significantly induced. The induction of these genes suggests that they may contribute to PTI and basal defense (Bi et al., 2018).

Although there are more members in the Raf-like MAPKKK group, very few Raf-like MAPKKK genes have been shown to function in plant immunity. Raf-like MAPKKKs CONSTITUTIVE TRIPLE RESPONSE 1 (CTR1) and ENHANCED DISEASE RESISTANCE 1 (EDR1) have been reported to be involved in ethylene signaling (Shakeel et al., 2015; Zhao et al., 2014). The loss-of-function mutant *ctr1* shows constitutive ethylene signaling. Co-purification experiments showed that CTR1 interacts with multiple ethylene receptors to negatively regulate ET signaling (Shakeel et al., 2015). EDR1 is another negative regulator of ethylene signaling (Frye et al., 2001). *edr1* mutant plants display enhanced resistance and cell death (Frye et al., 2001). Both genetic and biochemical data suggest that EDR1 protein negatively regulates the MKK4/MKK5-MPK3/MPK6 cascade to modulate defense response (Zhao et al., 2014). However, there is no evidence that CTR1 and EDR1 serve as *bona fide* MAPKKKs.

1.8 Thesis objective

My PhD thesis project mainly focuses on the MAP kinase module MKK4/MKK5-MPK3/MPK6 that is activated upon flg22 treatment. The thesis objectives are as follows:

1. Identify the previously unknown MAPKKK(s) upstream of MKK4/MKK5-MPK3/MPK6 module in plant immunity.
2. Characterize the function of the MAP kinase cascade that comprises the identified MAPKKK(s), MKK4/MKK5 and MPK3/MPK6 in plant immunity.

3. Identify components that transduce signal from FLS2 receptor complex to the identified MAPKKK(s).

Chapter 2: Method and Materials

2.1 Plant materials and mutant characterization

Plants were grown at 23 °C under 16 h light/8 h dark (long day) or 12 h light/12 h dark (short day) regime. *mapkkk3-1* (SALK_203147), *mapkkk5-1* (SAIL_1219_E11), *mpk3-1* (SALK_151594) and *mpk6-3* (SALK_127507) were obtained from the *Arabidopsis* Biological Resource Centre. Homozygous plants for *mapkkk3-1*, *mapkkk5-1*, *mpk3-1* and *mpk6-3* were identified using gene-specific primers (Table 2.1). The *mapkkk3-1 mapkkk5-1* double mutant was isolated from the F2 progeny of a cross between *mapkkk3-1* and *mapkkk5-1*. *mapkkk3-1 mapkkk5-1 mpk3-1* triple mutant was identified from F2 progeny of a cross between *mapkkk3-1 mapkkk5-1* and *mpk3-1*. *mapkkk3-1 mapkkk5-1mpk6-3* triple mutant was identified from F2 progeny of a cross between *mapkkk3-1 mapkkk5-1* and *mpk6-3*. Mutations in *MKK4* and *MKK5* were separately introduced into *mapkkk3-1 mapkkk5-1* double mutant using CRISPR-Cas9 gene editing tool to generate CRISPR alleles of *mapkkk3-1 mapkkk5-1 mkk4* and *mapkkk3-1 mapkkk5-1 mkk5*. *MKK4* was silenced in *mapkkk3-1 mapkkk5-1 mkk5* using artificial microRNA to generate *mapkkk3-1 mapkkk5-1 mkk5 amiMKK4*. *mekk1-1* and *chs3-2D* were described previously (D. Bi, Johnson, Zhu, et al., 2011; Z Zhang et al., 2012). The *mapkkk3-1 mapkkk5-1 mekk1-1^{+/-}* was isolated from the F2 progeny of a cross between *mapkkk3-1 mapkkk5-1* and *mekk1-1^{+/-}* and the *mapkkk3-1 mapkkk5-1 mekk1-1* triple mutant was isolated from the progeny of *mapkkk3-1 mapkkk5-1 mekk1-1^{+/-}*. The *mapkkk3-1 mapkkk5-1 chs3-2D^{+/-}* was isolated from the F2 progeny of a cross between *mapkkk3-1 mapkkk5-1* and *chs3-2D* and the *mapkkk3-1 mapkkk5-1 chs3-2D^{+/-}* triple mutant was isolated from the progeny of *mapkkk3-1 mapkkk5-1 chs3-2D^{+/-}*.

2.2 Construction of plasmids

For transgene complementation, a *MAPKKK3* genomic fragment containing its own promoter and coding region was amplified using primers MAPKKK3gDNA-F and MAPKKK3gDNA-R. A *MAPKKK5* genomic fragment containing its promoter and coding region was amplified using primers MAPKKK5gDNA-F and MAPKKK5gDNA-R. The DNA fragments were cloned into pCAMBIA1305-3xFLAG.

To generate the *MAPKKK3*^{K243M} and *MAPKKK5*^{K375M} mutant plasmids for use in the BiFC assay, *MAPKKK3* and *MAPKKK5* genomic coding sequences were amplified using primers MAPKKK3cds-F and MAPKKK3gDNA-R or primers MAPKKK5cds-F and MAPKKK5gDNA-R, and cloned into pUC19 to obtain pUC19-MAPKKK3 and pUC19-MAPKKK5. The mutation sites were introduced by overlapping PCR using primers MAPKKK3K243M-F, MAPKKK3K243M-R, MAPKKK3-intronF, and MAPKKK3-exonR for *MAPKKK3*^{K243M} or primers MAPKKK5K375M-F, MAPKKK5K375M-R, MAPKKK5-junctionF, and MAPKKK5-exonR for *MAPKKK5*^{K375M}. The resulting PCR fragments carrying the mutations were digested with restriction enzymes *NheI* and *AflIII* for the *MAPKKK3*^{K243M} fragment or *XhoI* and *BstEII* for the *MAPKKK5*^{K375M} fragment and used to replace the wild type fragments in pUC19-MAPKKK3 or pUC19-MAPKKK5 to obtain pUC19-MAPKKK3^{K243M} and pUC19-MAPKKK5^{K375M}. The MKK4 and MKK5 coding sequences were amplified by PCR using primers MKK4-SpeI-KpnI-F and MKK4-XhoI-R or primers MKK5-SpeI-KpnI-F and MKK5-XhoI-R, and cloned into vector pUC19-YNE (Walter et al., 2004) for BiFC assays.

For expression of recombinant proteins used in the kinase assay, the plasmid for 6×His-MBP-MAPKKK3 was generated by amplifying the full-length MAPKKK3 cDNA using the MAPKKK3-SfiI-F and R primers and inserted into the pLou3 vector. The plasmid for 6×His-MBP-MAPKKK3^{K243M} was generated by amplifying the previous MAPKKK3^{K243M} fragment using the MAPKKK3-SfiI-F and R primers and inserted into the pLou3 vector. The plasmid for 6×His-MBP-MAPKKK3ΔN was generated by amplifying the full-length MAPKKK3 cDNA using the M3KA-KD-SfiI-F and MAPKKK3-SfiI-R primers and inserted into the pLou3 vector. The plasmid for 6×His-MBP-MAPKKK3ΔC were generated by amplifying the full-length MAPKKK3 cDNA using the MAPKKK3-SfiI-F and MAPKKK3-Cdel2-SfiI-R primers and inserted into the pLou3 vector. The plasmid for 6×His-MKK5 was created by inserting the full-length MKK5 fragment amplified by MKK5-Nde1Kpn1-NF and MKK5-BamHIXho1-NR and using the KpnI and XhoI restriction enzyme sites to insert it into a modified pET15b vector. The mutations in the MKK5EE plasmid were introduced using primers MKK5EE-F, MKK5EE-R, MKK5-Nde1kpn1-NF and MKK5-BamHIXho1-NR. The plasmid for MPK6-6×His was generated by amplifying the full length MPK6 cDNA using MPK6-NdeI-F and MPK6-Sall-R and inserting it into pET21a.

For the Co-immunoprecipitation and biotinylation assays between PCRK2 and MAPKKK3/MAPKKK5, the PCRK2 cDNA was amplified using 616B-KpnI-F and 616B-speI-R. The resulting fragment was digested with KpnI and SpeI and inserted into a modified pBasta-35S-2HA-TurboID vector.

2.3 Analysis of MAPK activation

To examine the phosphorylated MAP kinases, 12-day-old seedlings grown on half-strength MS medium were treated with 100 nM of different elicitors (flg22, efl18, nlp20, or pep23) or 20 µg/ml of chitin containing 0.01% silwet L-77. Untreated and treated tissue samples were ground and denatured by boiling in 2× SDS loading buffer. The protein samples were separated by SDS-PAGE and analyzed by western blot using the α-p44/42-ERK antibody (Cell Signaling Technology, #9102). The same samples were also analyzed by immunoblot using a-AtMPK3 (Sigma, M8318) and a-AtMPK6 (Sigma, A7104) antibodies to detect the MPK3 and MPK6 protein levels. Loading consistency was examined by staining the membrane with Ponceau S. The intensity of relevant protein bands was measured using ImageJ (<http://imagej.nih.gov>).

2.4 Gene expression analysis

For flg22-induced FRK1 and WRKY29 expression analysis, seedlings from 12-day-old seedlings grown on half-strength MS medium treated with 100 nM of flg22 were collected. For *Pto* DC3000 *AvrRpt2*-induced *ALD1* and *FMO1* expression analysis, two fully extended leaves of each four-week-old plant were infiltrated with *Pto* DC3000 *AvrRpt2* ($OD_{600} = 0.025$) and leaf samples were collected 24 h after infiltration. For *PR* gene expression, seedlings from 12-day-old seedlings grown on half-strength MS medium were collected. RNA was extracted using the EZ-10 Spin Column Plant RNA mini-preps kit (Bio Basic Inc.) The RNA was reverse transcribed using EasyScript (Applied Biological Materials, Inc.) to obtain the complementary DNA for subsequent quantitative PCR analysis. Quantitative PCR was conducted on the cDNA using the SYBR Premix Ex TaqII kit (Takara) with primers specific to *FRK1*, *WRKY29*, *ALD1*, *FMO1*, *PR1*, *PR2* and *ACTIN1* (Table 2.1).

Table 2.1 Primers used in this study.

cloning primers	
MAPKKK3-Cdel2-sfiI-R	acgcccGGCCCATGAGGCCcctaTAGAAAAGGGTGTTCCTAGAA
MAPKKK3cds-F	TCGGGGTACCATGCCTACTTGGTGGGGAAG
MAPKKK3-exonR	GTACTGTATTTCTGTCATGT
MAPKKK3gDNA-F	TCGGGGTACCtagacacgtggcagcagac
MAPKKK3gDNA-R	GCTGCGGTCGACCACCAGTCTTGATCTCAATG
MAPKKK3-intronF	Ggtaacttcactgcaatc
MAPKKK3K243M-F	GGAAAATGTGTGCTATTATGGAGGTCAAGGTCATTTCTGA
MAPKKK3K243M-R	GAAATGACCTTGACCTCCATAATAGCACACATTTCCCTT
MAPKKK3-KD-SfiI-F	GGAAAATGTGTGCTATTATGGAGGTCAAGGTCATTTCTGA
MAPKKK3-SfiI-F	CGCGGATCCGGCCGTCAAGGCCAATGCCTACTTGGTGGGGAAG
MAPKKK3-SfiI-R	CGCGGATCCGGCCCATGAGGCCCTACACCAGTCTTGATCTCAA
MAPKKK5cds-F	TCGGGGTACCATGCGTTGGCTTCCGCAAAT
MAPKKK5-exonR	TCGCTACCAAATACTGCACA
MAPKKK5gDNA-F	TCGGGGTACCtggactagctgatagcctg
MAPKKK5gDNA-R	GCTGCGGTCGACAAGGTGATCTGAAGTGACGC
MAPKKK5-junctionF	tgtgtaatcagCGTCAATGG
MAPKKK5K375M-F	TGGAGCATTGTGTGCGATGATGGAAGTTGAGCTATTTCTG
MAPKKK5K375M-R	CAGGAAATAGCTCAACTTCCATCATCGCACACAATGCTCCA
MKK4-SpeI-KpnI-F	cggactagtgtaccATGAGACCGATTCAATCGCC
MKK4-XhoI-R	ccgctcgagTGTGGTTGGAGAAGAAGACG
MKK5-BamHIXhoI-NR	acgcGGATCCtcaCTCGAGTGTGGTTGGAGAAGAAGAC
MKK5-NdeI kpn1-NF	GGGAATTCCATATGGGTACCATGAGACCGATTCAATCGC
MKK5-EE-F	TCTTGGCACAagaAATGGATCCTTGTAATgaATCTGTTGGTAC
MKK5-EE-R	GTACCAACAGATtcATTACAAGGATCCATTtcTTGTGCCAAGA
MKK5-SpeI-KpnI-F	cggactagtgtaccATGAAACCGATTCAATCTCC
MKK5-XhoI-R	ccgctcgagAGAGGCAGAAGGAAGAGGAC
PCRK2-KpnI-F	ccgggtaccATGAAATGCTTCTTATTCCCTCT

PCRK2-spe1-R	AAAGAATGTGAGAGCTTGTACTAGTAGGCCTAGA
T-DNA primers	
MPK3-B1	CCGTATGTTGGATTGAGTGCTA
MPK3-F1	TGCGCTTATTGACAGAGgtaaa
MPK6-B1	GAAGGTGGGCTATCATAACA
MPK6-F1	CACTCACCCCAAAATTACAAAAA
MAPKKK3-salk203147-F	Ggttcgctttttccccttta
MAPKKK3-salk203147-R	Tgaaggctttgctacaacca
MAPKKK5-SAIL1219E11F	CTTCCGCAAATCTCGTTCTC
MAPKKK5-SAIL1219E11R	TGGGCTTCTGATCTGTTTCC
Real-time qPCR primers	
WRKY29-RT-NF	GGATCTCCATACCCAAGGAGT
WRKY29-RT-NR	ATCAGCGGATGGGATCATAG
ALD1-RT-NF	TGCTAGAGAGGTTCGCGATTG
ALD1-RT-NR	CGACCGTATCTCCTTAAGGC
FMO1-RT-NF	TGCCTTTATACAGGGGAACA
FMO1-RT-NR	TGGAAATGCAATGACGTTTG
FRK1-RT-NF	TTAGATGCAGCGCAAGGACT
FRK1-RT-NR	CGAATAGTACTCGGGGTCAA
PR1 F-2	Aggcaactgcagactcatac
PR1 R-2	Ttgttacacctcactttggc
PR2-A	Gcttccttttcaaccacacagc
PR2-B	Cggtgatgtaccggaatctgac
ACT1-F	Cgatgaagctcaatccaacga
ACT1-R	Cagagtcgagcacaataccg

2.5 Pathogen infection assay

For the disease resistance assay, two fully extended leaves of each four-week-old plant grown in short-day condition were infiltrated with *Pto* DC3000 at a dose of $OD_{600} = 0.0002$. Samples were collected at 0 and 3 d after infiltration. For the *Pto* DC3000 *hrcC*⁻ spray infection assay, two fully extended leaves of each plant were spray-inoculated with the bacteria at a dose of $OD_{600} =$

0.2. The inoculated plants were subsequently covered with a clear lid for 1 d, and samples were taken 3 d post inoculation. For *Pto* DC3000 *AvrRpt2*, *Pto* DC3000 *AvrRps4* and *Pto* DC3000 *AvrPphB* infection assay, two fully extended leaves of each plant were infiltrated with the bacteria at a dose of $OD_{600} = 0.0005$. Samples were collected at 0 and 3 d after infiltration. For *Pto* DC3000 *AvrRpt2*-induced SAR, three local leaves of each four-week-old plant grown in short-day condition were infiltrated with *Pto* DC3000 *AvrRpt2* at a dose of $OD_{600} = 0.001$. 10mM $MgCl_2$ was infiltrated as mock treatment. Two systemic leaves were infiltrated with *Pma* ES 4326 at a dose of $OD_{600} = 0.001$. Systemic samples were collected 3 d after infiltration. One leaf disk was punched from each infected leaf, and two leaf disks from each plant were collected as one sample. The samples were ground, diluted serially in 10 mM $MgCl_2$, and plated on lysogeny broth (LB) agar plates with proper antibiotics. After incubation at 28 °C for 36 h, bacterial colonies were counted from selected dilutions and the colony numbers were used to calculate colony forming units (CFU).

2.6 Measurement of Oxidative Burst

Leaf strips with a size of approximately 4 × 5 mm from four-week-old plants grown under short-day conditions were placed in a 96-well plate, with each well containing 200 mL water. After incubation at room temperature for about 12 h, the liquid was removed, and 180 mL elicitor solution containing 20 mM luminol, 10 mg/mL horseradish peroxidase, and 1 mM flg22 were added to each sample. Luminescence was recorded using a Synergy 2 microplate luminometer (BioTek). This is modified from a previous protocol (Liu et al., 2013).

2.7 Ion leakage measurement

For ion leakage measurement, two fully extended leaves of each four-week-old plant grown in short-day condition were infiltrated with *Pto* DC3000 *AvrRpt2* at a dose of $OD_{600} = 0.025$. Each sample contains 8 leaves from 4 plants and each genotype contains 6 samples. Samples were collected in 15 ml 10 mM $MgCl_2$ buffer and shaken at 220 rpm for 30 min before initial measurement by conductivity meter (Model 2052; Amber Science, San Diego, CA, USA). Samples were then boiled for 30 min and cooled down to measure the maximum conductivity value.

For one-time-point ion leakage measurement, infiltrated leaves were collected 16 h post inoculation for T16h conductivity values. The ratio of cell death was calculated using the T16h conductivity value divided by the maximum conductivity value. For ion leakage measurement over time, infiltrated leaves were collected right after infiltration. Conductivity values at different time points were measured until 24-26 h post inoculation. The ratio of cell death at time n was calculated as $(T_n \text{ conductivity value} - T_0 \text{ conductivity value}) / (\text{maximum conductivity value} - T_0 \text{ conductivity value})$.

2.8 Recombinant protein expression and purification

For protein expression, the constructs were transformed into the *E. coli* BL21 strain. The bacteria were cultured in LB media containing 100 $\mu\text{g/ml}$ Ampicillin and 34 $\mu\text{g/ml}$ chloramphenicol to an OD_{600} of 0.4 at 37°C and then switch to a lower temperature. One h after switching, IPTG was added to a final concentration of 0.4 mM to induce protein expression. Bacteria expressing 6×His-MBP-MAPKKK3, 6×His-MBP-MAPKKK3^{K243M} and 6×His-MBP-MAPKKK3 Δ C were incubated with IPTG at 28 °C for 2 h. Bacteria expressing 6×His-MBP-MAPKKK3 Δ N were

incubated with IPTG at 28 °C for 1 h. Bacteria expressing 6×His-MKK5, 6×His-MKK5EE and MPK6-6×His were incubated with IPTG at 16 °C for 16 h. The bacteria were collected by centrifugation and stored at -80 °C until use.

The recombinant proteins were purified following a previous procedure. The bacteria were resuspended in lysis buffer (50 mM tris-HCl pH 7.4, 500 mM NaCl, 10% glycerol, 20 mM imidazole, 0.1% triton X-100 and 1 mM PMSF) and lysed by sonication. After spinning at 15000 g for 30 min at 4 °C, the clear supernatant was applied to a Ni-NTA column and then the column was washed three times with 10 ml of lysis buffer supplemented with imidazole (20, 30 and 40 mM). Proteins were eluted by adding lysis buffer containing 250 mM of imidazole. The eluted proteins were dialyzed three times (20 mM tris-HCl pH 7.4, 10 mM MgCl₂, 100 mM NaCl, 10 % glycerol, 0.05 % triton X-100, 0.2 mM DTT and 1 mM PMSF) at 4 °C. The protein after dialysis was aliquoted and stored at -80 °C until use.

2.9 *In vitro* kinase assay

Purified recombinant proteins and ATP were diluted in kinase buffer (50 mM HEPES 7.4, 10 mM MgCl₂, 10 mM MnCl₂, 1 mM DTT, 1 mM PMSF, and 1 mM protease inhibitor) on ice. 0.02 µg 6×His-MBP-MAPKKK3 /MAPKKK3 mutant version protein, 0.01 µg 6×His-MKK5, 0.4 µg MPK6-6×His and 3 µl of 1mM ATP were sequentially added into each kinase reaction to reach a final volume of 30 µl. Reaction tubes were gently mixed, spun down and incubated at 30 °C for 30 min. The reactions were ended by boiling in 2× SDS loading buffer for 10 min. The samples were separated by SDS-PAGE and MPK6 phosphorylation was analyzed by western blot using the α-p44/42-ERK antibody (Cell Signaling Technology, #9102).

2.10 Bimolecular fluorescence complementation assay

Arabidopsis mesophyll protoplasts were isolated as previously reported (F.-H. Wu et al., 2009). The constructs for expressing MAPKKK3^{K243M}-YFPC, MKK4-YFPN, MKK5-YFPN, YFPC, and YFPN were purified using a plasmid large prep kit (Promega) and co-transfected into protoplasts through PEG-mediated transformation. After incubation at RT for 12–16 h, the transfected cells were examined using a Nikon ECLIPSE 80i confocal microscope.

2.11 Co-immunoprecipitation and biotinylation assay

For co-immunoprecipitation of MKK4/MKK5 by MAPKKK3/MAPKKK5, the mutant DNA fragments for MAPKKK3 and MAPKKK5 were subcloned into modified vector the pCAMBIA1300-35S-3FLAG, and MKK4 and MKK5 coding sequences were subcloned into modified vector the pCAMBIA1300-35S-3HA. MKK4-3HA or MKK5-3HA was co-expressed with MAPKKK3^{K243M}-3FLAG or MAPKKK5^{K375M}-3FLAG through *Agrobacterium*-mediated transient expression in *Nicotiana benthamiana* (*N.b.*) leaves. Forty-eight hour after inoculation, leaf tissue was collected and frozen in liquid nitrogen. Co-immunoprecipitation assay was performed as described before (Zhang et al., 2012). Western blot analysis was carried out with anti-HA (Roche, Cat# 11867423001) or anti-FLAG (Sigma, Cat# F3165) antibodies.

For co-immunoprecipitation of PCRK2 by MAPKKK3/MAPKKK5 and biotinylation assay, PCRK2 coding sequences were subcloned into modified vector pBasta-2HA-TurboID. PCRK2-2HA-TurboID was co-expressed with MAPKKK3^{K243M}-3FLAG or MAPKKK5^{K375M}-3FLAG through *Agrobacterium*-mediated transient expression in *N. b.* leaves. Forty-eight h after inoculation, leaf tissue was collected and frozen in liquid nitrogen. Co-immunoprecipitation assay was performed as described before (Z Zhang et al., 2012). Western blot analysis was

carried out with anti-HA (Roche, Cat# 11867423001), anti-FLAG (Sigma, Cat# F3165) antibodies and Streptavidin-HRP (Abcam, Cat# ab7403).

2.12 Statistical analysis

Error bars in figures represent standard deviations. Statistical comparison among different samples was performed by Student's t-test, one-way ANOVA with Tukey HSD test

(http://astatsa.com/OneWay_Anova_with_TukeyHSD/) or two-way ANOVA

(<https://scistatcalc.blogspot.com/2013/11/two-factor-anova-test-calculator.html#>). The P-values of statistical comparison were provided in figure legends. Stars (*) are used to show statistically significant differences between two samples. For comparisons involved in more than two samples, different letters (a, b, c, etc.) are used to mark the samples with statistically significant differences, whereas the same letter is used to label the samples with no statistical difference.

“ab” is used to label samples with no statistical difference to two statistically different samples marked with “a” or “b”.

Chapter 3: Results

3.1 flg22-induced activation of MPK3 and MPK6 is compromised in the *mapkkk3 mapkkk5* double mutant.

As mentioned earlier, the MAPKKK upstream of MKK4/MKK5-MPK3/MPK6 in the flg22-induced MAPK cascade was unknown. Despite that truncated MEKK1 is able to phosphorylate MKK5 *in vitro*, the *mekk1* single mutant doesn't show a reduction in flg22-induced MPK3 and MPK6 phosphorylation, suggesting that MEKK1 is likely not the MAPKKK responsible for this phosphorylation (Ichimura et al., 2006; Suarez-Rodriguez et al., 2007). To search for the MAPKKK responsible for flg22-induced MPK3 and MPK6 activation, we examined the phylogenetic tree of *Arabidopsis* MAPKKKs. We focused on the MEKK-type MAPKKKs because almost all MAPKKKs known to function in MAPK cascades belong to this type.

The *Arabidopsis* genome contains 12 MEKK-type MAPKKKs that can be divided into four groups. Besides the group containing MEKK1, there are three other groups. One group includes ANP1, ANP2 and ANP3. While the triple mutant is lethal, the double mutant *anp2 anp3* shows elevated basal immunity (Lian et al., 2018). Another group includes MAPKKK6 and MAPKKK7. Similarly, the double mutant is lethal and *mapkkk7* shows enhanced basal immunity and flg22-induced defense responses (Chaiwongsar et al., 2012; Mithoe et al., 2016). The last group includes MAPKKK3, MAPKKK5 and YDA. It is known that YDA forms a MAPK cascade with MKK4/MKK5-MPK3/MPK6 regulating stomatal development (Bergmann et al., 2004). However, the biological functions of MAPKKK3 and MAPKKK5 are unknown. Both *MAPKKK3* and *MAPKKK5* were identified as candidate targets of SARD1, a master

transcription factor for plant immunity, in a chromatin immunoprecipitation-sequencing (ChIPseq) study, implying that they may be involved in regulating plant defense responses.

To test whether MAPKKK3 and MAPKKK5 regulate flg22-induced MPK3/MPK6 phosphorylation, we obtained the *mapkkk3-1* (*mapkkk3*) and *mapkkk5-1* (*mapkkk5*) mutants from *Arabidopsis* Biological Resource Center (ABRC) and generated the *mapkkk3-1 mapkkk5-1* (*mapkkk3 mapkkk5*) double mutant by crossing the two single mutants. These mutants were subsequently tested for MAPK activation induced by flg22 treatment.

Previously it was reported that activation of MPK3 and MPK6 in response to flg22 is much stronger in *mapkkk5* mutant plants (Yamada et al., 2016). However, no clear change in flg22-induced MAPK activation was observed in the *mapkkk3* and *mapkkk5* single mutants under our experimental condition (Figure 3.1A). Interestingly, activation of MPK3 and MPK6 following flg22 treatment is clearly reduced in the *mapkkk3 mapkkk5* double mutant compared to that in the wild type (WT) and the single mutants (Figure 3.1A). The amount of phosphorylated MPK3 and MPK6 in flg22-treated *mapkkk3 mapkkk5* plants is less than half of those in the wild type plants (Figure 3.1B). Consistent with the reduced MAPK activation, flg22-induced *FRK1* and *WRKY29* expression is also reduced in the double mutant (Figure 3.1C and D). However, flg22-induced ROS production is not affected in the *mapkkk3 mapkkk5* plants (Figure 3.2).

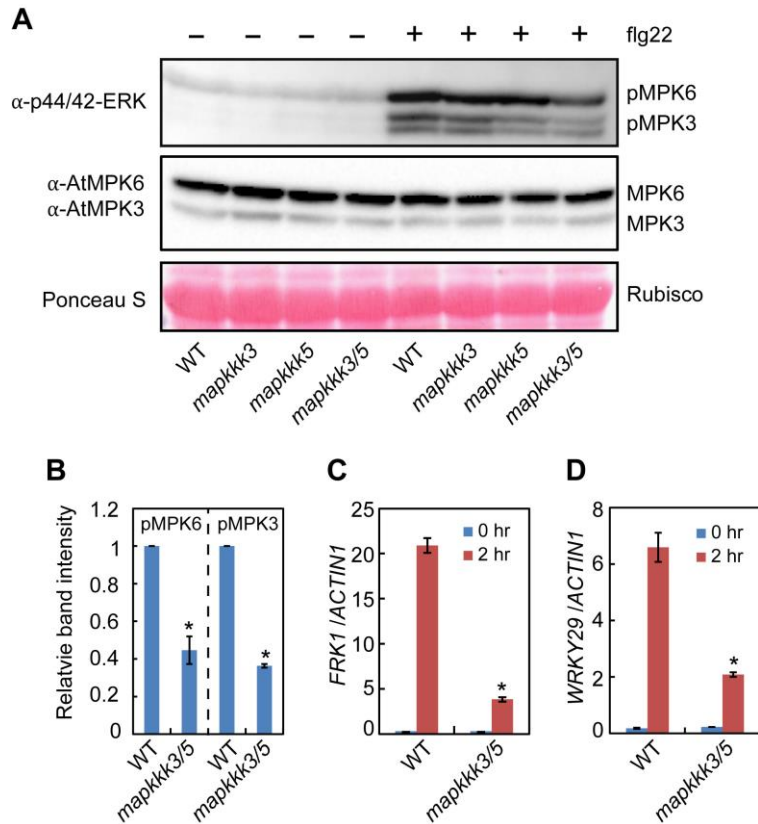


Figure 3.1 flg22-induced activation of MPK3 and MPK6 are compromised in the *mapkkk3 mapkkk5* double mutant.

(A) flg22-induced MAP kinase activation in wild type (WT), *mapkkk3*, *mapkkk5* and *mapkkk3 mapkkk5* (*mapkkk3/5*). Samples were collected 10 min after treatment with 100 nM flg22. Activated MAPKs were detected by immunoblots using α -p44/42-ERK antibody. MPK3 and MPK6 protein levels in the same samples were detected using the α -AtMPK3 and α -AtMPK6 antibodies. Equal loading is indicated by the Ponceau S staining of Rubisco.

(B) Quantification of the relative intensity of the pMPK6 and pMPK3 bands in WT and *mapkkk3/5* after flg22 treatment. The relative intensity of pMPK6 and pMPK3 bands in WT was set was 1. Significant difference compared with WT: *P < 0.01 (Student's t-test). Error bars represent means \pm s.d. from three independent experiments.

(C-D) Quantitative RT-PCR analysis of flg22-induced *FRK1* (C) and *WRKY29* (D) expression in WT and *mapkkk3/5*. Samples were collected at 0 and 2 h after treatment with 100 nM flg22. Values were normalized to the level of *ACTIN1*. Error bars represent means \pm s.d. (n = 3). Significant difference compared with WT: *P < 0.01 (Student's t-test).

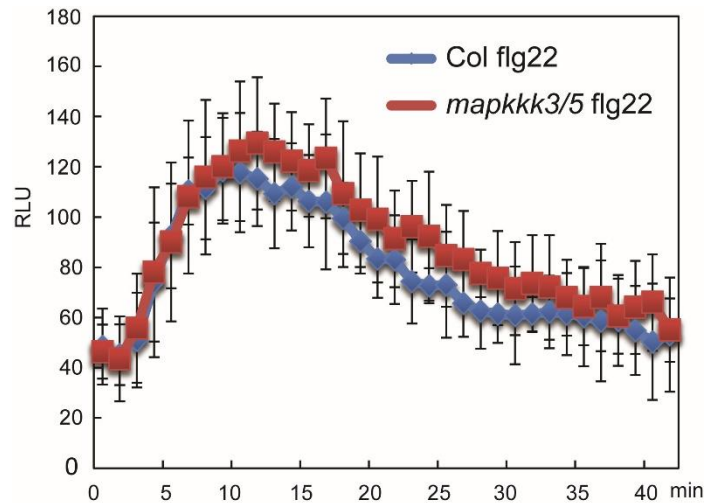


Figure 3.2 ROS burst triggered by flg22 is not affected in *mapkkk3 mapkkk5*.

Leaf slices of four-week-old plants were treated with 1 μ M of flg22. ROS was measured using the luminol dependent assay. Error bars represent standard deviations from averages of eight samples. Experiments were repeated twice with similar results.

To confirm that the observed reduction of flg22-induced MPK3/MPK6 phosphorylation in the double mutant is indeed caused by mutations in both genes, wild type copies of *MAPKKK3* and *MAPKKK5* were transformed into *mapkkk3 mapkkk5* double mutant separately. Two transgenic lines for each gene were examined for flg22-induced MPK3/MPK6 phosphorylation. All four lines complemented the reduction of MPK3/MPK6 phosphorylation in *mapkkk3 mapkkk5* double

mutant, indicating that MAPKKK3 and MAPKKK5 are required for flg22-induced MPK3 and MPK6 phosphorylation (Figure 3.3).

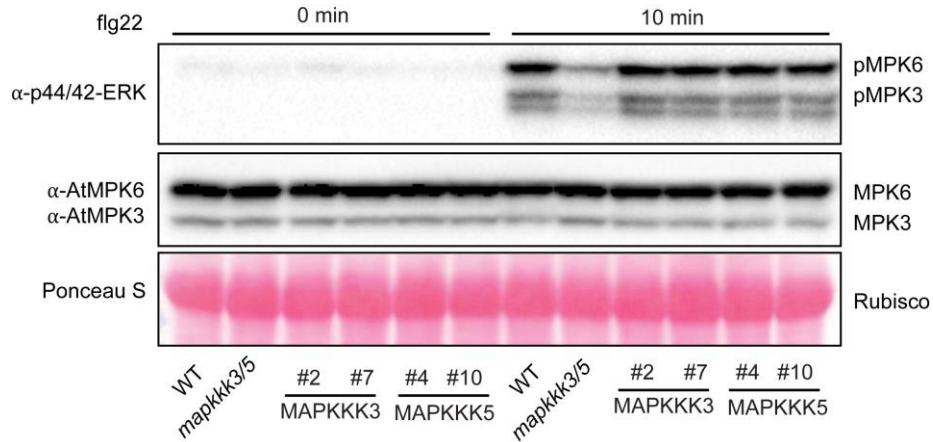


Figure 3.3 The reduced flg22-induced MAPK activation in *mapkkk3 mapkkk5* can be complemented by MAPKKK3 or MAPKKK5.

Western blot analysis of flg22-induced MAPK activation in wild type (WT), *mapkkk3 mapkkk5* (*mapkkk3/5*), and transgenic lines expressing *MAPKKK3* (#2 and #7) or *MAPKKK5* (#4 and #10) in *mapkkk3/5*. Twelve-day-old seedlings were sprayed with 100 nM flg22. Samples were collected at 0 and 10 min after flg22 treatment. Activated MAPKs were detected by immunoblots using the α -p44/42-ERK antibody. MPK3 and MPK6 protein levels in the same samples were detected using the α -AtMPK3 and α -AtMPK6 antibodies. Equal loading is indicated by the Ponceau S staining of Rubisco.

3.2 MAPKKK3 and MAPKKK5 are required for MPK3/MPK6 phosphorylation induced by multiple elicitors.

To test whether MPK3/MPK6 phosphorylation induced by other PAMPs is affected by the loss of MAPKKK3 and MAPKKK5, the *mapkkk3 mapkkk5* double mutant was treated with elf18 (a

peptide derived from the N terminus of bacterial EF-Tu) and nlp20 (a conserved 20 amino acid fragment of NLPs). Similarly, MPK3 and MPK6 activation is attenuated in *mapkkk3 mapkkk5* plants (Figure 3.4 A and B). Induction of MPK3/MPK6 phosphorylation by the endogenous DAMP signal pep23 (a 23 amino acid fragment derived from Plant Elicitor Peptide 1) was also examined. As shown in figure 3.4 C, phosphorylation of MPK3 and MPK6 following pep23 treatment is not affected in the single mutants, but it is clearly reduced in the *mapkkk3 mapkkk5* double mutant. Altogether, these data suggest that MAPKKK3 and MAPKKK5 are required for MPK3 and MPK6 activation upon treatment with different elicitors.

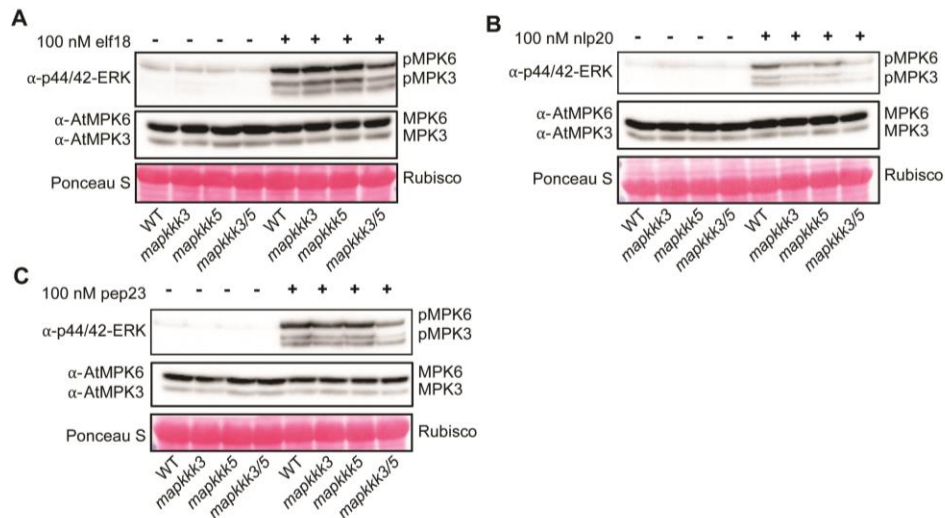


Figure 3.4 MAPKKK3 and MAPKKK5 are required for elf18, nlp20 and pep23-induced activation of MPK3 and MPK6.

elf18 (A), nlp20 (B) and pep23 (C)-induced MAP kinase activation in wild type (WT), *mapkkk3*, *mapkkk5* and *mapkkk3 mapkkk5* (*mapkkk3/5*). Samples were collected 10 min after treatment with 100 nM elf18, 100 nM nlp20 and 100 nM pep23. Activated MAPKs were detected by immunoblots using α-p44/42-ERK antibody. MPK3 and MPK6 protein levels in the same

samples were detected using the α -AtMPK3 and α -AtMPK6 antibodies. Equal loading is indicated by the Ponceau S staining of Rubisco.

3.3 Loss of *MEKK1*, *MEKK2*, and *MEKK3* does not enhance the compromised activation of MPK3/MPK6 by flg22.

MEKK1, *MEKK2*, and *MEKK3* encode three closely related MAPKKs in a tandem repeat. *MEKK1* is required for flg22-induced activation of MPK4, but not MPK3 and MPK6 (Ichimura et al., 2006; Suarez-Rodriguez et al., 2007). To test whether loss of these three MEKKs can further reduce flg22-induced MAPK activation in *mapkkk3 mapkkk5*, a *mekk1 mekk2 mekk3* triple mutant was crossed into *mapkkk3 mapkkk5*. Analysis of flg22-induced activation of MPK3 and MPK6 showed that it is comparable in the *mapkkk3 mapkkk5* double mutant and the *mekk1 mekk2 mekk3 mapkkk3 mapkkk5* quintuple mutant (Figure 3.5), suggesting that these three MEKKs most likely do not contribute to the activation of MPK3 and MPK6 induced by flg22.

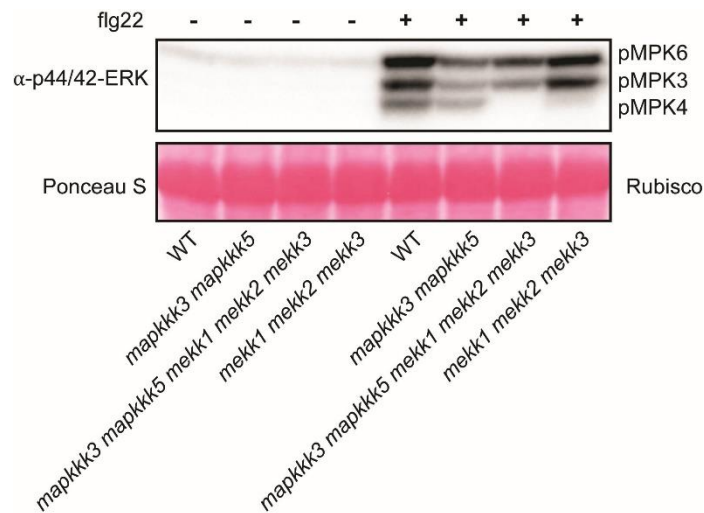


Figure 3.5 flg22-induced MAPK activation in *mapkkk3 mapkkk5* is not further reduced by *mekk1 mekk2 mekk3*.

Twelve-day-old seedlings of the indicated genotypes were treated with 100 nM of flg22 for 10 min and protein extracts were analysed by western blot using the α -p44/42-ERK antibody. Equal loading is indicated by the Ponceau S staining of Rubisco. Experiments were repeated twice with similar results.

3.4 MAPKKK3/MAPKKK5 interact with MKK4/MKK5.

As MKK4 and MMK5 function upstream of MPK3 and MPK6 in development and immune signaling (Asai et al., 2002; Wang et al., 2007), we tested whether MAPKKK3/MAPKKK5 interact with MKK4/MKK5. We co-expressed 3 \times HA-tagged MKK4 or MKK5 with 3 \times FLAG-tagged MAPKKK3^{K243M} or MAPKKK5^{K375M} in *Nicotiana benthamiana* (*N.b.*). MAPKKK3^{K243M} and MAPKKK5^{K375M} contain mutations in the ATP binding sites of MAPKKK3 and MAPKKK5 separately that are predicted to be essential for the kinase activity. They were used because overexpression of MAPKKK3 causes cell death in *N.b.* Immunoprecipitation was carried out using anti-FLAG beads, and the precipitated proteins were detected by anti-HA and anti-FLAG antibodies. As shown in figure 3.6 A–C, MAPKKK3^{K243M}-3FLAG and MAPKKK5^{K375M}-3FLAG co-immunoprecipitated with MKK4-3HA as well as with MKK5-3HA, suggesting that MAPKKK3/MAPKKK5 interact with MKK4/MKK5. The interaction between MAPKKK3^{K243M} and MKK4/MKK5 was further confirmed by bimolecular fluorescence complementation (BiFC) assays (Figure 3.6 D).

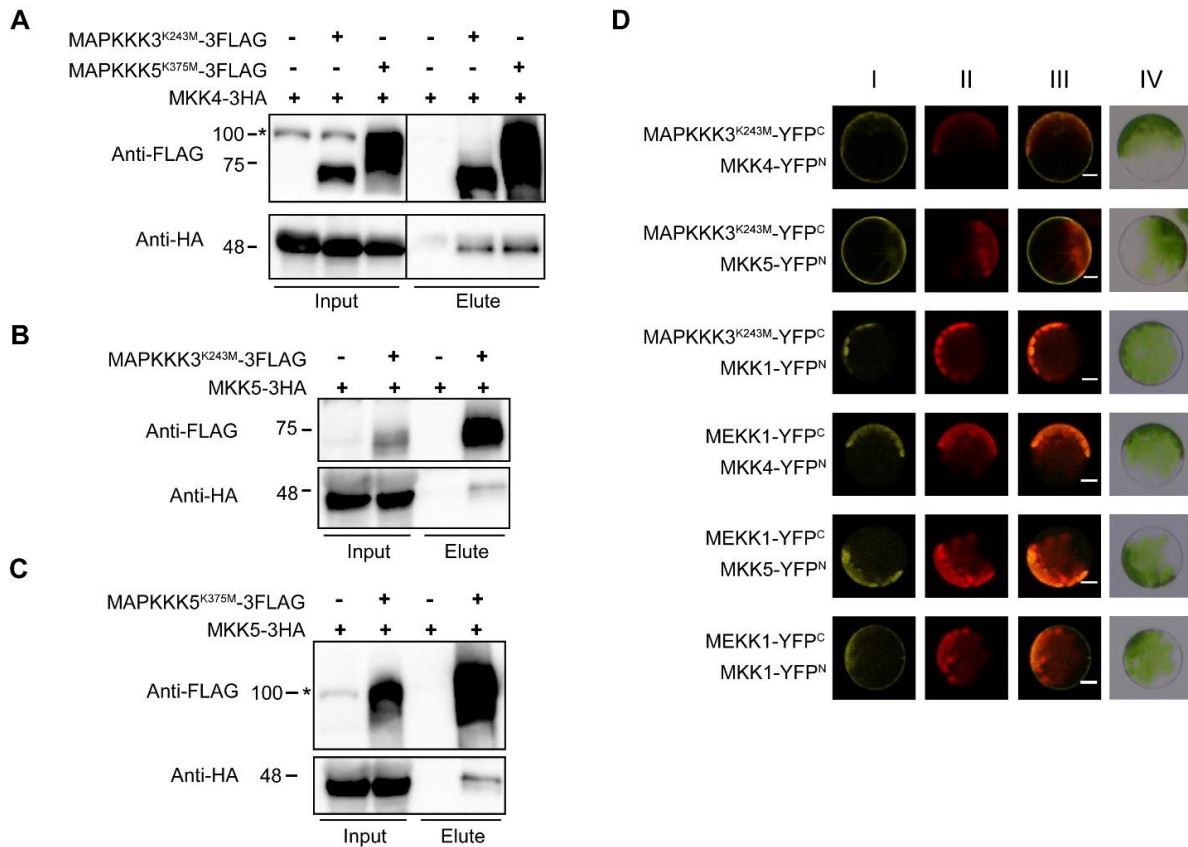


Figure 3.6 MAPKKK3/MAPKKK5 interact with MKK4/MKK5.

(A-C) MKK4/MKK5 interact with MAPKKK3/MAPKKK5 *in planta*. MKK4-3HA (A) or MKK5-3HA (B, C) was co-expressed with MAPKKK3^{K243M}-3FLAG or MAPKKK5^{K375M}-3FLAG through *Agrobacterium*-mediated transient expression in *Nicotiana benthamiana* (*N.b.*) leaves. Total protein was immunoprecipitated with anti-FLAG M2 agarose beads. Fusion proteins in input and eluate were detected using anti-FLAG or anti-HA antibodies. *Indicates the unspecific band in *N.b.* tissue detected by anti-FLAG antibody. Experiments are repeated twice with similar result.

(D) Analysis of interaction between MAPKKK3^{K243M} and MKK4/MKK5 by bimolecular fluorescence complementation (BiFC) assay. Epifluorescence (I), chloroplast autofluorescence (II), merged (III), bright field (IV) images of *Arabidopsis* mesophyll protoplasts co transfected with constructs expressing different fusion proteins. MEKK1-YFPC and MKK1-YFPN were used as controls. Scale bar = 10 μ m. Experiments are repeated three times with similar result.

3.5 MAPKKK3 and MAPKKK5 are required for PTI and basal resistance.

To evaluate the role of MAPKKK3 and MAPKKK5 in PTI, wild type and the mutant plants were challenged with *Pto* DC3000 *hrcC*⁻, a bacterial strain that is deficient in the delivery of type III effectors and is only able to induce PTI responses. As shown in figure 3.7 A, growth of *Pto* DC3000 *hrcC*⁻ in *mapkkk3* and *mapkkk5* single mutants is comparable with wild type, but the *mapkkk3 mapkkk5* double mutant supports significantly higher level of bacterial growth, suggesting that MAPKKK3 and MAPKKK5 function redundantly in positive regulation of PTI.

We also challenged wild type and the mutant plants with the virulent bacterial strain *Pto* DC3000. Growth of *Pto* DC3000 on *mapkkk3 mapkkk5* is significantly higher than in the wild type and single mutants (Figure 3.7 B). To confirm the observed enhanced susceptibility towards *Pto* DC3000 in the *mapkkk3 mapkkk5* double mutant is indeed caused by mutations in both genes, complementing lines expressing wild type copies of *MAPKKK3* or *MAPKKK5* in *mapkkk3 mapkkk5* double mutant were challenged with *Pto* DC3000. All four lines complemented the enhanced susceptibility in *mapkkk3 mapkkk5* double mutant (Figure 3.7 C), suggesting that MAPKKK3 and MAPKKK5 are required for basal resistance.

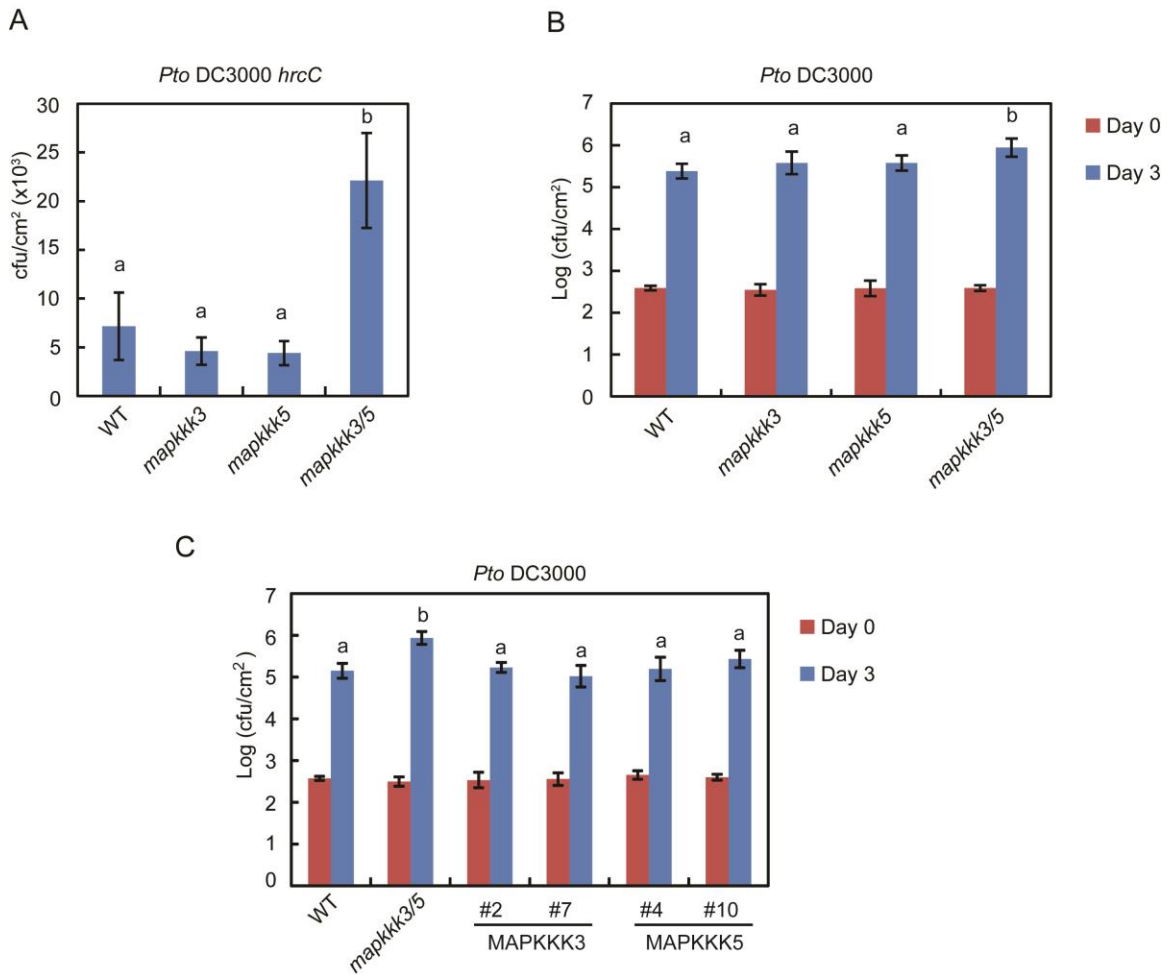


Figure 3.7 *mapkkk3 mapkkk5* plants are more susceptible to *Pto DC3000 hrcC*⁻ and *Pto DC3000*.

(A) Growth of *Pto DC3000 hrcC*⁻ on wild type (WT), *mapkkk3*, *mapkkk5*, and *mapkkk3 mapkkk5* (*mapkkk3/5*). Four-week-old plants were sprayed with *Pto DC3000 hrcC*⁻ (OD₆₀₀ = 0.2) at the abaxial surface of leaves. Samples were collected 3 days after inoculation. (B) Growth of *Pto DC3000* on WT, *mapkkk3*, *mapkkk5*, and *mapkkk3/5* plants. Four-week-old plants were infiltrated with *Pto DC3000* (OD₆₀₀ = 0.0002). (C) Growth of *Pto DC3000* on WT, *mapkkk3/5*, and transgenic lines expressing MAPKKK3 (#2 and #7) or MAPKKK5 (#4 and #10) in *mapkkk3 mapkkk5*. Four-week-old plants were infiltrated with *Pto DC3000* (OD₆₀₀ = 0.0002). Samples in (B) and (C) were taken at 0 h (day 0) and 72 h (day 3).

Experiments were repeated three times, each showing similar results. Error bars represent standard deviations of six biological samples ($n = 6$). Statistical differences among different genotypes are labeled with different letters (one-way ANOVA with Tukey's HSD test, $P < 0.01$ in panel A and C, $P < 0.05$ in panel B).

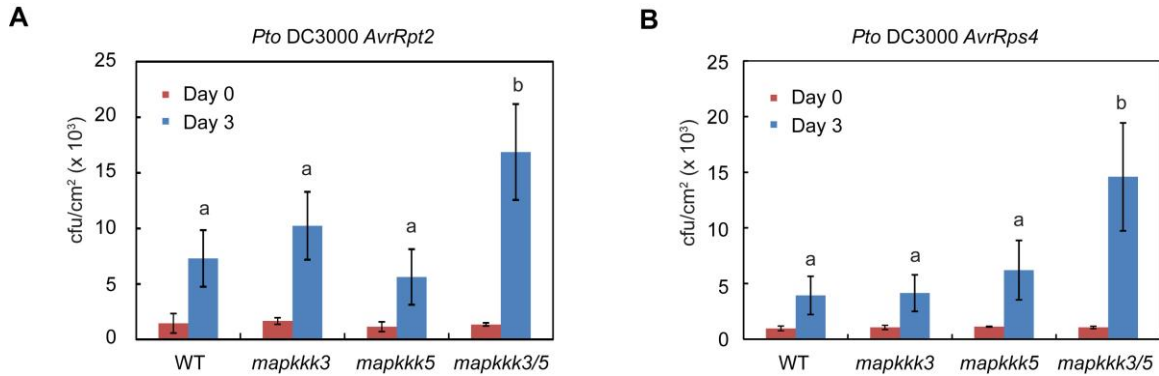


Figure 3.8 Growth of *Pto* DC3000 *AvrRpt2* and *Pto* DC3000 *AvrRps4* on wild type (WT), *mapkkk3*, *mapkkk5*, and *mapkkk3 mapkkk5* plants.

Four-week-old plants were infiltrated with the *Pto* DC3000 *AvrRpt2* (A) and *Pto* DC3000 *AvrRps4* (B) ($OD_{600} = 0.0005$). Samples were taken at 0 h (day 0) and 72 h (day 3). Experiments in (A, B) represent one of three biological replicates, each showing similar results. Error bars represent standard deviations of six biological samples ($n = 6$). Statistical differences among different genotypes are labeled with different letters (one-way ANOVA with Tukey's HSD test, $P < 0.01$).

3.6 MAPKKK3 and MAPKKK5 are required for ETI.

To test the role of MAPKKK3 and MAPKKK5 in ETI, wild type and *mapkkk3* and *mapkkk5* mutants were challenged with *Pto* DC3000 *AvrRpt2*, a bacterial strain carrying the effector *AvrRpt2* that can be recognized by the CNL protein RPS2. While the *mapkkk3* and *mapkkk5*

single mutants allow similar amount of bacterial growth as wild type plants, the *mapkkk3* *mapkkk5* double mutant supports about twice as much bacterial growth compared with wild type plants (Figure 3.8 A). Plants of the same genotypes were also challenged with *Pto* DC3000 *AvrRps4*, a bacterial strain carrying the effector AvrRps4 that can be recognized by the TNL protein RPS4. Similarly, the *mapkkk3 mapkkk5* double mutant, but not the *mapkkk3* or *mapkkk5* single mutant, shows significantly enhanced susceptibility (Figure 3.8 B). The enhanced avirulent bacteria growth in the *mapkkk3 mapkkk5* double mutant suggests that MAPKKK3 and MAPKKK5 contribute to ETI.

3.7 The *mapkkk3 mapkkk5* double mutant cannot suppress the autoimmune phenotypes of *chs3-2D* and *mekk1-1*.

To test whether mutations in *MAPKKK3* and *MAPKKK5* can suppress the dwarfism in autoimmune mutants with constitutive ETI-like responses, *mapkkk3 mapkkk5* mutant plants were crossed with two autoimmune mutants, *chs3-2D* and *mekk1-1*, to generate the *chs3-2D mapkkk3-1 mapkkk5-1* and *mekk1-1 mapkkk3-1 mapkkk5-1* triple mutants. *chs3-2D* contains a gain-of-function mutation in the TNL protein CHS3, which results in severe dwarfism and constitutively activated immune responses. In the *mekk1-1* mutant, disruption of the MEKK1-MKK1/2-MPK4 cascade leads to constitutive activation of the CNL protein SUMM2, which monitors the integrity of the MAPK cascade. Constitutive activation of SUMM2-mediated immunity in *mekk1-1* is coupled with extreme dwarfism and seedling lethality. As shown in figure 3.9 A and D, the *chs3-2D mapkkk3-1 mapkkk5-1* and *mekk1-1 mapkkk3-1 mapkkk5-1* triple mutants are morphologically indistinguishable from the *chs3-2D* and *mekk1-1* single mutants, indicating that mutations in *MAPKKK3* and *MAPKKK5* do not suppress the dwarfism in *chs3-2D* and *mekk1-1*.

Analysis of *PR* gene expression in the triple mutants further confirms that *mapkkk3 mapkkk5* double mutant cannot suppress the constitutive defense response in *chs3-2D* and *mekk1-1* (Figure 3.9 B-C, E-F).

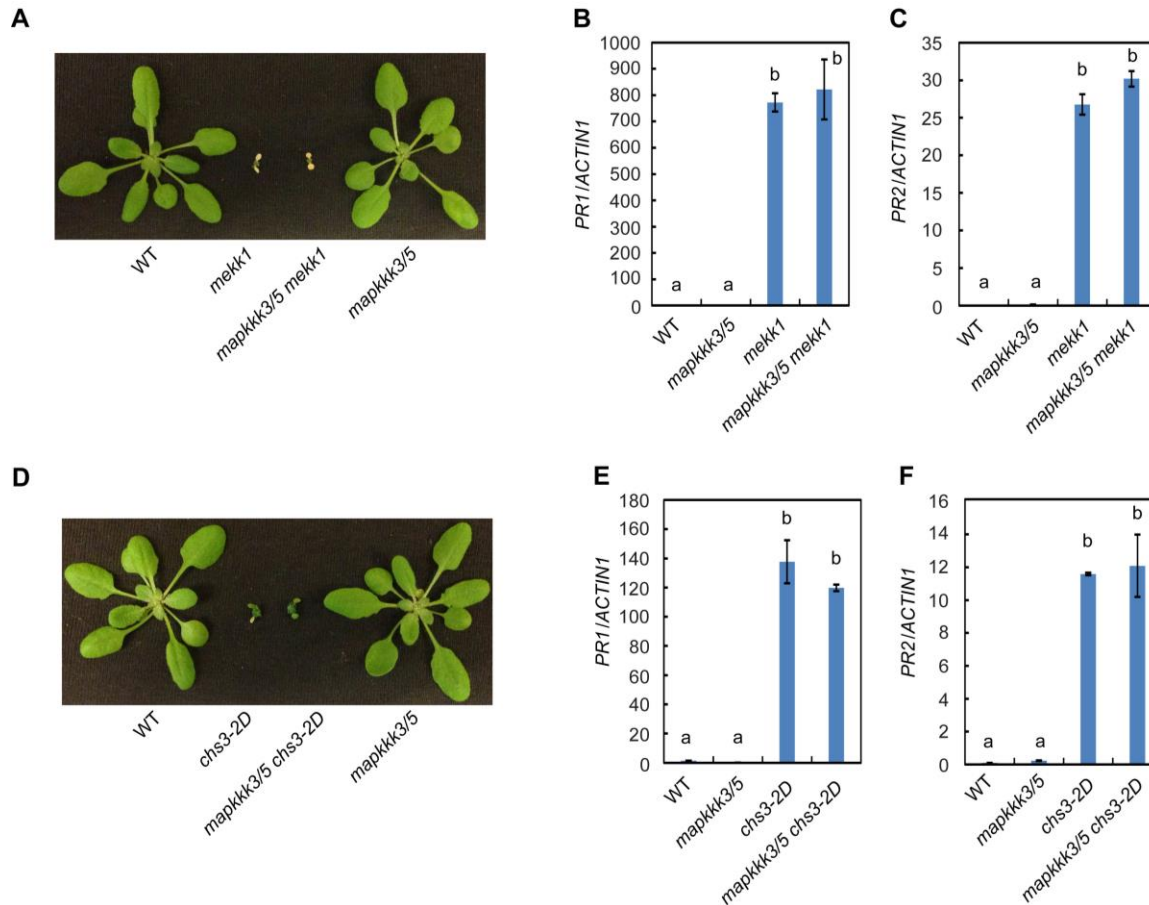


Figure 3.9 *mapkkk3 mapkkk5* double mutant can't suppress the autoimmune phenotype in *mekk1-1* and *chs3-2D*.

(A-C) Morphological phenotypes (A), *PR1* (B) and *PR2* (C) expression of wild type (WT), *mekk1*, *mapkkk3/5 mekk1* and *mapkkk3/5* plants. (D-F) Morphological phenotypes (D), *PR1* (E) and *PR2* (F) expression of WT, *chs3-2D*, *mapkkk3/5 chs3-2D* and *mapkkk3/5* plants. Pictures in (A) and (D) were taken with three-week-old plants. Gene expression in (C-D) and (E-F) were determined by quantitative RT-PCR using two-week-old seedlings grown on 1/2 MS plates.

Values were normalized to the expression levels of *ACTIN1*. Error bars represent means \pm s.d. (n = 3). The experiments were repeated twice with similar results. Statistical differences among different genotypes are labeled with different letters (one-way ANOVA with Tukey's HSD test, $P < 0.01$).

3.8 MAPKKK3 and MAPKKK5 are required for ETI-induced cell death.

To test whether MAPKKK3 and MAPKKK5 are required for cell death associated with ETI, *mapkkk3 mapkkk5* double mutant plants were infiltrated with *Pto* DC3000 *AvrRpt2* and the cell death progress was monitored. *mapkkk3 mapkkk5* double mutant plants exhibited delayed cell death as shown by reduced leaf collapse 16 hours after infiltration (Figure 3.10 A, B and C).

To quantify cell death in wild type and *mapkkk3 mapkkk5* double mutant plants induced by *Pto* DC3000 *AvrRpt2*, the infiltrated leaves were collected to measure the ion leakage from dead cells. As shown in figure 3.10 D, wild type plants showed about 21 % ion leakage, whereas the *mapkkk3 mapkkk5* double mutant plants showed about 16 % ion leakage 16 hours after infiltration with the bacteria. Ion leakage measurement of wild type and *mapkkk3 mapkkk5* double mutant plant leaves infiltrated with *Pto* DC3000 *AvrRpt2* over time also showed delayed cell death in the *mapkkk3 mapkkk5* double mutant (Figure 3.10 E).

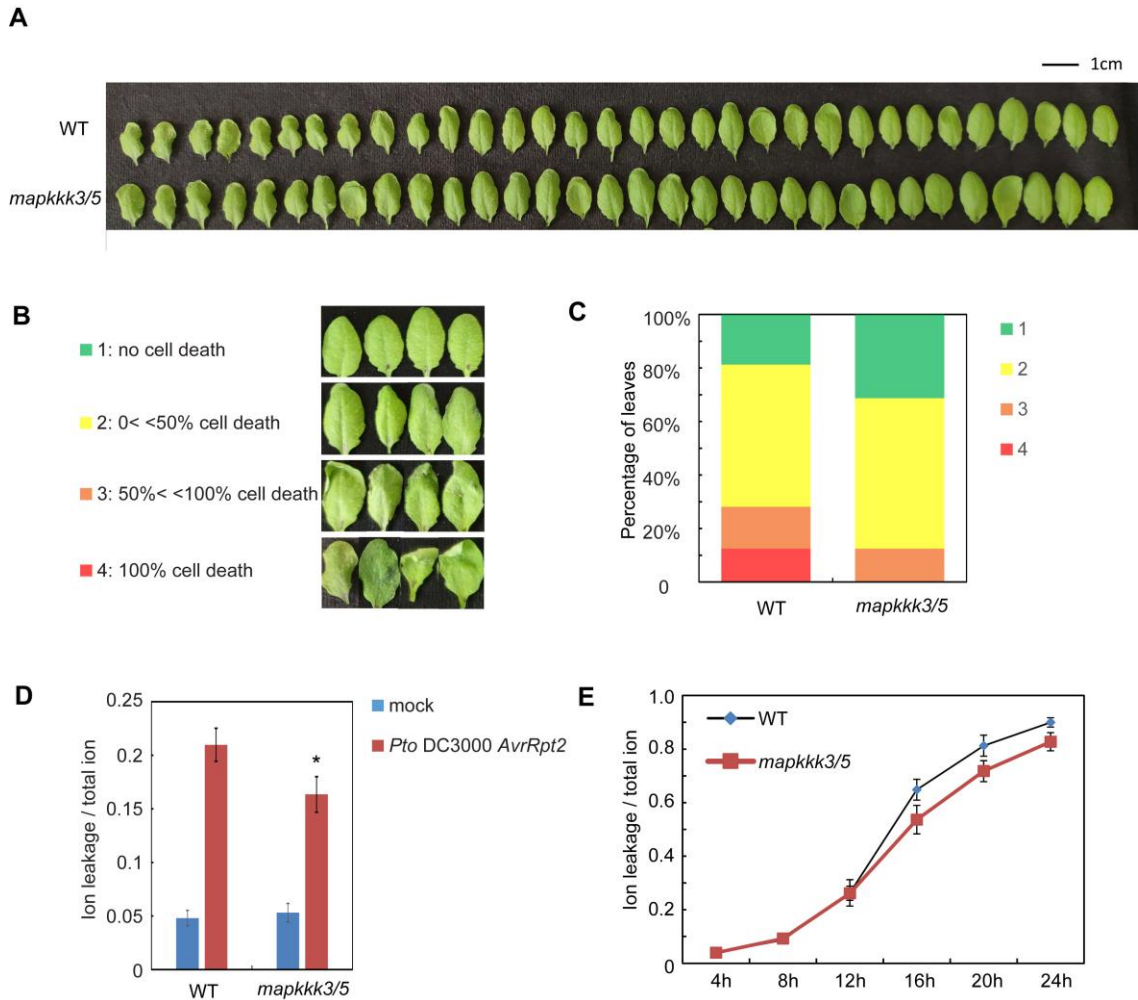


Figure 3.10 *mapkkk3 mapkkk5* double mutant plants show delayed cell death after infection by *Pto* DC3000 *AvrRpt2*.

(A) Leaves of wild type (WT) and *mapkkk3 mapkkk5* (*mapkkk3/5*) 16 hours after infiltration with *Pto* DC3000 *AvrRpt2* ($OD_{600} = 0.025$). (B) Representative leaf morphology with different levels of cell death. The percentages of cell death are quantified by percentages of the area of leaves collapse. (C) Quantification of cell death in leaf samples from (A) by ranking the levels of cell death. (D) Ion leakage in wild type (WT) and *mapkkk3/5* 16 hours after infiltration with *Pto* DC3000 *AvrRpt2* ($OD_{600} = 0.025$). (E) Ion leakage in WT and *mapkkk3/5* in 10 mM MgCl₂ over time after infiltration with *Pto* DC3000 *AvrRpt2* ($OD_{600} = 0.025$). All the experiments were

repeated three times with similar results. Statistical differences among different genotypes are labeled with a star (one-way ANOVA with Tukey's HSD test, $P < 0.01$).

One possible explanation for the relative weak phenotype in delayed ETI-induced cell death in *mapkkk3 mapkkk5* is the likely existence of other functional redundant MAPKKs upstream of MKK4/MKK5-MPK3/MPK6. In this scenario, introducing mutations in the downstream MKK4/MKK5 or MPK3/MPK6 would further reduce the output of the kinase cascade and may enhance the delayed cell death phenotype. To test whether mutations in the downstream kinases can enhance the delayed cell death phenotype, *mapkkk3 mapkkk5* was crossed into *mpk3* and *mpk6* mutants. Meanwhile, mutations in *MKK4* and *MKK5* were separately introduced into *mapkkk3 mapkkk5* by gene editing using CRISPR-Cas9. Wild type, *mapkkk3 mapkkk5*, *mpk3*, *mpk6*, *mkk4*, *mkk5*, and the four triple mutants were challenged with *Pto* DC3000 *AvrRpt2*, *Pto* DC3000 *AvrRps4* and another avirulent strain *Pto* DC3000 *AvrPphB* separately. As shown in figure 3.11 A, B and C, cell death triggered by the different bacterial strains is further reduced in four triple mutants. To further weaken the MAPK cascade, *MKK4* was silenced in the *mapkkk3/5 mkk5* triple mutant using amiRNA targeting *MKK4*. Analysis of two *mapkkk3 mapkkk5 mkk5* *amiMKK4* transgenic lines showed that cell death after *Pto* DC3000 *AvrRpt2* infection was further reduced as revealed by the ion leakage assay (Figure 3.11 D and E). The *mapkkk3 mapkkk5 mkk5* *amiMKK4* transgenic plants also displayed enhanced susceptibility towards the three avirulent bacterial strains (Figure 3.11 F, G and H). Together, these data suggest that MAPKKK3/MAPKKK5 and their downstream kinase module MKK4/MKK5-MPK3/MPK6 are required for ETI-induced cell death.

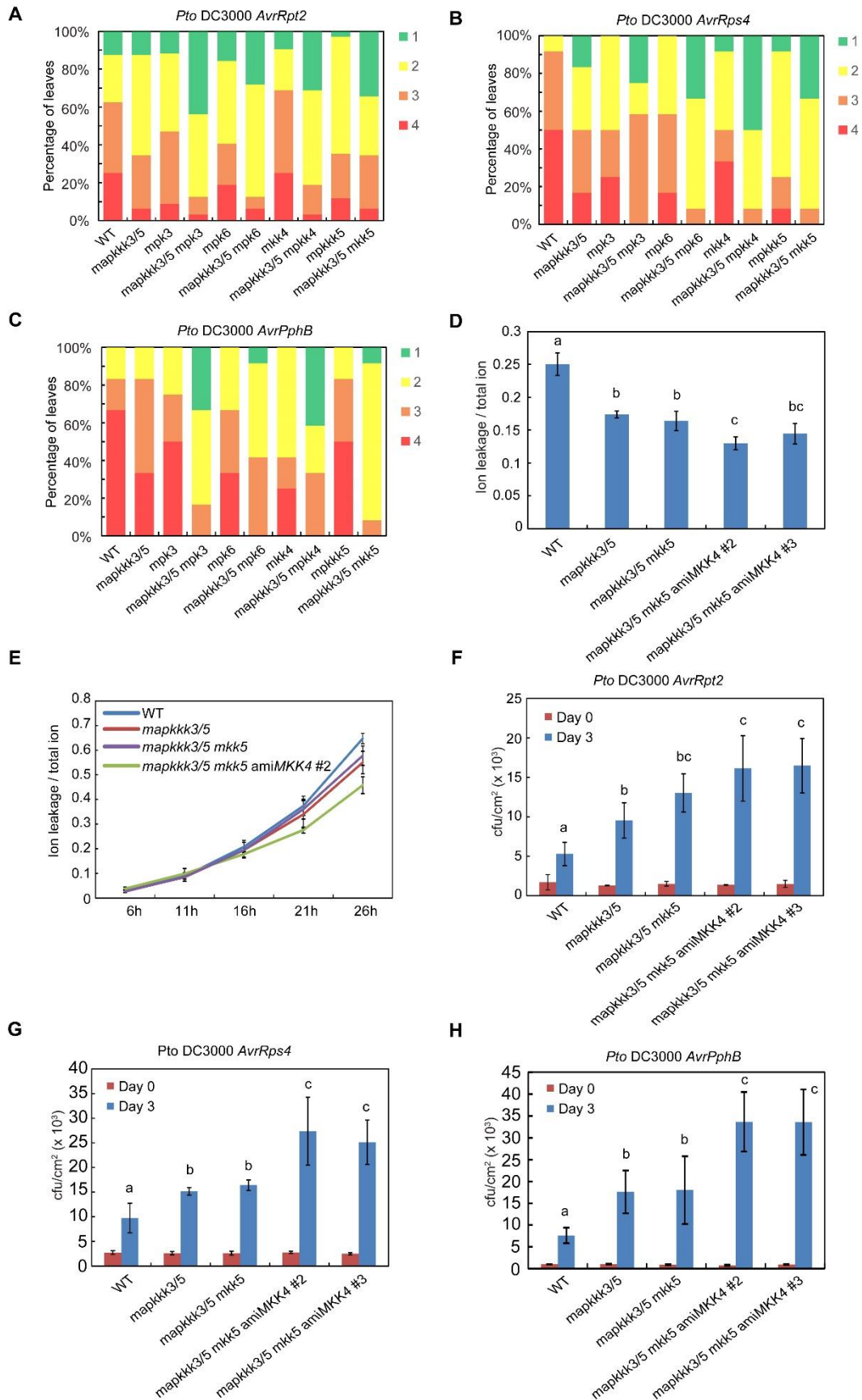


Figure 3.11 Mutations in *MKK4/MKK5* and *MPK3/MPK6* further reduce ETI-induced cell death and enhance susceptibility to avirulent pathogens in *mapkkk3 mapkkk5*.

(A-C) Percentage of leaves with different levels of cell death in the indicated genotypes 16 hours after infiltration with *Pto* DC3000 *AvrRpt2* (A), *Pto* DC3000 *AvrRps4* (B) and *Pto* DC3000 *AvrPphB* (C) ($OD_{600} = 0.025$). (D) Ion leakage in wild type (WT), *mapkkk3/5*, *mapkkk3/5 mkk5* and two *mapkkk3/5 mkk5* lines expressing artificial microRNA targeting *MKK4* (*amiMKK4*). The samples were collected 16 hours after infiltration with *Pto* DC3000 *AvrRpt2* ($OD_{600} = 0.025$). (E) Ion leakage in WT, *mapkkk3/5*, *mapkkk3/5 mkk5* and *mapkkk3/5 mkk5 amiMKK4 #2* in 10 mM $MgCl_2$ over time after infiltration with *Pto* DC3000 *AvrRpt2* ($OD_{600} = 0.025$). (F-H) Growth of *Pto* DC3000 *AvrRpt2* (F), *Pto* DC3000 *AvrRps4* (G) and *Pto* DC3000 *AvrPphB* (H) on WT, *mapkkk3/5*, *mapkkk3/5 mkk5* and two *mapkkk3/5 mkk5 amiMKK4* lines. Four-week-old plants were infiltrated with the bacterial pathogens ($OD_{600} = 0.0005$). Samples were taken at 0 h (day 0) and 72 h (day 3). Error bars represent standard deviations of six biological repeats ($n = 6$). Statistical differences among different genotypes are labeled with different letters (one-way ANOVA with Tukey's HSD test, $P < 0.05$ in panel F and G, $P < 0.01$ in panel H). The experiments were carried out twice with similar results.

3.9 SAR induced by *Pto* DC3000 *AvrRpt2* is compromised in the *mapkkk3 mapkkk5* double mutant.

To test the role of MAPKKK3 and MAPKKK5 in the induction of SAR by ETI, *Pto* DC3000 *AvrRpt2*-induced SAR on wild type and *mapkkk3 mapkkk5* double mutant plants was analyzed. The *mpk3* single mutant was used as a positive control, as it was previously shown to have a defect in *Pto* DC3000 *AvrRpt2*-induced SAR (Wang et al., 2018). In the mock treated *mapkkk3 mapkkk5* double mutant, there is significantly increased bacteria growth compared with wild type (Figure 3.12A), which is consistent with the previous result that basal resistance is compromised in the *mapkkk3 mapkkk5* double mutant. When challenged with *Pto* DC3000 *AvrRpt2*, wild type

plants allow significant reduced bacterial growth in the distal leaves. In the *mapkkk3 mapkkk5* double mutant, *Pto* DC3000 *AvrRpt2*-induced SAR is compromised (Figure 3.12A). Consistent with the defect in *Pto* DC3000 *AvrRpt2*-induced SAR, gene expression analysis showed that in the *mapkkk3 mapkkk5* double mutant there is reduced induction of *FMO1* and *ALD1*, two genes required for establishment of SAR, after *Pto* DC3000 *AvrRpt2* infection (Figure 3.12 B and C).

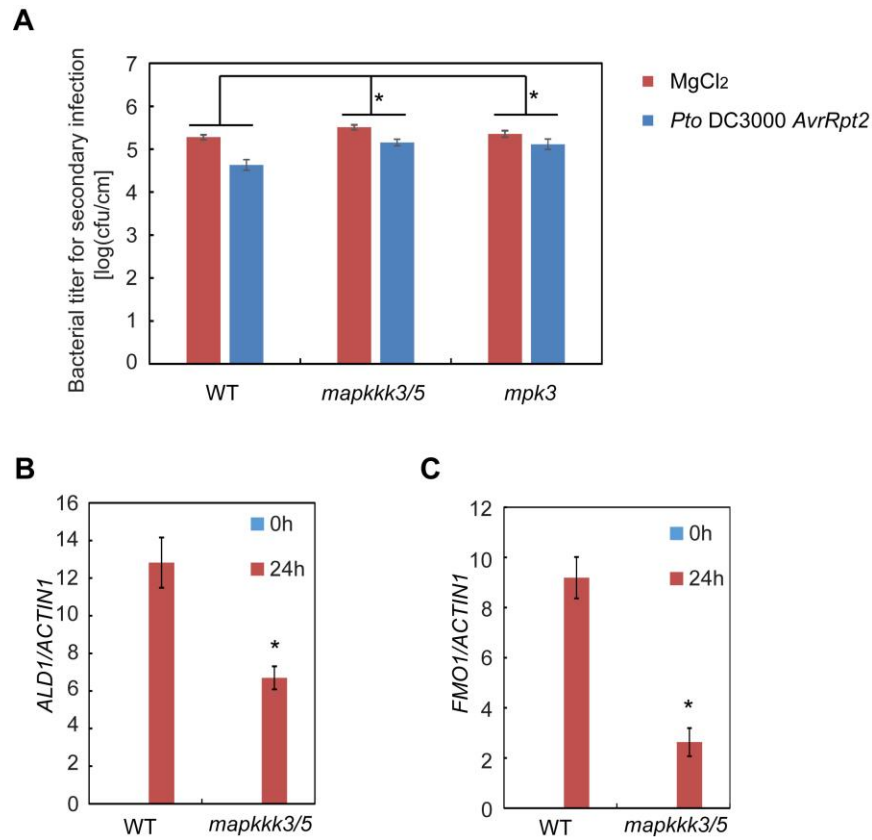


Figure 3.12 *mapkkk3 mapkkk5* double mutant shows a defect in *Pto* DC3000 *AvrRpt2* induced SAR.

(A) Growth of *Pseudomonas syringae* pv. *maculicola* (*Pma*) ES4326 ($OD_{600} = 0.001$) on systemic leaves of the wild type (WT), *mapkkk3 mapkkk5* (*mapkkk3/5*) and *mpk3* after *Pto* DC3000 *AvrRpt2* or mock treatment. Error bars represent standard deviations of six biological samples ($n = 6$). The resistance induced by avirulent pathogen *Pto* DC3000 *AvrRpt2* in different

genotypes were compared using two-way ANOVA, $P < 0.01$. (B-C) Quantitative RT-PCR analysis of *Pto* DC3000 *AvrRpt2* ($OD_{600} = 0.001$) induced *ALD1* (B) and *FMO1* (C) expression in WT and *mapkkk3/5*. Two leaves of four-week-old plants were infiltrated with *Pto* DC3000 *AvrRpt2* and collected 24 h after infiltration. Values were normalized to the levels of *ACTIN1*. Bars represent means \pm s.d. from three biological repeats. Significant difference compared with WT: * $P < 0.01$ (Student's t-test).

Experiments were repeated twice (B-C) or three times (A) with similar results.

3.10 The MAPKKK3-MKK5-MPK6 MAPK cascade can be reconstituted *in vitro*.

The reduced flg22-induced MPK3/MPK6 phosphorylation in the *mapkkk3 mapkkk5* double mutant and interactions between MAPKKK3/MAPKKK5 and MKK4/MKK5 suggest that MAPKKK3 and MAPKKK5 function redundantly upstream of MKK4/MKK5 and MPK3/MPK6. To gain additional insights about this MAPK cascade, I tried to reconstitute the cascade *in vitro*. Recombinant 6 \times His-MBP-MAPKKK3 protein purified from *E. coli* was used to test whether it can enhance phosphorylation of MPK6-6 \times His by 6 \times His-MKK5 *in vitro*. As shown in figure 3.13 B, no phosphorylation was detected on the recombinant MPK6-6 \times His protein purified from *E. coli* using the p44-42-ERK antibody. Adding the wild type 6 \times His-MKK5 protein to the reaction resulted in only weak MPK6 phosphorylation. However, adding the constitutively active kinase 6 \times His-MKK5EE in the reaction leads to strong MPK6 phosphorylation. This data suggest that the activity of the wild type 6 \times His-MKK5 protein purified from *E. coli* is very low. Next, we added recombinant 6 \times His-MBP-MAPKKK3 protein purified from *E. coli* to the kinase assay. The 6 \times His-MBP-MAPKKK3 protein showed a ladder-like pattern in an SDS-PAGE gel when stained with coomassie blue, most likely due to

degradation (Figure 3.13A). While 6×His-MBP-MAPKKK3 alone cannot phosphorylate MPK6, adding 6×His-MBP-MAPKKK3 together with 6×His-MKK5 to the kinase assay leads to strong MPK6 phosphorylation (Figure 3.13 C), suggesting that the MAPKKK3-MKK5-MPK6 cascade was reconstituted successfully *in vitro*.

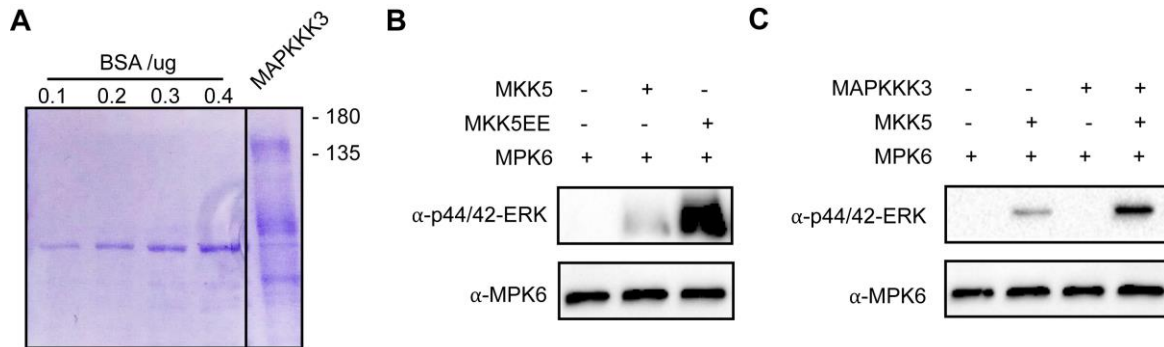


Figure 3.13 MAPKKK3-MKK5-MPK6 cascade can be reconstituted *in vitro*.

(A) Coomassie blue staining of full length recombinant MAPKKK3 protein purified from *E. coli*. 1 μ l of protein was loaded with BSA as control. (B) Phosphorylation of MPK6 by MKK5 and MKK5EE. 0.01 μ g recombinant MKK5/ MKK5EE protein and 0.4 μ g recombinant MPK6 protein were used in each reaction. (C) Phosphorylation of MPK6 by MKK5 in the presence of full length MAPKKK3. 0.02 μ g recombinant MAPKKK3 protein, 0.01 μ g recombinant MKK5 protein and 0.4 μ g recombinant MPK6 protein were used in each reaction.

All the proteins were expressed and purified from *E. coli*. After incubation with ATP and the indicated proteins in kinase buffer for 30 min, the reactions were terminated by heat treatment. MPK6 phosphorylation was detected using the α -p44/42-ERK antibody. MPK6 protein levels in the samples were detected using α -AtMPK6 antibodies. The experiments were repeated three times with similar results.

3.11 The kinase domain and C terminal domain, but not the N terminal domain of MAPKKK3 are required for its function *in vitro*.

We further analyzed the importance of different domains of MAPKKK3 using the *in vitro* kinase assay by generating several mutant versions of MAPKKK3. MAPKKK3 has an N terminal regulatory domain predicted to negatively regulate its activity, a kinase domain and a C terminal domain (Figure 3.14 A). To evaluate the function of the N terminal domain, the recombinant 6×His-MBP-MAPKKK3ΔN protein with an N-terminal deletion was used in the *in vitro* kinase assay. As shown in figure 3.14 B, MPK6 phosphorylation is comparable in the presence of full length 6×His-MBP-MAPKKK3 and 6×His-MBP-MAPKKK3ΔN, suggesting that the N terminal domain of MAPKKK3 is not required for its activity in the kinase assay.

To investigate the function of MAPKKK3 C terminal domain using the *in vitro* kinase assay, a truncated recombinant 6×His-MBP-MAPKKK3ΔC protein was expressed and purified from *E. coli*. As shown in figure 3.14 C, compared with the full length recombinant MAPKKK3, recombinant MAPKKK3ΔC protein has very low activity in stimulating phosphorylation of MPK6 by MKK5. However, increasing the amount of recombinant MAPKKK3ΔC protein leads to increased MPK6 phosphorylation, suggesting that the recombinant MAPKKK3ΔC protein may be partially active in activating MKK5 *in vitro*.

To determine whether the kinase activity is necessary for the function of MAPKKK3, a conserved lysine in the ATP binding pocket was mutated to methionine to generate the kinase dead recombinant protein 6×His-MBP-MAPKKK3^{K243M}. As shown in figure 3.14 D, recombinant MAPKKK3^{K243M} protein is clearly less active in stimulating MPK6 phosphorylation by MKK5. However, as the amount of recombinant MAPKKK3^{K243M} protein used in the kinase

assay increases, there is increased phosphorylation of MPK6. It suggests that the kinase activity of MAPKKK3 is required for its function, but the kinase dead protein still maintains some activity.

To test the contribution of MAPKKK3 kinase activity to its function *in vivo*, *MAPKKK3*^{K243M} driven by its native promoter was transformed into the *mapkkk3 mapkkk5* double mutant. While wild type copies of *MAPKKK3* can complement the reduced flg22-induced MPK3/MPK6 phosphorylation, the reduced flg22-induced MPK3/MPK6 phosphorylation in *mapkkk3 mapkkk5* double mutant was not complemented in transgenic lines transformed with the *MAPKKK3*^{K243M} mutant gene (Figure 3.14 E), suggesting that the kinase activity of MAPKKK3 is required in flg22-induced MPK3 and MPK6 activation *in planta*.

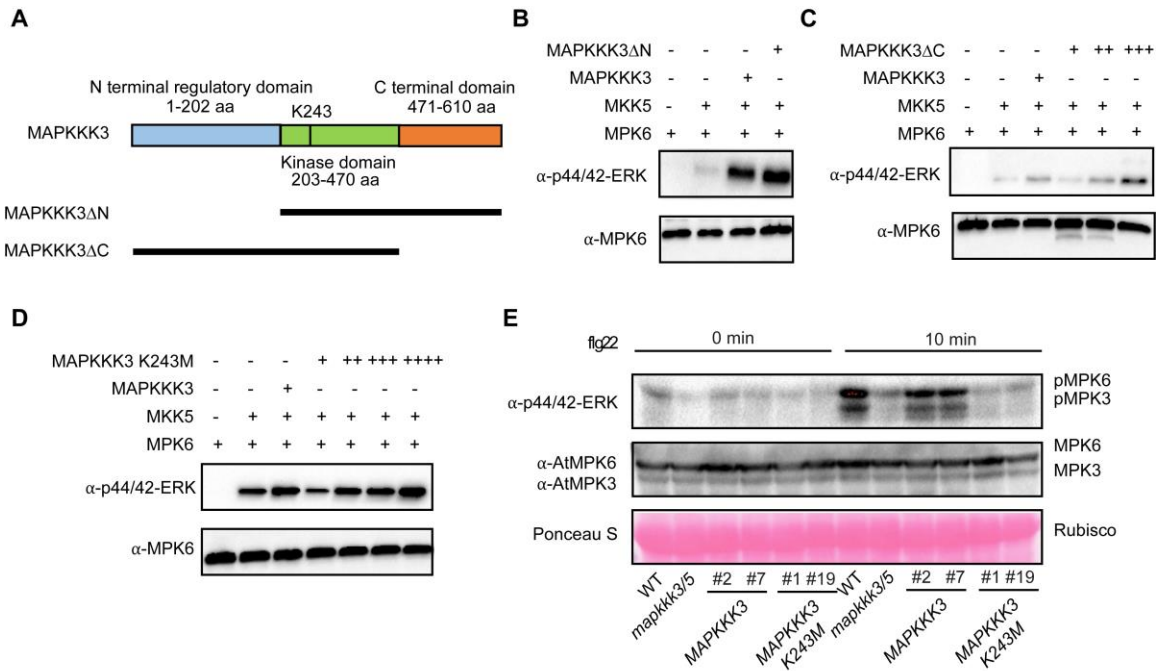


Figure 3.14 Analysis of the N-terminal domain, the C-terminal domain, and the kinase activity of MAPKKK3 in its function.

(A) Schematic representation of MAPKKK3 domain structure and deletion constructs.

(B-D) phosphorylation of MPK6 by MKK5 in the presence of MAPKKK3 Δ N (A), MAPKKK3 Δ C (B) and MAPKKK^{K243M} (C). All the proteins are purified from *E. coli*. After incubation with ATP and the indicated proteins in kinase buffer for 30 min, the reactions were terminated by heat treatment. MPK6 phosphorylation was detected using α -p44/42-ERK antibody. MPK6 protein levels in the same samples were detected using α -AtMPK6 antibodies. One extra plus sign (++) means the amount of protein used is doubled. Two extra plus sign (+++) means the amount of protein used is 4 times of regular amount.

(E) flg22-induced MAP kinase activation in wild type (WT), *mapkkk3 mapkkk5* (*mapkkk3/5*), transgenic lines expressing *MAPKKK3* (#2 and #7) and *MAPKKK3*^{K243M} (#1 and #19) in *mapkkk3/5*. Samples were collected 10 min after treatment with 100 nM flg22. Activated MAPKs were detected by immunoblots using α -p44/42-ERK antibody. MPK3 and MPK6 protein levels in the same samples were detected using the α -AtMPK3 and α -AtMPK6 antibodies. Equal loading is indicated by the Ponceau S staining of Rubisco.

All experiments were repeated three times with similar results.

3.12 PCRK2 interacts with MAPKKK3 and MAPKKK5.

Although it is known that activation of PRR complexes leads to MAP kinase activation within a few minutes, it was unclear how the activated FLS2/BAK1 complex transduces the signal to MAPKKK3/MAPKKK5. As mentioned earlier in the introduction, the RLCK BIK1 is released from the PRR complex upon activation and phosphorylates RBOHD and CNGC2/CNGC4 (Kadota et al., 2014; Li et al., 2014; Tian et al., 2019). However, *bik1* mutant plants exhibit defect in flg22-induced ROS production, but not in flg22-induced MAP kinase activation (Feng

et al., 2012; Zhang et al., 2010). It is very likely that other RLCKs are involved in transducing the signals from the FLS2/BAK1 complex to MAPKKK3 and MAPKKK5.

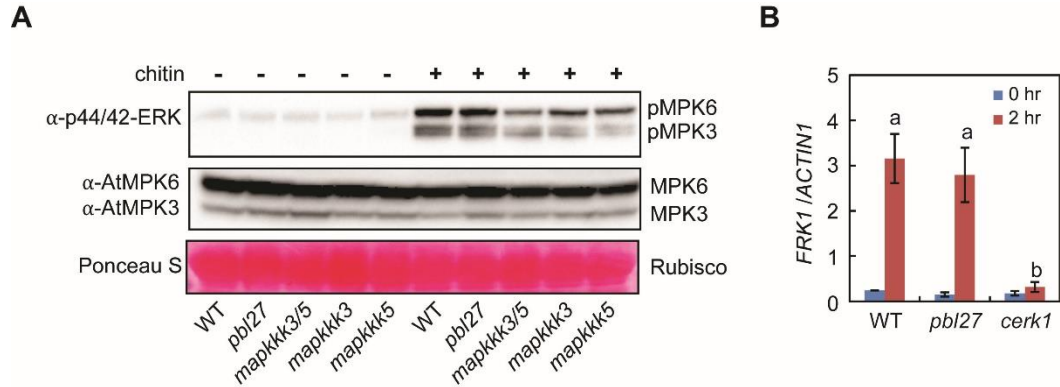


Figure 3.15 Chitin-induced MAPK activation and *FRK1* expression are not significantly altered in the *pbl27* mutant.

(A) Twelve-day-old seedlings of the indicated genotypes were treated with 20 µg/ml of chitin for 10 min and protein extracts were analyzed by western blot using the α-p44/42-ERK antibody. MPK3 and MPK6 protein levels in the same samples were detected using the α-AtMPK3 and α-AtMPK6 antibodies. Equal loading is indicated by the Ponceau S staining of Rubisco. Experiments were repeated twice with similar results.

(B) Quantitative RT-PCR analysis of chitin-induced *FRK1* expression in wild type, *pbl27* and *cerk1*. Twelve-day-old seedlings were collected at 0 and 2 hr after treatment with 20 µg/ml of chitin. Values were normalized to the level of *ACTIN1*. Bars represent means ± s.d. from three independent experiments. Statistical differences among different samples are labelled with different letters (one-way ANOVA with Tukey’s HSD test, $P < 0.01$).

It was previously reported that PBL27 interacts with chitin receptor CERK1 and can phosphorylate MAPKKK5 *in vitro* (Yamada et al., 2016). However, chitin-induced MAP kinase activation and defense gene expression are not significantly altered in *pbl27* in my experimental condition (Figure 3.15 A and B). It is very likely that there are genetic redundant RLCKs transducing signals from PRRs to MAPKKK3 and MAPKKK5.

The RLCKs PCRK1 and PCRK2 were previously shown to interact with FLS2 and are phosphorylated upon flg22 treatment (Kong et al., 2016). In addition, *pcrk1 pcrk2* double mutant shows modestly reduced flg22-induced MPK3/MPK6 phosphorylation (Kong et al., 2016). These findings make PCRK1 and PCRK2 promising candidates for transducing signals from PRR complexes to MAPKKK3 and MAPKKK5 and prompted us to examine whether PCRK2 can interact with MAPKKK3 and MAPKKK5. PCRK2 instead of PCRK1 was used in the analysis because it shows higher protein expression levels when transiently expressed in *N.b.*.

To test whether PCRK2 can interact with MAPKKK3 and MAPKKK5, PCRK2 with a 2HA-TurboID tag was co-expressed with 3×FLAG-tagged MAPKKK3 or MAPKKK5 in *N.b.* leaves using *Agrobacterium*-mediated transient transformation. The GFP-2HA-TurboID was used as a negative control. TurboID is an engineered biotin ligase with high efficiency in proximity labeling (Zhang et al., 2019). When the 3×FLAG-tagged MAPKKK3 and MAPKKK5 were immunoprecipitated with anti-FLAG beads, the PCRK2-2HA-TurboID protein was detected in the eluted samples by the anti-HA antibody, suggesting that PCRK2 interacts with both MAPKKK3 and MAPKKK5 (Figure 3.16).

In vivo biotinylation assay was used to further confirm the interaction between PCRK2 and MAPKKK3/MAPKKK5. In this assay, biotinylation of interacting proteins occurs when the

physical distance of the two proteins is close enough (Zhang et al., 2019). As shown in figure 3.16, both MAPKKK3^{K243M}-3FLAG and MAPKKK5^{K375M}-3FLAG proteins are biotinylated by PCRK2-2HA-TurboID but not the GFP-2HA-TurboID as shown by western blot using streptavidin-HRP, confirming that PCRK2 interacts with MAPKKK3 and MAPKKK5.

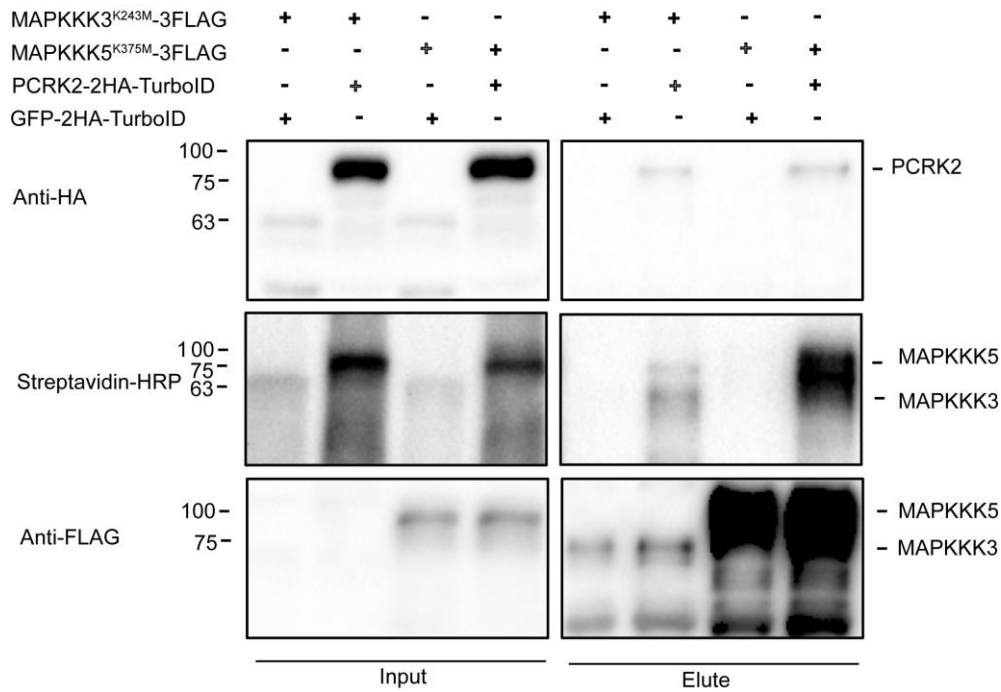


Figure 3.16 PCRK2 interacts with MAPKKK3 and MAPKKK5 in planta.

MAPKKK3^{K243M}-3FLAG or MAPKKK5^{K375M}-3FLAG was co-expressed with PCRK2-2HA-TurboID or GFP-2HA-TurboID through *Agrobacterium*-mediated transient expression in *Nicotiana benthamiana* (*N.b.*) leaves. Total protein was immunoprecipitated with anti-FLAG M2 agarose beads. Fusion proteins in input and eluate were detected using anti-FLAG, streptavidin-HRP or anti-HA antibodies. Experiments are repeated twice with similar result.

Chapter 4: Discussion

4.1 MAPKKK3 and MAPKKK5 function upstream of MKK4/MKK5-MPK3/MPK6.

Arabidopsis MKK4/MKK5 and MPK3/MPK6 function in a MAP kinase cascade downstream of PAMP receptor FLS2. The identity of the MAPKKK(s) in this cascade was previously unknown. As shown in Chapter 3, the *mapkkk3 mpakkk5* double mutant has a defect in *flg22*, *elf18* and *nlp20*-induced MPK3 and MPK6 activation, suggesting that both MAPKKK3 and MAPKKK5 are required for PAMP-induced MAP kinase activation. Interestingly, the *mapkkk3 mapkkk5* double mutant also showed reduced activation of MPK3 and MPK6 in response to *pep23*, suggesting that MAPKKK3 and MAPKKK5 are also required for DAMP-induced MAP kinase activation. In Co-IP and BiFC assays, MAPKKK3/MAPKKK5 were found to interact with MKK4/MKK5. Using recombinant MAPKKK3, MKK5 and MPK6 proteins purified from *E.coli*, the full length MAPKKK3 protein was shown to enhance MPK6 phosphorylation by MKK5, suggesting that the MAPKKK3-MKK5-MPK6 cascade can be reconstituted *in vitro*. All together, these results suggest that MAPKKK3 and MAPKKK5 serve as the MAPKKKs upstream of the MKK4/MKK5-MPK3/MPK6 module. This is confirmed by independent data from Dr. Jian-min Zhou's group, which also found that MAPKKK3 and MAPKKK5 are required for MPK3/MPK6 activation triggered by various PAMPs (Bi et al., 2018).

Although elicitor-induced activation of MPK3 and MPK6 in the *mapkkk3 mpakkk5* double mutant is clearly reduced, it is not completely blocked, suggesting that other MAPKKKs share overlapping functions with MAPKKK3/MAPKKK5. Previously it was shown that the expression of a truncated MEKK1 protein lacking the N-terminal regulation domain leads to activation of MKK5 (Asai et al., 2002). However, activation of MPK3/MPK6 in the *mekk1* knockout mutant

is not affected (Ichimura et al., 2006; Suarez-Rodriguez et al., 2007). In the *mapkkk3 mapkkk5 mekk1 mekk2 mekk3* quintuple mutant, flg22 induces similar levels of MPK3/MPK6 phosphorylation as in *mapkkk3 mapkkk5* double mutant, suggesting that MEKK1 is unlikely to function redundantly with MAPKKK3 and MAPKKK5 in flg22-induced MPK3 and MPK6 activation (Figure 3.5).

Recently, a Raf-like MAPKKK, MAPKKK DELTA 1 (MKD1) was reported to be required for flg22-induced MPK3 and MPK6 activation (Asano et al., 2020). MKD1 protein was isolated from a complex including the transcription factor NF-X-LIKE 1(NFXL1), which is involved in trichothecene phytotoxin response and disease resistance against *Pto* DC3000. Y2H assay and BiFC assay showed that MKD1 interacts with MKK1, MKK2 and MKK5 (Asano et al., 2020). *In vitro* kinase assay showed that N terminal truncated MKD1 could phosphorylate MKK1, MKK2 and MKK5. Thus, MKD1 may contribute to the remaining MPK3/MPK6 phosphorylation in the *mapkkk3 mapkkk5* double mutant (Asano et al., 2020). It will be interesting to knock out *MKD1* in the *mapkkk3 mapkkk5* double mutant and examine flg22-induced MPK3/MPK6 activation in the resulting triple mutant in the future.

4.2 The MAPKKK3/MAPKKK5-MKK4/MKK5-MPK3/MPK6 cascade plays critical roles in PTI and basal resistance.

Upon flg22 treatment, the MEKK1-MKK1/MKK2-MPK4 is activated. This kinase cascade has been shown to positively contribute to basal resistance. Our study showed that the flg22-activated MAPKKK3/MAPKKK5-MKK4/MKK5-MPK3/MPK6 cascade also plays important roles in basal immunity as suggested by the enhanced susceptibility in mutants towards *Pto* DC3000. In addition, the *mapkkk3 mapkkk5* double mutant displays reduced flg22-induced

MPK3/MPK6 phosphorylation and support increased growth of *Pto* DC3000 *hrcC*, suggesting that MAPKKK3 and MAPKKK5 are required for PTL.

It was previously reported that the conditional *mpk3 mpk6* double mutant exhibits compromised stomata immunity and allows increased pathogen entry (Su et al., 2017). Increased malate and citrate accumulation are observed in conditional *mpk3 mpk6* double mutant after pathogen infection (Su et al., 2017). In addition, exogenous application of organic acid impairs pathogen-induced stomata closure. Thus, MPK3 and MPK6 were proposed to regulate organic acid metabolism during pathogen infection, which is critical to pathogen-induced stomata immunity. It will be interesting to determine whether the increased bacterial growth in *mapkkk3 mapkkk5* is caused by reduced stomata defense due to reduced MPK3/MPK6 activities.

Several MPK3/MPK6 substrates, such as the ethylene biosynthesis enzymes ACS2 and ACS6 and transcription factors WRKY33 and ERF6, play critical roles in plant defense. Ethylene positively regulates resistance against bacterial and fungal pathogens. WRKY33 promotes pathogen-induced phytoalexin biosynthesis. ERF6 promotes the biosynthesis of indole glucosinolates that contribute to plant immunity (Meng et al., 2013). It is likely the reduced activation of MPK3/MPK6 in the *mapkkk3 mapkkk5* double mutant leads to reduced phosphorylation of WRKY33, ERF1 and ACS2/ACS6, resulting in compromised basal defense.

4.3 MAPKKK3 and MAPKKK5 contribute to ETI and are required for AvrRpt2-induced cell death and SAR.

When the *mapkkk3 mapkkk5* double mutant plants were challenged with avirulent *Pto* DC3000 strains carrying *AvrRpt2*, *AvrPphB* or *AvrRps4*, they supported significantly higher growth of the avirulent pathogens than wild type plants. Introducing mutations in *MKK4* and *MKK5* into the *mapkkk3 mapkkk5* double mutant further increased the growth of avirulent strains. These data suggest that MAPKKK3 and MAPKKK5 contribute positively to promote ETI.

Interestingly, *mapkkk3 mapkkk5* does not suppress the autoimmune phenotypes in *mekk1* and *chs3-2D*. This could be due to the existence of other MAPKKKs that function redundantly with MAPKKK3/MAPKKK5. It is also possible that MAPKKK3 and MAPKKK5 only play a minor role in defense signaling downstream of SUMM2 and CHS3.

In addition to supporting increased growth of avirulent bacterial pathogens, the *mapkkk3 mapkkk5* double mutant shows reduced cell death upon infection by the avirulent *Pto* DC3000 strains. When combined with mutations in *MKK4/MKK5* and *MPK3/MPK6*, cell death triggered by the avirulent pathogens is further reduced. These data suggest that MAPKKK3 and MAPKKK5 play an important role in activation of cell death during ETI. This is consistent with previous findings that cell death triggered by ETI is compromised in *mpk3 mpk6* double mutant (Su et al., 2018). MAPKKK α , a homolog of MAPKKK3 and MAPKKK5, previously was also reported to be required for cell death triggered by different pathogen effector proteins in *N.b.*, suggesting that the function of MAPKKK3 and MAPKKK5 in promoting HR during ETI is evolutionarily conserved (Pozo et al., 2004).

MPK3 and MPK6 were previously shown to contribute to SAR induced by *Pto* DC3000 *AvrRpt2* (Wang et al., 2018). In the *mapkkk3 mapkkk5* double mutant, *Pto* DC3000 *AvrRpt2*-induced SAR is also compromised, suggesting that MAPKKK3 and MAPKKK5 are required for SAR induced by ETI. Quantitative RT-PCR analysis of *ALD1* and *FMO1*, which encodes two key enzymes in the biosynthesis of Pip and NHP respectively, showed that their induction by *Pto* DC3000 *AvrRpt2* is significantly reduced in the *mapkkk3 mapkkk5* double mutant, suggesting that the compromised SAR in *mapkkk3 mapkkk5* could be due to reduced Pip/NHP biosynthesis. It is important to compare Pip and NHP levels in wild type and *mapkkk3 mapkkk5* in the future.

4.4 MAPKKK3 kinase activity and C terminal domain but not its N terminal regulatory domain is required for its function in signal transduction.

As shown in figure 3.14 A, MAPKKK3 consists of an N terminal regulatory domain, a kinase domain and C terminal domain. N terminal regulatory domains of MAPKKKs are believed to negatively regulate MAPKKK's function. For example, overexpression of the N terminal truncated but not the full length tobacco MAPKKK NPK1 complemented the growth defect in yeast *bck1* mutant (Banno et al., 1993). Deletion of the N-terminal domain of YDA, a MAPKKK involved in the negative function of stomata development leads to constitutive activation of YDA and almost complete elimination of stomata (H. Wang et al., 2007). In the *in vitro* kinase assay, MAPKKK3 with deletion of the N terminal domain has similar activity in stimulating MPK6 phosphorylation by MKK5, suggesting that N terminal domain is not essential for the activity *in vitro*. Since the *E.coli* expressed full length MAPKKK3 shows auto-phosphorylation and can activate downstream MPK6 phosphorylation, the N terminal domain of MAPKKK3 may

not be able to inhibit its activity *in vitro*. Additional factors may be required *in planta* to keep MAPKKK3 inactive in the absence of upstream stimuli.

Previously it was shown that N terminal truncated MEKK1 is able to phosphorylate MKK5 and activate downstream MPK3 and MPK6 in protoplasts despite that the full length MEKK1 is unlikely to contribute to flg22-induced MPK3/MPK6 activation *in planta*, suggesting a loss of specificity due to the N terminal truncation. Whether the N terminal domain of MAPKKK3 contributes to its specificity is unknown. It will be interesting to test whether MAPKKK3 Δ N can phosphorylate MKKs other than MKK4 and MKK5.

Analysis of flg22-induced MAP kinase activation in *Arabidopsis* transgenic lines showed that the kinase dead *mapkkk3* mutant cannot complement the reduced MPK3/MPK6 phosphorylation in *mapkkk3 mapkkk5*, suggesting that the kinase activity of MAPKKK3 is required for signal transduction *in vivo*. In the *in vitro* reconstituted MAPK kinase assay, the kinase dead MAPKKK3 protein purified from *E.coli* was less active but still retained some activity in stimulating MPK6 phosphorylation. Previously it was reported that a kinase dead mutant of MEKK1 can fully complement the autoimmune phenotype of *mekk1*, suggesting that MEKK1 may function as a scaffold protein in the MEKK1-MKK1/MKK2-MPK4 kinase cascade (Suarez-Rodriguez et al., 2007). It remains to be determined whether MAPKKK3/MAPKKK5 also play a role in assembling the MAPKKK3/MAPKKK5-MKK4/MKK5-MPK3/MPK6 cascade.

In the reconstituted MAPK kinase assay, the activity of the MAPKKK3 Δ C protein is also reduced but not completely eliminated, suggesting that C terminal domain of MAPKKK3 is partially required for MAPKKK3's activity *in vitro*. Phosphorylation at three sites in the C-terminus of MAPKKK5 were previously reported to be promote its activity in MPK3/MPK6

activation (Bi et al., 2018). It is likely that the corresponding phosphorylation sites at the C terminus of MAPKKK3 are also critical to its activity.

4.5 PCRK2 interacts with MAPKKK3/MAPKKK5 and connects upstream PRRs to the MAPKKK3/MAPKKK5-MKK4/MKK5-MPK3/MPK6 cascade.

MPK3/MPK6 are activated upon treatment by different elicitors. However, how PRRs transduce defense signal to activate the downstream MAP kinase cascades was unclear. It was reported that PBL27 interacts with the chitin receptor CERK1 and can phosphorylate MAPKKK5 (Yamada et al., 2016). However, no reduction in chitin-induced MPK3/MPK6 phosphorylation was observed in the *pbl27* mutant under our experimental condition (Figure 3.15).

Two redundant RLCKs, PCRK1 and PCRK2, were previously shown to interact with FLS2 and be rapidly phosphorylated upon treatment with flg22 (Kong et al., 2016). In addition, the *pcrk1 pcrk2* double mutant shows a modestly reduced MPK3/MPK6 activation after flg22 treatment, suggesting that PCRK1 and PCRK2 may be involved in transducing signal from FLS2 to MAPKKK3 and MAPKKK5 (Kong et al., 2016). In Co-IP and *in vivo* biotinylation assays using proteins transiently expressed in *N. b.* leaves, both MAPKKK3 and MAPKKK5 were found to interact with PCRK2, further supporting that PCRK2 and most likely its redundant homologue PCRK1 connect FLS2 to MAPKKK3/MAPKKK5 to activate downstream MAPK signaling (Figure 3.16). PCRK1 and PCRK2 belong to the RLCK VII-4 subgroup. Another member of the RLCK VII-4 subgroup, PBL19, was shown to phosphorylate the C terminal tail of MAPKKK5 (Bi et al., 2018). In the *rlck vii-4* sextuple mutant, phosphorylation of C terminus of MAPKKK5 induced chitin treatment is significantly reduced (Bi et al., 2018).

When we tested whether PCRK2-HA protein transiently expressed and purified from flg22-treated *N.b.* leaves can stimulate MPK6 phosphorylation using the reconstituted *in vitro* MAPK pathway assay, it failed to further enhance MPK6 phosphorylation in the presence of MAPKKK3 and MKK5. It is possible that the amount of the PCRK2-HA protein from *N.b.* is too low or the MAPKKK3 protein purified from *E. coli* is auto-phosphorylated and already fully activated.

In summary, our data suggest that the MAPKKK3/MAPKKK5-MKK4/MKK5-MPK3/MPK6 cascade plays broad roles in plant immunity as summarized in figure 4.1. It contributes to PTI, basal resistance, ETI-triggered cell death and SAR. The cascade is activated by flg22 and multiple other elicitors. Additionally, PCRK2 is involved in connecting the upstream FLS2/BAK1 complex and MAPKKK3/MAPKKK5 in the signal transduction.

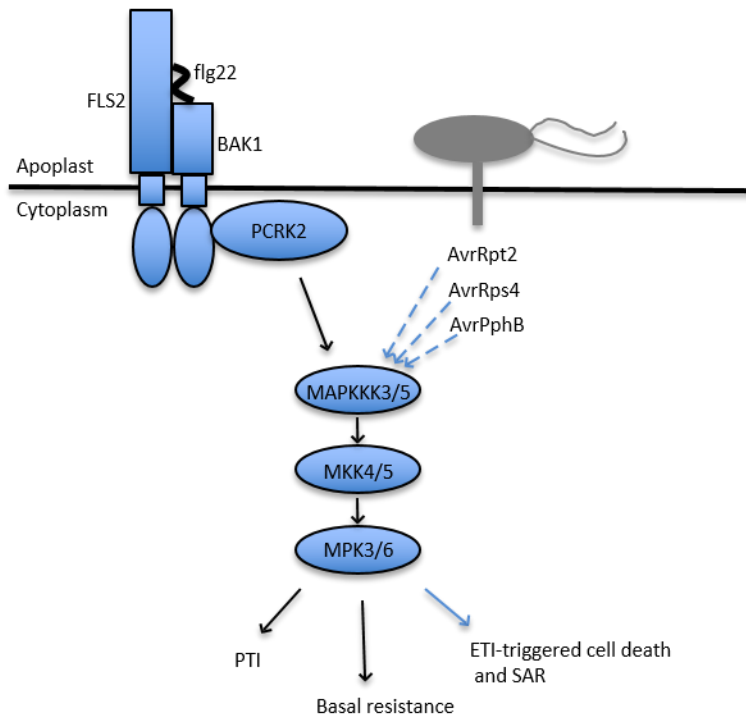


Figure 4.1 The MAPKKK3/MAPKKK5-MKK4/MKK5-MPK3/MPK6 cascade plays broad roles in plant immunity.

This MAPK cascade is activated upon flg22 treatment by the activated PCRK2 from FLS2 complex. It contributes to PTI and basal resistance. The MAPK cascade is also required for *Pto* DC3000 *AvrRpt2*, *Pto* DC3000 *AvrRps4* and *Pto* DC3000 *AvrPphB* induced cell death and SAR.

Bibliography

- Ade, J., DeYoung, B. J., Golstein, C., & Innes, R. W. (2007). Indirect activation of a plant nucleotide binding site-leucine-rich repeat protein by a bacterial protease. *Proc Natl Acad Sci U S A*, *104*(7), 2531–2536.
- Albert, I., Bohm, H., Albert, M., Feiler, C. E., Imkampe, J., Wallmeroth, N., Brancato, C., Raaymakers, T. M., Oome, S., Zhang, H., Krol, E., Grefen, C., Gust, A. A., Chai, J., Hedrich, R., Van den Ackerveken, G., & Nurnberger, T. (2015). An RLP23-SOBIR1-BAK1 complex mediates NLP-triggered immunity. Albert, I., Bohm, H., Albert, M., Feiler, C. E., Imkampe, J., Wallmeroth, N., Brancato, C., Raaymakers, T. M., Oome, S., Zhang, H., Krol, E., Grefen, C., Gust, A. A., Chai, J., Hedrich, R., Van d. *Nat Plants*, *1*, 15140.
- Asai, T., Tena, G., Plotnikova, J., Willmann, M. R., Chiu, W. L., Gomez-Gomez, L., Boller, T., Ausubel, F. M., & Sheen, J. (2002). MAP kinase signalling cascade in Arabidopsis innate immunity. *Nature*, *415*(6875), 977–983.
- Asano, T., Nguyen, T. H. N., Yasuda, M., Sidiq, Y., Nishimura, K., Nakashita, H., & Nishiuchi, T. (2020). Arabidopsis MAPKKK δ -1 is required for full immunity against bacterial and fungal infection. *Journal of Experimental Botany*, *71*(6), 2085–2097.
- Banno, H., Hirano, K., Nakamura, T., Irie, K., Nomoto, S., Matsumoto, K., & Machida, Y. (1993). NPK1, a tobacco gene that encodes a protein with a domain homologous to yeast BCK1, STE11, and Byr2 protein kinases. *Molecular and Cellular Biology*, *13*(8), 4745–4752.
- Bednarek, P., & Osbourn, A. (2009). Plant-Microbe Interactions: Chemical Diversity in Plant

Defense. *Science*, 324(5928), 746 LP – 748.

Bergmann, D. C., Lukowitz, W., & Somerville, C. R. (2004). Stomatal development and pattern controlled by a MAPKK kinase. *Science*, 304(5676), 1494–1497.

Bi, D., Johnson, K. C. M., Zhu, Z., Huang, Y., Chen, F., Zhang, Y., & Li, X. (2011). Mutations in an atypical TIR-NB-LRR-LIM resistance protein confer autoimmunity. *Frontiers in Plant Science*, 2(OCT), 1–10.

Bi, D., Johnson, K., Huang, Y., Zhu, Z., Li, X., & Zhang, Y. (2011). Mutations in an atypical TIR-NB-LRR-LIM resistance protein confers autoimmunity. *Frontiers in Plant Science*, 2.

Bi, G., Zhou, Z., Wang, W., Li, L., Rao, S., Wu, Y., Zhang, X., Menke, F. L. H., Chen, S., & Zhou, J. M. (2018). Receptor-like cytoplasmic kinases directly link diverse pattern recognition receptors to the activation of mitogen-activated protein kinase cascades in arabidopsis. *Plant Cell*, 30(7), 1543–1561.

Böhm, H., Albert, I., Oome, S., Raaymakers, T. M., Van den Ackerveken, G., & Nürnberger, T. (2014). A Conserved Peptide Pattern from a Widespread Microbial Virulence Factor Triggers Pattern-Induced Immunity in Arabidopsis. *PLoS Pathogens*, 10(11).

Boller, T., & Felix, G. (2009). A renaissance of elicitors: perception of microbe-associated molecular patterns and danger signals by pattern-recognition receptors. *Annu Rev Plant Biol*, 60, 379–406.

Boudsocq, M., Willmann, M. R., McCormack, M., Lee, H., Shan, L., He, P., Bush, J., Cheng, S. H., & Sheen, J. (2010). Differential innate immune signalling via Ca²⁺ sensor protein

- kinases. *Nature*, 464(7287), 418–422.
- Cao, H., Glazebrook, J., Clarke, J. D., Volko, S., & Dong, X. (1997). The Arabidopsis NPR1 gene that controls systemic acquired resistance encodes a novel protein containing ankyrin repeats. *Cell*, 88(1), 57–63.
- Chaiwongsar, S., Strohm, A. K., Su, S. H., & Krysan, P. J. (2012). Genetic analysis of the Arabidopsis protein kinases MAP3Kε1 and MAP3Kε2 indicates roles in cell expansion and embryo development. *Frontiers in Plant Science*, 3(OCT), 1–10.
- Chinchilla, D., Zipfel, C., Robatzek, S., Kemmerling, B., Nurnberger, T., Jones, J. D., Felix, G., & Boller, T. (2007). A flagellin-induced complex of the receptor FLS2 and BAK1 initiates plant defence. *Nature*, 448(7152), 497–500.
- Chung, E. H., da Cunha, L., Wu, A. J., Gao, Z., Cherkis, K., Afzal, A. J., Mackey, D., & Dangl, J. L. (2011). Specific threonine phosphorylation of a host target by two unrelated type III effectors activates a host innate immune receptor in plants. *Cell Host Microbe*, 9(2), 125–136.
- Couto, D., & Zipfel, C. (2016). Regulation of pattern recognition receptor signalling in plants. *Nature Reviews Immunology*, 16(9), 537–552.
- Day, B., Dahlbeck, D., Huang, J., Chisholm, S. T., Li, D., & Staskawicz, B. J. (2005). Molecular basis for the RIN4 negative regulation of RPS2 disease resistance. *Plant Cell*, 17(4), 1292–1305.
- de Jonge, R., Peter van Esse, H., Kombrink, A., Shinya, T., Desaki, Y., Bours, R., van der Krol,

- S., Shibuya, N., Joosten, M. H. A. J., & Thomma, B. P. H. J. (2010). Conserved Fungal LysM Effector Ecp6 Prevents Chitin-Triggered Immunity in Plants. *Science*, 329(5994), 953 LP – 955.
- Del Pozo, O., Pedley, K. F., & Martin, G. B. (2004). MAPKKK α is a positive regulator of cell death associated with both plant immunity and disease. *EMBO Journal*, 23(15), 3072–3082.
- Ding, P., Rekhter, D., Ding, Y., Feussner, K., Busta, L., Haroth, S., Xu, S., Li, X., Jetter, R., Feussner, I., Zhang, Y., & Ding Rekhter, D., Ding, Y., Feussner, K., Busta, L., Haroth, S., Xu, S., Li, X., Jetter, R., Feussner, I. and Zhang, Y., P. (2016). Characterization of a Pipecolic Acid Biosynthesis Pathway Required for Systemic Acquired Resistance. *Plant Cell*, 28(10), 2603–2615.
- Ding, Y., Sun, T., Ao, K., Peng, Y., Zhang, Y., Li, X., & Zhang, Y. (2018). Opposite Roles of Salicylic Acid Receptors NPR1 and NPR3/NPR4 in Transcriptional Regulation of Plant Immunity. *Cell*, 173(6), 1454-1467.e10.
- Dubiella, U., Seybold, H., Durian, G., Komander, E., Lassig, R., Witte, C.-P., Schulze, W. X., & Romeis, T. (2013). Calcium-dependent protein kinase/NADPH oxidase activation circuit is required for rapid defense signal propagation. *Proceedings of the National Academy of Sciences*, 110(21), 8744–8749.
- Felix, G., Duran, J. D., Volko, S., & Boller, T. (1999). Plants have a sensitive perception system for the most conserved domain of bacterial flagellin. *The Plant Journal*, 18(3), 265–276.
- Feng, F., Yang, F., Rong, W., Wu, X., Zhang, J., Chen, S., He, C., & Zhou, J. M. (2012). A

- Xanthomonas uridine 5'-monophosphate transferase inhibits plant immune kinases. *Nature*, 485(7396), 114–118.
- Frye, C. A., Tang, D., & Innes, R. W. (2001). Negative regulation of defense responses in plants by a conserved MAPKK kinase. *Proceedings of the National Academy of Sciences of the United States of America*, 98(1), 373–378.
- Galan, J. E., & Collmer, A. (1999). Type III secretion machines: bacterial devices for protein delivery into host cells. *Science*, 284(5418), 1322–1328.
- Gao, M., Liu, J., Bi, D., Zhang, Z., Cheng, F., Chen, S., & Zhang, Y. (2008). MEKK1, MKK1/MKK2 and MPK4 function together in a mitogen-activated protein kinase cascade to regulate innate immunity in plants. *Cell Res*, 18(12), 1190–1198.
- Gao, M., Wang, X., Wang, D., Xu, F., Ding, X., Zhang, Z., Bi, D., Cheng, Y. T., Chen, S., Li, X., & Zhang, Y. (2009). Regulation of cell death and innate immunity by two receptor-like kinases in Arabidopsis. *Cell Host Microbe*, 6(1), 34–44.
- Gassmann, W., & Bhattacharjee, S. (2012). Effector-triggered immunity signaling: From gene-for-gene pathways to protein-protein interaction networks. *Molecular Plant-Microbe Interactions*, 25(7), 862–868.
- Gomez-Gomez, L., & Boller, T. (2000). FLS2: an LRR receptor-like kinase involved in the perception of the bacterial elicitor flagellin in Arabidopsis. *Mol Cell*, 5(6), 1003–1011.
- Guo, H., Ahn, H.-K., Sklenar, J., Huang, J., Ma, Y., Ding, P., Menke, F. L. H., & Jones, J. D. G. (2020). Phosphorylation-Regulated Activation of the Arabidopsis RRS1-R/RPS4 Immune

Receptor Complex Reveals Two Distinct Effector Recognition Mechanisms. *Cell Host & Microbe*, 27(5), 769-781.e6.

Halter, T., Imkampe, J., Mazzotta, S., Wierzba, M., Postel, S., Bucherl, C., Kiefer, C., Stahl, M., Chinchilla, D., Wang, X., Nurnberger, T., Zipfel, C., Clouse, S., Borst, J. W., Boeren, S., de Vries, S. C., Tax, F., & Kemmerling, B. (2014). The leucine-rich repeat receptor kinase BIR2 is a negative regulator of BAK1 in plant immunity. *Curr Biol*, 24(2), 134–143.

Han, L., Li, G., Yang, K., Mao, G., Wang, R., Liu, Y., & Zhang, S. (2010). Mitogen-activated protein kinase 3 and 6 regulate Botrytis cinerea-induced ethylene production in Arabidopsis. *The Plant Journal*, 64(1), 114–127.

Hartmann, M., Zeier, T., Bernsdorff, F., Reichel-Deland, V., Kim, D., Hohmann, M., Scholten, N., Schuck, S., Bräutigam, A., Hölzel, T., Ganter, C., & Zeier, J. (2018). Flavin Monooxygenase-Generated N-Hydroxypipicolinic Acid Is a Critical Element of Plant Systemic Immunity. *Cell*, 173(2), 456-469.e16.

Hückelhoven, R. (2007). Cell Wall–Associated Mechanisms of Disease Resistance and Susceptibility. *Annual Review of Phytopathology*, 45(1), 101–127.

Ichimura, K., Casais, C., Peck, S. C., Shinozaki, K., & Shirasu, K. (2006). MEKK1 is required for MPK4 activation and regulates tissue-specific and temperature-dependent cell death in Arabidopsis. *J Biol Chem*, 281(48), 36969–36976.

Imkampe, J., Halter, T., Huang, S., Schulze, S., Mazzotta, S., Schmidt, N., Manstretta, R., Postel, S., Wierzba, M., Yang, Y., van Dongen, W. M. A. M., Stahl, M., Zipfel, C., Goshe, M. B.,

- Clouse, S., de Vries, S. C., Tax, F., Wang, X., & Kemmerling, B. (2017). The arabidopsis leucine-rich repeat receptor kinase BIR3 negatively regulates BAK1 receptor complex formation and stabilizes BAK1. *Plant Cell*, 29(9), 2285–2303.
- Jacob, F., Vernaldi, S., & Maekawa, T. (2013). Evolution and Conservation of Plant NLR Functions. *Front Immunol*, 4, 297.
- Jehle, A K, Lipschis, M., Albert, M., Fallahzadeh-Mamaghani, V., Furst, U., Mueller, K., & Felix, G. (2013). The receptor-like protein ReMAX of Arabidopsis detects the microbe-associated molecular pattern eMax from Xanthomonas. *Plant Cell*, 25(6), 2330–2340.
- Jehle, Anna Kristina, Fürst, U., Lipschis, M., Albert, M., & Felix, G. (2013). Perception of the novel MAMP eMax from different Xanthomonas species requires the Arabidopsis receptor-like protein remax and the receptor kinase SOBIR. *Plant Signaling and Behavior*, 8(12), 11–13.
- Jewaria, P. K., Hara, T., Tanaka, H., Kondo, T., Betsuyaku, S., Sawa, S., Sakagami, Y., Aimoto, S., & Kakimoto, T. (2013). Differential effects of the peptides stomagen, EPF1 and EPF2 on activation of MAP kinase MPK6 and the SPCH protein level. *Plant and Cell Physiology*, 54(8), 1253–1262.
- Jones, J. D., & Dangl, J. L. (2006). The plant immune system. *Nature*, 444(7117), 323–329.
- Kadota, Y., Sklenar, J., Derbyshire, P., Stransfeld, L., Asai, S., Ntoukakis, V., Jones, J. D., Shirasu, K., Menke, F., Jones, A., & Zipfel, C. (2014). Direct regulation of the NADPH oxidase RBOHD by the PRR-associated kinase BIK1 during plant immunity. *Mol Cell*,

54(1), 43–55.

Kanneganti, T. D., Lamkanfi, M., & Nunez, G. (2007). Intracellular NOD-like receptors in host defense and disease. *Immunity*, 27(4), 549–559.

Kim, M. G., da Cunha, L., McFall, A. J., Belkhadir, Y., DebRoy, S., Dangl, J. L., & Mackey, D. (2005). Two *Pseudomonas syringae* type III effectors inhibit RIN4-regulated basal defense in *Arabidopsis*. *Cell*, 121(5), 749–759.

Kim, Y., Gilmour, S. J., Chao, L., Park, S., & Thomashow, M. F. (2019). *Arabidopsis* CAMTA Transcription Factors Regulate Pipecolic Acid Biosynthesis and Priming of Immunity Genes. *Molecular Plant*, 13(1), 157–168.

Klessig, D. F., Choi, H. W., & Dempsey, D. A. (2018). Systemic acquired resistance and salicylic acid: Past, present, and future. *Molecular Plant-Microbe Interactions*, 31(9), 871–888.

Kong, Q., Sun, T., Qu, N., Ma, J., Li, M., Cheng, Y.-T., Zhang, Q., Wu, D., Zhang, Z., & Zhang, Y. (2016). Two redundant receptor-like cytoplasmic kinases function downstream of pattern recognition receptors to regulate activation of SA biosynthesis. *Plant Physiology*, 171(2).

Kong, Q., Sun, T., Qu, N., Ma, J., Li, M., Cheng, Y. T., Zhang, Q., Wu, D., Zhang, Z., & Zhang, Y. (2016). Two redundant receptor-like cytoplasmic kinases function downstream of pattern recognition receptors to regulate activation of SA biosynthesis. *Plant Physiology*, 171(2), 01954.2015.

Krasileva, K. V., Dahlbeck, D., & Staskawicz, B. J. (2010). Activation of an *Arabidopsis*

resistance protein is specified by the in planta association of its leucine-rich repeat domain with the cognate oomycete effector. *Plant Cell*, 22(7), 2444–2458.

Kumar, D., & Klessig, D. F. (2003). High-affinity salicylic acid-binding protein 2 is required for plant innate immunity and has salicylic acid-stimulated lipase activity. *Proc Natl Acad Sci U S A*, 100(26), 16101–16106.

Kunze, G., Zipfel, C., Robatzek, S., Niehaus, K., Boller, T., & Felix, G. (2004). The N terminus of bacterial elongation factor Tu elicits innate immunity in Arabidopsis plants. *Plant Cell*, 16(12), 3496–3507.

Lal, N. K., Nagalakshmi, U., Hurlburt, N. K., Flores, R., Bak, A., Sone, P., Ma, X., Song, G., Walley, J., Shan, L., He, P., Casteel, C., Fisher, A. J., & Dinesh-Kumar, S. P. (2018). The Receptor-like Cytoplasmic Kinase BIK1 Localizes to the Nucleus and Regulates Defense Hormone Expression during Plant Innate Immunity. *Cell Host Microbe*, 23(4), 485–497 e5.

Lee, W. S., Rudd, J. J., Hammond-Kosack, K. E., & Kanyuka, K. (2014). *Mycosphaerella graminicola* lysm effector-mediated stealth pathogenesis subverts recognition through both *cerk1* and *cebip* homologues in wheat. *Molecular Plant-Microbe Interactions*, 27(3), 236–243.

Li, B., Ferreira, M. A., Huang, M., Camargos, L. F., Yu, X., Teixeira, R. M., Carpinetti, P. A., Mendes, G. C., Gouveia-Mageste, B. C., Liu, C., Pontes, C. S. L., Brustolini, O. J. B., Martins, L. G. C., Melo, B. P., Duarte, C. E. M., Shan, L., He, P., & Fontes, E. P. B. (2019). The receptor-like kinase NIK1 targets FLS2/BAK1 immune complex and inversely modulates antiviral and antibacterial immunity. *Nature Communications*, 10(1), 1–14.

- Li, L., Li, M., Yu, L., Zhou, Z., Liang, X., Liu, Z., Cai, G., Gao, L., Zhang, X., Wang, Y., Chen, S., & Zhou, J. M. (2014). The FLS2-associated kinase BIK1 directly phosphorylates the NADPH oxidase RbohD to control plant immunity. *Cell Host Microbe*, *15*(3), 329–338.
- Li, Xin, Kapos, P., & Zhang, Y. (2015). NLRs in plants. *Current Opinion in Immunology*, *32*, 114–121.
- Li, Y., Dong, O. X., Johnson, K., Li-Sup, X., & Zhang, Y. (2011). MOS1 epigenetically regulates the expression of plant Resistance gene SNC1. *Plant Signaling and Behavior*, *6*(3), 434–436.
- Lian, K., Gao, F., Sun, T., Wersch, R. van, Ao, K., Kong, Q., Nitta, Y., Wu, D., Krysan, P. J., Zhang, Y., van Wersch, R., Ao, K., Kong, Q., Nitta, Y., Wu, D., Krysan, P. J., & Zhang, Y. (2018). MKK6 functions in two parallel MAP kinase cascades in immune signaling. *Plant Physiology*, *178*(3), 1284–1295.
- Liebrand, T. W., van den Burg, H. A., & Joosten, M. H. (2014). Two for all: receptor-associated kinases SOBIR1 and BAK1. *Trends Plant Sci*, *19*(2), 123–132.
- Liu, J., Ding, P., Sun, T., Nitta, Y., Dong, O., Huang, X., Yang, W., Li, X., Botella, J. R., & Zhang, Y. (2013). Heterotrimeric G proteins serve as a converging point in plant defense signaling activated by multiple receptor-like kinases. *Plant Physiology*, *161*(4).
- Liu, Y., & Zhang, S. (2004). Phosphorylation of 1-aminocyclopropane-1-carboxylic acid synthase by MPK6, a stress-responsive mitogen-activated protein kinase, induces ethylene biosynthesis in Arabidopsis. *Plant Cell*, *16*(12), 3386–3399.

- Lu, D., Wu, S., Gao, X., Zhang, Y., Shan, L., & He, P. (2010). A receptor-like cytoplasmic kinase, BIK1, associates with a flagellin receptor complex to initiate plant innate immunity. *Proc Natl Acad Sci U S A*, *107*(1), 496–501.
- Mao, G., Meng, X., Liu, Y., Zheng, Z., Chen, Z., & Zhang, S. (2011). Phosphorylation of a WRKY transcription factor by two pathogen-responsive MAPKs drives phytoalexin biosynthesis in Arabidopsis. *The Plant Cell*, *23*(4), 1639–1653.
- MAPK-Group. (2002). Mitogen-activated protein kinase cascades in plants: a new nomenclature. *Trends Plant Sci.*, *7*(7), 301–308.
- Melotto, M., Underwood, W., Koczan, J., Nomura, K., & He, S. Y. (2006). Plant stomata function in innate immunity against bacterial invasion. *Cell*, *126*(5), 969–980.
- Melotto, Maeli, Zhang, L., Oblessuc, P. R., & He, S. Y. (2017). Stomatal defense a decade later. *Plant Physiology*, *174*(2), 561–571.
- Meng, X., Xu, J., He, Y., Yang, K. Y., Mordorski, B., Liu, Y., & Zhang, S. (2013). Phosphorylation of an ERF transcription factor by Arabidopsis MPK3/MPK6 regulates plant defense gene induction and fungal resistance. *Plant Cell*, *25*(3), 1126–1142.
- Meng, X., & Zhang, S. (2013). MAPK cascades in plant disease resistance signaling. *Annu Rev Phytopathol*, *51*, 245–266.
- Mithoe, S. C., Ludwig, C., Pel, M. J., Cucinotta, M., Casartelli, A., Mbengue, M., Sklenar, J., Derbyshire, P., Robatzek, S., Pieterse, C. M., Aebersold, R., & Menke, F. L. (2016). Attenuation of pattern recognition receptor signaling is mediated by a MAP kinase kinase

- kinase . *EMBO Reports*, 17(3), 441–454.
- Miya, A., Albert, P., Shinya, T., Desaki, Y., Ichimura, K., Shirasu, K., Narusaka, Y., Kawakami, N., Kaku, H., & Shibuya, N. (2007). CERK1, a LysM receptor kinase, is essential for chitin elicitor signaling in Arabidopsis. *Proc Natl Acad Sci U S A*, 104(49), 19613–19618.
- Möbius, N., & Hertweck, C. (2009). Fungal phytotoxins as mediators of virulence. *Current Opinion in Plant Biology*, 12(4), 390–398.
- Monaghan, J., & Zipfel, C. (2012). Plant pattern recognition receptor complexes at the plasma membrane. *Curr Opin Plant Biol*, 15(4), 349–357.
- Navarova, H., Bernsdorff, F., Doring, A. C., & Zeier, J. (2012). Pipecolic acid, an endogenous mediator of defense amplification and priming, is a critical regulator of inducible plant immunity. *Plant Cell*, 24(12), 5123–5141.
- Ngou, P. M., Ahn, H., Ding, P., & Jones, J. D. (2020). Mutual Potentiation of Plant Immunity by Cell-surface and Intracellular Receptors. *BioRxiv*, 1–29.
- Nishihama, R., Banno, H., Kawahara, E., Irie, K., & Machida, Y. (1997). Possible involvement of differential splicing in regulation of the activity of Arabidopsis ANP1 that is related to mitogen-activated protein kinase kinase kinases (MAPKKKs). *Plant Journal*, 12(1), 39–48.
- Nitta, Y., Qiu, Y., Yaghmaiean, H., Zhang, Q., Huang, J., Adams, K., & Zhang, Y. (2020). MEKK2 inhibits activation of MAP kinases in Arabidopsis. *The Plant Journal*, 1–10.
- Oome, S., Raaymakers, T. M., Cabral, A., Samwel, S., Böhm, H., Albert, I., Nürnberger, T., &

- Van Den Ackerveken, G. (2014). Nep1-like proteins from three kingdoms of life act as a microbe-associated molecular pattern in Arabidopsis. *Proceedings of the National Academy of Sciences of the United States of America*, *111*(47), 16955–16960.
- Piršelová, B., & Matušíková, I. (2013). Callose: The plant cell wall polysaccharide with multiple biological functions. *Acta Physiologiae Plantarum*, *35*(3), 635–644.
- Reina-Pinto, J. J., & Yephremov, A. (2009). Surface lipids and plant defenses. *Plant Physiology and Biochemistry*, *47*(6), 540–549.
- Ryals, J., Weymann, K., Lawton, K., Friedrich, L., Ellis, D., Steiner, H. Y., Johnson, J., Delaney, T. P., Jesse, T., Vos, P., & Uknes, S. (1997). The Arabidopsis NIM1 protein shows homology to the mammalian transcription factor inhibitor I kappa B. *Plant Cell*, *9*(3), 425–439.
- Saucet, S. B., Ma, Y., Sarris, P. F., Furzer, O. J., Sohn, K. H., & Jones, J. D. G. (2015). Two linked pairs of Arabidopsis TNL resistance genes independently confer recognition of bacterial effector AvrRps4. *Nature Communications*, *6*.
- Schulze, B., Mentzel, T., Jehle, A. K., Mueller, K., Beeler, S., Boller, T., Felix, G., & Chinchilla, D. (2010). Rapid heteromerization and phosphorylation of ligand-activated plant transmembrane receptors and their associated kinase BAK1. *J Biol Chem*, *285*(13), 9444–9451.
- Shah, J., Tsui, F., & Klessig, D. F. (1997). Characterization of a salicylic acid-insensitive mutant (sai1) of Arabidopsis thaliana, identified in a selective screen utilizing the SA-inducible

- expression of the *tms2* gene. *Mol Plant Microbe Interact*, 10(1), 69–78.
- Shakeel, S. N., Gao, Z., Amir, M., Chen, Y. F., Rai, M. I., Haq, N. U., & Schaller, G. E. (2015). Ethylene regulates levels of ethylene receptor/CTR1 signaling complexes in *Arabidopsis thaliana*. *Journal of Biological Chemistry*, 290(19), 12415–12424.
- Shi, H., Shen, Q., Qi, Y., Yan, H., Nie, H., Chen, Y., Zhao, T., Katagiri, F., & Tang, D. (2013). BR-SIGNALING KINASE1 physically associates with FLAGELLIN SENSING2 and regulates plant innate immunity in *Arabidopsis*. *Plant Cell*, 25(3), 1143–1157.
- Shibuya, N., & Minami, E. (2001). Oligosaccharide signalling for defence responses in plant. *Physiological and Molecular Plant Pathology*, 59(5), 223–233.
- Shiu, S., Karlowski, W., Pan, R., Sd, O., Duf, O., Osi, K., Duf, A., Egf, S., Thn, S., & Sd, R. (2004). Phylogeny of RLK/Pelle members from *Arabidopsis* and rice. *The Plant Cell* ..., 16(May), 33.
- Smakowska-Luzan, E., Mott, G. A., Parys, K., Stegmann, M., Howton, T. C., Layeghifard, M., Neuhold, J., Lehner, A., Kong, J., Grünwald, K., Weinberger, N., Satbhai, S. B., Mayer, D., Busch, W., Madalinski, M., Stolt-Bergner, P., Provar, N. J., Mukhtar, M. S., Zipfel, C., ... Belkhadir, Y. (2018). An extracellular network of *Arabidopsis* leucine-rich repeat receptor kinases. *Nature*, 553(7688), 342–346.
- Su, J., Zhang, M., Zhang, L., Sun, T., Liu, Y., Lukowitz, W., Xu, J., & Zhang, S. (2017). Regulation of Stomatal Immunity by Interdependent Functions of a Pathogen-Responsive MPK3/MPK6 Cascade and Abscisic Acid. *Plant Cell*, 29(3), 526–542.

- Su, Jianbin, Yang, L., Zhu, Q., Wu, H., He, Y., Liu, Y., Xu, J., Jiang, D., & Zhang, S. (2018). Active photosynthetic inhibition mediated by MPK3/MPK6 is critical to effector-triggered immunity. *PLoS Biology*, *16*(5), 1–29.
- Su, S. H., Bush, S. M., Zaman, N., Stecker, K., Sussman, M. R., & Krysan, P. (2013). Deletion of a tandem gene family in Arabidopsis: increased MEKK2 abundance triggers autoimmunity when the MEKK1-MKK1/2-MPK4 signaling cascade is disrupted. *Plant Cell*, *25*(5), 1895–1910.
- Suarez-Rodriguez, M. C., Adams-Phillips, L., Liu, Y., Wang, H., Su, S. H., Jester, P. J., Zhang, S., Bent, A. F., & Krysan, P. J. (2007). MEKK1 is required for flg22-induced MPK4 activation in Arabidopsis plants. *Plant Physiol*, *143*(2), 661–669.
- Sun, T., Huang, J., Xu, Y., Verma, V., Jing, B., Sun, Y., Ruiz Orduna, A., Tian, H., Huang, X., Xia, S., Schafer, L., Jetter, R., Zhang, Y., & Li, X. (2019). Redundant CAMTA Transcription Factors Negatively Regulate the Biosynthesis of Salicylic Acid and N-Hydroxypipicolinic Acid by Modulating the Expression of SARD1 and CBP60g. *Molecular Plant*, *13*(1), 144–156.
- Sun, Y., Li, L., Macho, A. P., Han, Z., Hu, Z., Zipfel, C., Zhou, J. M., & Chai, J. (2013). Structural basis for flg22-induced activation of the Arabidopsis FLS2-BAK1 immune complex. *Science*, *342*(6158), 624–628.
- Tang, W., Kim, T. W., Osés-Prieto, J. A., Sun, Y., Deng, Z., Zhu, S., Wang, R., Burlingame, A. L., & Wang, Z. Y. (2008). BSKs mediate signal transduction from the receptor kinase BRI1 in Arabidopsis. *Science*, *321*(5888), 557–560.

- Tian, W., Hou, C., Ren, Z., Wang, C., Zhao, F., Dahlbeck, D., Hu, S., Zhang, L., Niu, Q., Li, L., Staskawicz, B. J., & Luan, S. (2019). A calmodulin-gated calcium channel links pathogen patterns to plant immunity. *Nature*, *572*(7767), 131–135.
- Torres, M. A., Dangl, J. L., & Jones, J. D. G. (2002). Arabidopsis gp91phox homologues AtrbohD and AtrbohF are required for accumulation of reactive oxygen intermediates in the plant defense response. *Proceedings of the National Academy of Sciences*, *99*(1), 517–522.
- Toruño, T. Y., Stergiopoulos, I., & Coaker, G. (2016). Plant-Pathogen Effectors: Cellular Probes Interfering with Plant Defenses in Spatial and Temporal Manners. *Annual Review of Phytopathology*, *54*(1), 419–441.
- Uchida, N., & Tasaka, M. (2013). Regulation of plant vascular stem cells by endodermis-derived EPFL-family peptide hormones and phloem-expressed ERECTA-family receptor kinases. *Journal of Experimental Botany*, *64*(17), 5335–5343.
- van der Hoorn, R. A., & Kamoun, S. (2008). From Guard to Decoy: a new model for perception of plant pathogen effectors. *Plant Cell*, *20*(8), 2009–2017.
- van Wersch, R., Li, X., & Zhang, Y. (2016). Mighty dwarfs: Arabidopsis autoimmune mutants and their usages in genetic dissection of plant immunity. *Frontiers in Plant Science*, *7*(NOVEMBER2016), 1–8.
- Walter, M., Chaban, C., Schutze, K., Batistic, O., Weckermann, K., Nake, C., Blazevic, D., Grefen, C., Schumacher, K., Oecking, C., Harter, K., & Kudla, J. (2004). Visualization of protein interactions in living plant cells using bimolecular fluorescence complementation.

Plant J, 40(3), 428–438.

Wang, G., Ellendorff, U., Kemp, B., Mansfield, J. W., Forsyth, A., Mitchell, K., Bastas, K., Liu, C. M., Woods-Tor, A., Zipfel, C., de Wit, P. J., Jones, J. D., Tor, M., & Thomma, B. P. (2008). A genome-wide functional investigation into the roles of receptor-like proteins in Arabidopsis. *Plant Physiol*, 147(2), 503–517.

Wang, H., Ngwenyama, N., Liu, Y., Walker, J. C., & Zhang, S. (2007). Stomatal development and patterning are regulated by environmentally responsive mitogen-activated protein kinases in Arabidopsis. *Plant Cell*, 19(1), 63–73.

Wang, Y., Schuck, S., Wu, J., Yang, P., Döring, A. C., Zeier, J., & Tsuda, K. (2018). A mpk3/6-wrky33-ald1-pipecolic acid regulatory loop contributes to systemic acquired resistance[open]. *Plant Cell*, 30(10), 2480–2494.

Wildermuth, M. C., Dewdney, J., Wu, G., & Ausubel, F. M. (2001). Isochorismate synthase is required to synthesize salicylic acid for plant defence. *Nature*, 414(6863), 562–565.

Wu, F.-H., Shen, S.-C., Lee, L.-Y., Lee, S.-H., Chan, M.-T., & Lin, C.-S. (2009). Tape-Arabidopsis Sandwich—a simpler Arabidopsis protoplast isolation method. *Plant Methods*, 5(1), 16.

Wu, Y., Zhang, D., Chu, J. Y., Boyle, P., Wang, Y., Brindle, I. D., De Luca, V., & Despres, C. (2012). The Arabidopsis NPR1 protein is a receptor for the plant defense hormone salicylic acid. *Cell Rep*, 1(6), 639–647.

Xiang, T. T., Zong, N., Zou, Y., Wu, Y., Zhang, J., Xing, W. M., Li, Y., Tang, X. Y., Zhu, L. H.,

- Chai, J. J., & Zhou, J. M. (2008). *Pseudomonas syringae* effector AvrPto blocks innate immunity by targeting receptor kinases. *Current Biology*, *18*(1), 74–80.
- Xin, X. F., Nomura, K., Aung, K., Velasquez, A. C., Yao, J., Boutrot, F., Chang, J. H., Zipfel, C., & He, S. Y. (2016). Bacteria establish an aqueous living space in plants crucial for virulence. *Nature*, *539*(7630), 524–529.
- Yamada, K., Yamaguchi, K., Shirakawa, T., Nakagami, H., Mine, A., Ishikawa, K., Fujiwara, M., Narusaka, M., Narusaka, Y., Ichimura, K., Kobayashi, Y., Matsui, H., Nomura, Y., Nomoto, M., Tada, Y., Fukao, Y., Fukamizo, T., Tsuda, K., Shirasu, K., ... Kawasaki, T. (2016). The Arabidopsis CERK1-associated kinase PBL27 connects chitin perception to MAPK activation. *EMBO J*, *35*(22), 2468–2483.
- Yamada, Kenta, Yamaguchi, K., Shirakawa, T., Nakagami, H., Mine, A., Ishikawa, K., Fujiwara, M., Narusaka, M., Narusaka, Y., Ichimura, K., Kobayashi, Y., Matsui, H., Nomura, Y., Nomoto, M., Tada, Y., Fukao, Y., Fukamizo, T., Tsuda, K., Shirasu, K., ... Kawasaki, T. (2016). The Arabidopsis CERK 1-associated kinase PBL 27 connects chitin perception to MAPK activation. *The EMBO Journal*, *35*(22), 2468–2483.
- Yan, H., Zhao, Y., Shi, H., Li, J., Wang, Y., & Tang, D. (2018). BRASSINOSTEROID-SIGNALING kinase1 phosphorylates MAPKKK5 to regulate immunity in arabidopsis. *Plant Physiology*, *176*(4), 2991–3002.
- Yang, Y., Liu, J., Yin, C., Vespoli, L. de S., Ge, D., Huang, Y., Feng, B., Xu, G., Manhães, A. M. E. de A., Dou, S., Criswell, C., Shan, L., Wang, X., & He, P. (2020). RNAi-based screen reveals concerted functions of MEKK2 and CRCK3 in plant cell death regulation. *Plant*

Physiology, pp.01555.2019.

Yuan, M., Jiang, Z., Bi, G., Nomura, K., Liu, M., He, S. Y., Zhou, J.-M., & Xin, X.-F. (2020).

Pattern-recognition receptors are required for NLR-mediated plant immunity. *BioRxiv*, 2020.04.10.031294.

Zeng, W., & He, S. Y. (2010). A prominent role of the flagellin receptor FLAGELLIN-

SENSING2 in mediating stomatal response to *Pseudomonas syringae* pv tomato DC3000 in *Arabidopsis*. *Plant Physiology*, 153(3), 1188–1198.

Zhang, J., Li, W., Xiang, T., Liu, Z., Laluk, K., Ding, X., Zou, Y., Gao, M., Zhang, X., Chen, S.,

Mengiste, T., Zhang, Y., & Zhou, J. M. (2010). Receptor-like cytoplasmic kinases integrate signaling from multiple plant immune receptors and are targeted by a *Pseudomonas syringae* effector. *Cell Host Microbe*, 7(4), 290–301.

Zhang, L., Kars, I., Essenstam, B., Liebrand, T. W., Wagemakers, L., Elberse, J., Tagkalaki, P.,

Tjoitang, D., van den Ackerveken, G., & van Kan, J. A. (2014). Fungal endopolygalacturonases are recognized as microbe-associated molecular patterns by the arabidopsis receptor-like protein RESPONSIVENESS TO BOTRYTIS POLYGALACTURONASES1. *Plant Physiol*, 164(1), 352–364.

Zhang, W., Fraiture, M., Kolb, D., Loffelhardt, B., Desaki, Y., Boutrot, F. F., Tor, M., Zipfel, C.,

Gust, A. A., & Brunner, F. (2013). Arabidopsis receptor-like protein30 and receptor-like kinase suppressor of BIR1-1/EVERSHED mediate innate immunity to necrotrophic fungi. *Plant Cell*, 25(10), 4227–4241.

Zhang, Y., Xu, S., Ding, P., Wang, D., Cheng, Y. T., He, J., Gao, M., Xu, F., Li, Y., Zhu, Z., Li, X., & Zhang, Y. (2010). Control of salicylic acid synthesis and systemic acquired resistance by two members of a plant-specific family of transcription factors. *Proceedings of the National Academy of Sciences*, *107*(42), 18220–18225.

Zhang, Y, Cheng, Y. T., Qu, N., Zhao, Q., Bi, D., & Li, X. (2006). Negative regulation of defense responses in Arabidopsis by two NPR1 paralogs. *Plant J*, *48*(5), 647–656.

Zhang, Y, Fan, W., Kinkema, M., Li, X., & Dong, X. (1999). Interaction of NPR1 with basic leucine zipper protein transcription factors that bind sequences required for salicylic acid induction of the PR-1 gene. *Proc Natl Acad Sci U S A*, *96*(11), 6523–6528.

Zhang, Yaxi, Xu, S., Ding, P., Wang, D., Cheng, Y. T., He, J., Gao, M., Xu, F., Li, Y., Zhu, Z., Li, X., & Zhang, Y. (2010). Control of salicylic acid synthesis and systemic acquired resistance by two members of a plant-specific family of transcription factors. *Proceedings of the National Academy of Sciences of the United States of America*, *107*(42), 18220–18225.

Zhang, Yongliang, Song, G., Lal, N. K., Nagalakshmi, U., Li, Y., Zheng, W., Huang, P. jui, Branon, T. C., Ting, A. Y., Walley, J. W., & Dinesh-Kumar, S. P. (2019). TurboID-based proximity labeling reveals that UBR7 is a regulator of N NLR immune receptor-mediated immunity. *Nature Communications*, *10*(1).

Zhang, Z, Wu, Y., Gao, M., Zhang, J., Kong, Q., Liu, Y., Ba, H., Zhou, J., & Zhang, Y. (2012). Disruption of PAMP-induced MAP kinase cascade by a *Pseudomonas syringae* effector activates plant immunity mediated by the NB-LRR protein SUMM2. *Cell Host Microbe*,

11(In press.), 253–263.

Zhang, Zhibin, Liu, Y., Huang, H., Gao, M., Wu, D., Kong, Q., & Zhang, Y. (2017). The NLR protein SUMM 2 senses the disruption of an immune signaling MAP kinase cascade via CRCK 3 . *EMBO Reports*, *18*(2), 292–302.

Zhao, C., Nie, H., Shen, Q., Zhang, S., Lukowitz, W., & Tang, D. (2014). EDR1 Physically Interacts with MKK4/MKK5 and Negatively Regulates a MAP Kinase Cascade to Modulate Plant Innate Immunity. *PLoS Genetics*, *10*(5).

Zipfel, C. (2014). Plant pattern-recognition receptors. *Trends in Immunology*, *35*(7), 345–351.

Zipfel, C., Kunze, G., Chinchilla, D., Caniard, A., Jones, J. D., Boller, T., & Felix, G. (2006). Perception of the bacterial PAMP EF-Tu by the receptor EFR restricts Agrobacterium-mediated transformation. *Cell*, *125*(4), 749–760.